PhD Thesis

Statistical analysis on the effect of precipitation on the variability of extreme sea levels along the coast of Bangladesh

Md. Anowarul Islam

Graduate School of Environmental Science

Hokkaido University

Sapporo, Japan

September 2022

ABSTRACT

The global mean sea level rise under climate change is an alarming issue to the sustainability of the coastal communities. The sea level rise enhances the vulnerability to cope with associated hazard for developing nations. Bangladesh is highly vulnerable to the adverse impacts of extreme sea levels (ESLs) because of its geographical location with low-lying deltaic coast and the inadequate infrastructure with high population exposure. In addition, as most downstream area of large Ganges-Brahmaputra-Meghna (GBM) River and Sangu-Matamuhuri River near Arakan hilly area, the central and eastern coast of Bangladesh receives abundant precipitated-water from the upstream, respectively. The resultant increase in precipitated-water discharge from the upstream areas may enhance the ESL-induced flood risk along the coast. The ESL arises from the combined interaction of different meteorological forcings. The effects of meteorological forcings like atmospheric pressure, storm-induced surges, and wind-induced waves to ESL have been investigated intensively. However, the influence of terrestrial precipitation to the ESL along the Bangladesh coast remains unknown despite the region is known as the highest precipitation-prone area in the world. In this study, the influence of precipitation on ESL was investigated for Cox's Bazar, Charchanga, and Khepupara stations, which represent three different geographical areas on the eastern, central, and western coast, respectively.

The ESL events were obtained from the available daily sea level data at Cox's Bazar (1983–2006), Charchanga (1980–2000), and Khepupara (1987–2000). To remove the seasonality in observed sea level, the anomalous sea level relative to the 91 days running mean was used. The 99th percentile values of daily sea level anomaly (SLA) were used as a threshold for the identification of ESL events. After excluding the consecutive days before and after the peak sea level, in total 35, 30, and 18 independent ESL events were selected for Cox's Bazar, Charchanga, and Khepupara, respectively. The variations in daily SLA during seven days prior to the ESL day were predicted by multivariate linear regression (MLR) using four meteorological variables of precipitation, sea level pressure, zonal, and meridional wind. The basin average accumulated precipitation over five days was used to account the delay effect in precipitation runoff. The daily sea level pressure and wind were averaged over the Bay of Bengal. The spatiotemporal variations of the meteorological variables during ESL events showed the presence of low pressure system and associated cyclonic circulation over the coast and high precipitation especially for Cox's Bazar area. It is revealed that the prediction of ESL height considering precipitation effects outperformed predictions without precipitation. To

understand the causality of the precipitation effect, each term of the MLR was investigated. The gradual increase in sea level towards the day of extreme was mainly brought by the contribution of precipitation term rather than the other atmospheric forcings for Cox's Bazar. In contrast, the influence of precipitation term is relatively small for Charchanga and Khepupara. Therefore, the benefit of incorporating precipitation effect is greater at Cox's Bazar than Charchanga and Khepupara. This is consistent with the hilly landscape of Sangu-Matamuhuri River basin near Cox's Bazar because a clear response of sea level to river runoff is expected there. The SLP and winds are the main drivers for ESL height during many ESL events at Charchanga and Khepupara. The analysis revealed that the sensitivity of ESL height to precipitation was high during the monsoon season. At Cox's Bazar, the effect of precipitation tended to be strong during June and July. This is presumably because high frequency of strong daily precipitation during the monsoon season. In contrast, at Charchanga and Khepupara the ESL events with high effect of precipitation was occurred during post-monsoon season.

The MLR created for each event had led to very high predictability. This is partly because the degree of freedom for predictand is closer to the number of explanatory variables. Therefore, a new MLR was built using all ESL days including their prior six days at each station to validate the robustness of precipitation's effect on ESL revealed by the MLR created for each event. In total 245, 210, and 126 sample days were used for Cox's Bazar, Charchanga, and Khepupara, respectively. The result again showed that the daily sea level is better predicted with incorporation of precipitation based on the evaluation using adjusted R^2. The MLR represent the large contribution of precipitation term to the ESL height at Cox's Bazar than Charchanga and Khepupara, as it was confirmed by the MLR for each event.

The intensive monitoring of the site-dependent key meteorological factors and the incorporation of their effects to prediction model are essential to improve the prediction of ESL. These efforts will be mandatory to develop early warning system of the ESL event for reducing the risk of the hazards and for better coastal management. In the context of changing climate, climate models projected the increase in the intensity of heavy precipitation, high winds, and strong cyclone events in future due to anthropogenic greenhouse gas emissions. Therefore, future changes in ESL events should be discussed based on the examination of the future changes in key meteorological forcings, which will help reduce the vulnerability of the coastal community and ensure coastal sustainability.

ABBREVIATION

APHRODITE	Asian Precipitation-Highly-Resolved Observational Data Integration Towards Evaluation
BoB	Bay of Bengal
BMD	Bangladesh Meteorological Department
BOM	Bureau of Meteorology
BWDB	Bangladesh Water Development Board
CCC	Climate Change Cell
C3S	Copernicus Climate Change Service
DMI	Dipole Mode Index
ENSO	El Niño–Southern Oscillation
ERSST	Extended Reconstructed Sea Surface Temperature
ESL	Extreme Sea Level (determined from SLA data using 99th percentiles threshold)
GBM	Ganges, Brahmaputra and Meghna River system
IMD	Indian Meteorological Department
IOD	Indian Ocean Dipole
IPCC	Intergovernmental Panel on Climate Change
JRA55	The Japanese 55-year Reanalysis
MLR	Multivariate Linear Regression
MSL	Mean Sea Level
NOAA	National Oceanic and Atmospheric Administration
OISST	Optimum Interpolation Sea Surface Temperature
ONI	Oceanic Niño Index
POT	Peak Over Threshold
RMSE	Root Mean Square Error
SLA	Sea Level Anomaly (obtained from observed sea level using 91 days running mean)
SLP	Sea Level Pressure
SST	Sea Surface Temperature
U	Zonal wind
UHSLC	University of Hawaii Sea Level Center
V	Meridional wind
WP	With Precipitation (to represent the multivariate linear regression with precipitation term; Equation 2)
WOP	Without Precipitation (to represent the multivariate linear regression without precipitation term; Equation 3)

LIST OF FIGURES

LIST OF TABLES

CONTENTS

Chapter 1: Introduction

1.1. Extreme sea level and coastal communities

Global mean sea level (MSL) rise induced by climate change is an alarming issue with respect to the sustainability of the world's coastal communities (Wu et al., 2002; Wahl et al., 2017). The global MSL is projected to increase by 0.52 to 0.98 m by the end of this century (IPCC, 2013). The increased MSL acts as a primary factor for enhancing the extremeness in sea level through the combined interaction of meteorological and oceanic drivers (Antony et al., 2016). At present, the extreme sea levels (ESLs) are more frequent along the low-lying coastal regions and the changing climate forcings accelerate the ESLs (Mehra et al., 2010; Kirezci et al., 2020; Woodworth et al., 2004). The impact of ESL on the highly productive coastal regions is a global concern, because the coast supports the livelihoods for more than half of the world's population (Adel, 2002; Ward et al., 2018). The ESL is anticipated to increase the risk of floods and deteriorate freshwater environments, particularly in low-lying coastal regions (Mirza, 2003; Karim and Mimura, 2008; Wahl et al., 2017). Inundation of saline water into agricultural land, severe floods, damages in infrastructures with loss of lives and properties are the major impact areas of ESL hazards along the coast of the developing nations. The ESL hazards cause a loss in the agro-based economy of the developing nations that increases their food-insecurity and forces them to migrate (IPCC, 2013; Wahl et al., 2017). Therefore, the high frequency and intensity of ESL hazard is a major concern for the people of the socioeconomically vulnerable coast of the world. Likewise other coastal regions, the country Bangladesh is considered to be highly vulnerable to the adverse impacts of ESL (Sarwar, 2013; Lee, 2013; Brammer, 2014).

1.2. Location of Bangladesh and vulnerability to ESL

Bangladesh is located in South Asia. It is one of the world's largest active deltaic country with flat and low-lying (1–5 m) coast (Rasid and Pramanik, 1990). Bangladesh is the most downstream country of the Ganges-Brahmaputra-Meghna (GBM) river system (Fig. 1.1). The GBM is one of the world's largest sets of river basin and an outlet of huge freshwater to the global ocean (Nishat and Rahman, 2009). The upstream of the GBM river basin receives plenty of precipitation and causes higher runoff to the downstream (Hassan, 2019; Dandapat et al., 2020). As a most downstream country, the coastal area of Bangladesh receives huge upstream flow that enhances the ESLs along the coast (Rahman and Rahaman, 2018; Antony

et al., 2016). The extremeness in sea level causes inundation and severe flooding along the coast (Lee, 2013; Karim and Mimura, 2008). The coastal area of Bangladesh is flooded every year and it is more frequent and intense in recent years (Singh et al., 2000; Wahiduzzaman, 2021). The geographical location with low coastal elevation (1–5 m), makes the country more vulnerable to ESL (Rasid and Paramanik, 1990; Brammer, 2014) (Fig. 1.1). Inadequate infrastructure and high population with poor economy also enhance the vulnerability of this area (Mirza, 2003; Sarwar, 2013; Dastagir, 2015). As a main economic activity of the coast, the agriculture is highly vulnerable to the adverse impacts of ESL (Brammer, 2014). The ESL-induced hazards cause a loss in agricultural land and production every year and that increases the vulnerability to the agro-based economy of the coast (Ali, 1999). It was revealed that a 1 m increase in MSL by the late 21st century could affect approximately 1,000 km^2 of coastal area in Bangladesh (Unnikrishnan et al., 2011; Antony et al., 2016). The vulnerabilities in people's livelihoods and properties due to the impact of ESL hazards are increasing over the coast (Mirza, 2003; Karim and Mimura, 2008). Therefore, it has importance to assess the magnitude of ESL hazards to reduce the vulnerability of the Bangladesh coast.

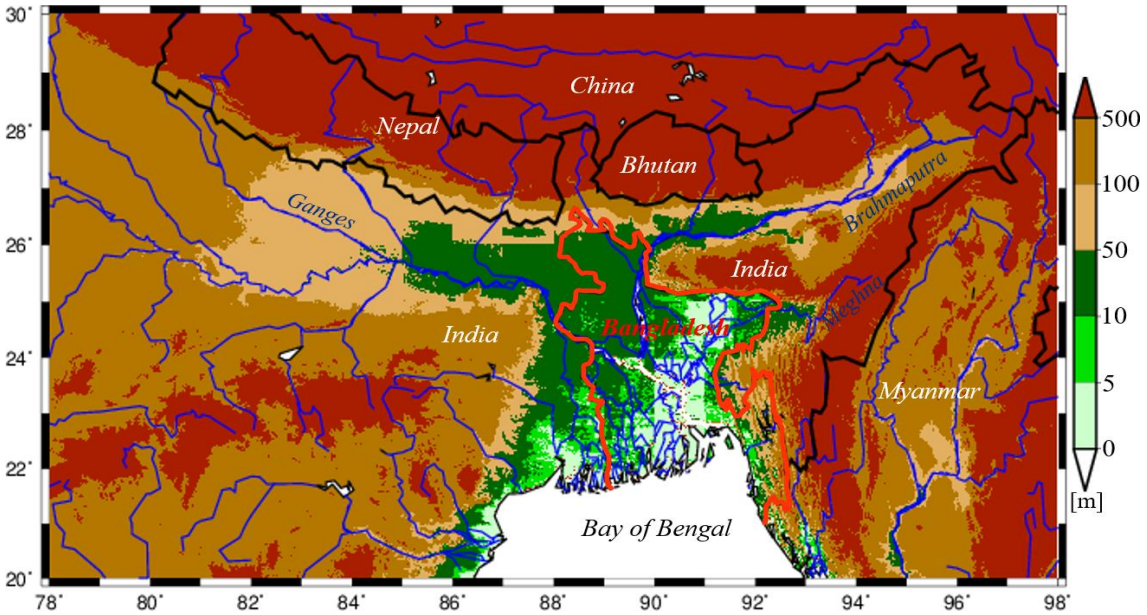

Figure 1.1 Topography and location of Bangladesh (red boundary) in South Asia.

1.3. Factors for ESL

ESL represents the high coastal water above MSL that are typically caused by meteorological and oceanic drivers (IPCC, 2019). In connection with the warming climate, the ocean thermal expansion caused by the excess heat absorption of the ocean water and melting

of the ice sheets acts as the main global drivers for sea level change (Fig. 1.2). The hydrological cycle, river runoff, and ocean currents are the dominant regional divers for sea level change. In association with global and regional divers the storm surges, waves and tides are the important atmospheric and oceanic factors, which modulate the ESL along the coast (IPCC, 2019).

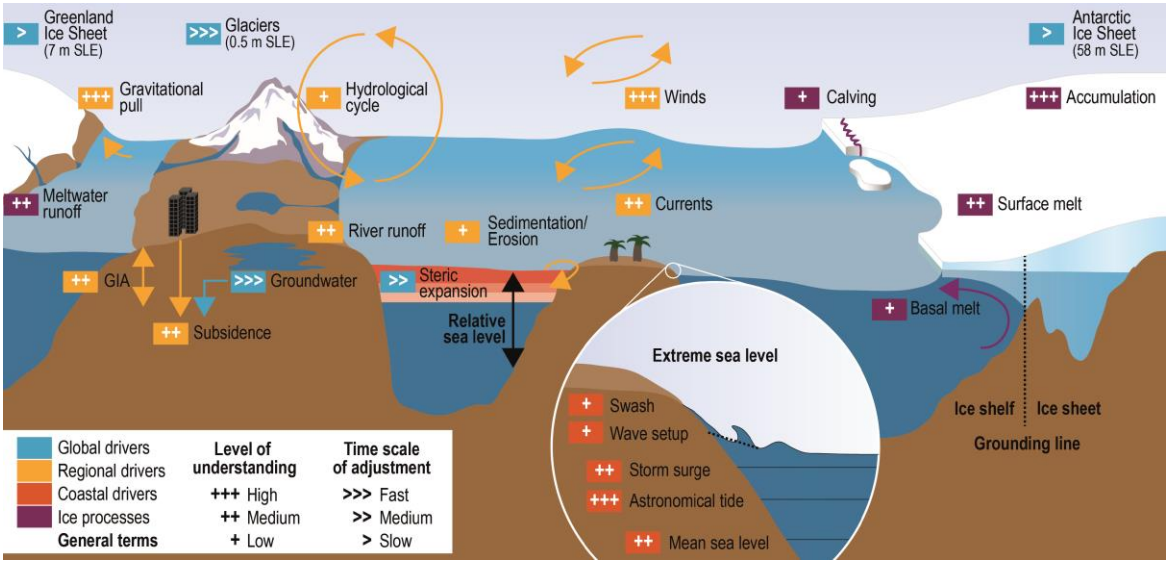

Figure 1.2 A schematic illustration of the climate and non-climate driven processes that can influence global, regional (green colors), relative and extreme sea level (ESL) events (red colors) along coasts. Major ice processes are shown in purple and general terms in black. SLE stands for Sea Level Equivalent and reflects the increase in GMSL if the mentioned ice mass is melted completely and added to the ocean (Source: IPCC, 2019).

It was noticed that the high precipitated-water discharge from continental upstream related to the hydrological cycle enhances the coastal sea level to be extreme (Svensson and Jones, 2002; Kuang et al., 2017; Piecuch et al., 2018; Ward et al., 2018). Likewise other coastal regions, it is hypothesized that in association with other factors, the abundant precipitated-water discharge from the GBM river basin may accelerate the ESL along the coast of Bangladesh. Therefore, regarding the target of this study a schematic of the considered contributing factors for ESL is illustrated in Figure 1.3. The interactions of the contributed factors from the atmosphere, ocean, and precipitated-water discharge as a part of the hydrological cycle to ESL will be discussed in the following sub-sections.

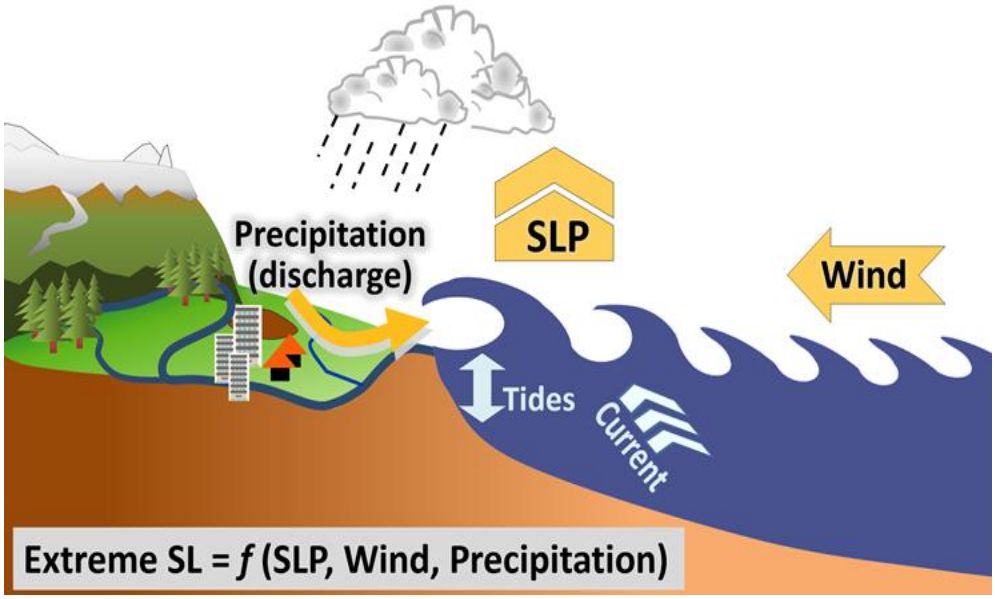

Figure 1.3 Contributing factors for ESL (Islam and Sato, 2021). The meteorological factors contributing to the ESL are indicated in orange. SLP represents sea level pressure.

1.3.1. Atmospheric and oceanic factors

The ESL along the coast mainly arises from the interactions of meteorological factors, such as low atmospheric pressure and associated high winds and oceanic factors, such as tides, surges, and oceanic waves (Moron and Ullmann, 2005; Han, 2005; Vialard e al., 2009; Iskandar and McPhaden, 2011; Lee, 2013; Tazkia et al., 2016; Karabil et al., 2017). It was revealed that during cyclones the low pressure induced storm surge is one of the main factors for ESL change along the coast (Karim and Mimura, 2008; Unnikrishnan et al., 2011; Lee, 2013). The frequent tropical cyclones over this region generate high winds and wind-induced surges enhance ESL along the coast (Dube et al., 2009; Iskandar and McPhaden, 2011; Suresh et al., 2013; Singh et al., 2021). The ESL along the coast is influenced by the winds-associated high waves and ocean currents (Vialard et al., 2009; Mehra et al., 2010; Anoop et al., 2015). The anomalous strong ocean current and its seasonal reversal modulates the high sea level variability along the coast (Dandapat et al., 2020). The ocean tidal component plays an important role for sea level variation along the coast and the large lunar tides modulate the rising sea level to be extreme (Tazkia et al., 2016). High sea surface temperature (SST) also enhances the sea level along the Bangladesh coast, because it leads to an increase in rainfall through the higher rate of evaporation (Salahudddin et al., 2006; Fan et al., 2016). The role of the above-mentioned ocean and atmospheric factors to ESL variability along the coast of Bangladesh have been studied intensively.

1.3.2. Precipitation as a factor related to the hydrological cycle

Likewise, the discussed role of the ocean and atmospheric factors to ESL in section 1.3.1, the effect of another factor related to the hydrological cycle is the discharge of precipitated-water from continental upstream which has been studied in many coastal areas across the world. The high precipitation enhances the surge-induced high sea levels along the eastern coast of Britain (Svensson and Jones, 2002). The high river discharge raises the sea level in the Yangtze River estuary near China (Kuang et al., 2017). The high sea level changes along the Atlantic coast of the United States are influenced by the upstream river discharge (Piecuch et al., 2018). The precipitation has an influence on the seasonal and spatial variability of the decadal sea levels along the Baltic coast (Karabil et al., 2017). Ward et al. (2018) studied that the high sea level is highly dependent on the river discharge for many deltas and estuaries over the global coast. It is known that as a downstream area of large GBM river basin, the coastal area of Bangladesh receives abundant precipitated-water that may enhance the high sea levels over this coast (Singh, 2001). However, the effect of precipitation on ESL variability remains unexplored along the coast of Bangladesh. The sensitivity experiment of the ocean model revealed that the river discharge affects the interannual variation of sea surface height near the river mouth (Dandapat et al., 2020). The earlier studies also mentioned that the high precipitated-water discharge modulates the intraseasonal variability of sea level along the coast of the northern Bay of Bengal (BoB) (Vialard et al., 2009; Cheng et al., 2013; Antony et al., 2016; Ghosh et al., 2018). The above-mentioned studies focus on the variability of sea level from monthly to seasonal time scale over different years. However, the influence of precipitation on ESLs at daily time scale along the coast of Bangladesh remains unknown.

1.4. Precipitation and ESL along the coast of Bangladesh

Bangladesh is one of the highest rainfall-prone areas in the world and it receives about one hundred percent of GBM river flow (Singh et al., 2000; Caesar et al., 2015). The monsoon is the peak precipitation season in Bangladesh area (Ahasan et al., 2010; Shahid, 2011). Figure 1.4 shows the monthly area average precipitation over the coast of Bangladesh during 1980–2006. It is revealed that the coastal area of Bangladesh receives high precipitation during peak monsoon (June to July). The previous study predicted that the rainfall over the Bangladesh area was increasing (Endo et al., 2015; Shahid, 2011) with the rate of +5.53 mm yr^{-1} during 1958–2007 (Shahid, 2009, 2010). Precipitation in and around the Bangladesh area has increased in recent decades (Shahid, 2010, 2011; Endo et al., 2015) and is projected to increase further by

the late 21st century (Turner and Annamalai, 2012; IPCC, 2013). The increase in future precipitation will enhance due to the increase in water vapor content. The intensity of monsoon circulation is, however, projected to be weak (Fan et al., 2012; Ma and Yu, 2014). As a low altitude basin area of the GBM rivers, the coastal area of Bangladesh receives abundant precipitated-water (Habib et al., 2019), that enhances the sea level near the coast and causes severe coastal flooding (Singh, 2002a, 2002b; Mirza, 2003; Shahid, 2011; Brammer, 2014; Dastagir, 2015). Hence, it is likely that the river discharge enhances the sea level in this region.

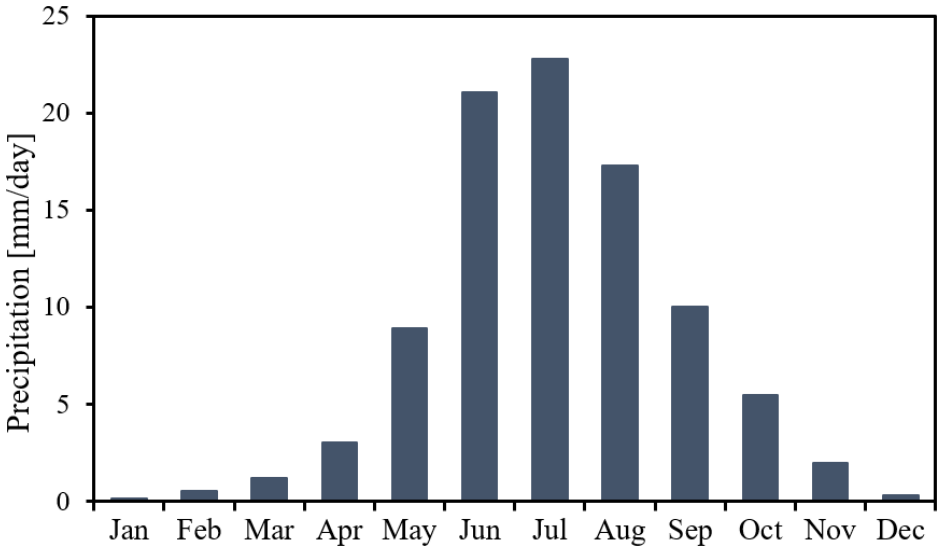

Figure 1.4 Monthly average precipitation (mm/day) during 1983–2006, averaged over Cox's Bazar area (21.00°–21.50° N and 92.00°–92.60° E). The daily precipitation data obtained from APHRODITE-V1003R1 was used (Yatagai et al., 2012).

It is hypothesized that the high sea level variation along the coast may follow the high precipitation over this region. Figure 1.5 illustrates the seasonal variation of the daily sea level and precipitation in 1999 observed at Cox's Bazar area (see Fig. 2.1 for location). There are marked sea level peaks during the monsoon season which appear to coincide with the precipitation peaks. Figure 1.5 strongly suggests that precipitation enhances the sea level at daily time scale and its impact seems to be large for ESL events. Meanwhile, Figure 1.5 also suggests the role of other forcing factors. The synchronized variation in daily sea level and precipitation shown in Figure 1.5 is a common character observed in many other years (Fig. 1.6). Strong precipitation events during the monsoon season are often caused by synoptic atmospheric disturbances (Hatsuzuka et al., 2014), which have the potential to increase sea level, even though precipitation-induced river discharge is absent, because the disturbances usually accompany changes in air pressure and wind speed/direction. The earlier studies

mentioned that the monsoonal precipitation also varies interannually in relation to the effect of the large-scale ocean and atmosphere dynamics (Salahuddin et al., 2006; Fan et al., 2016; Ahmed et al., 2017). The El Niño–Southern Oscillation (ENSO) and Indian Ocean Dipole (IOD) are the dominant climate modes to modulate the interannual variability of precipitation in this region (Singh et al., 2001; Salahuddin et al., 2006; Ahmed et al., 2017; Wahiduzzaman, 2021). The previous studies also mentioned the effect of local BoB SST forcings on the interannual variations of precipitation over Bangladesh area (Rahman et al., 2013; Roxy et al., 2013). Considering this specific geographical background and high precipitation over Bangladesh area, it is important to verify the contribution of precipitation variability during ESL events.

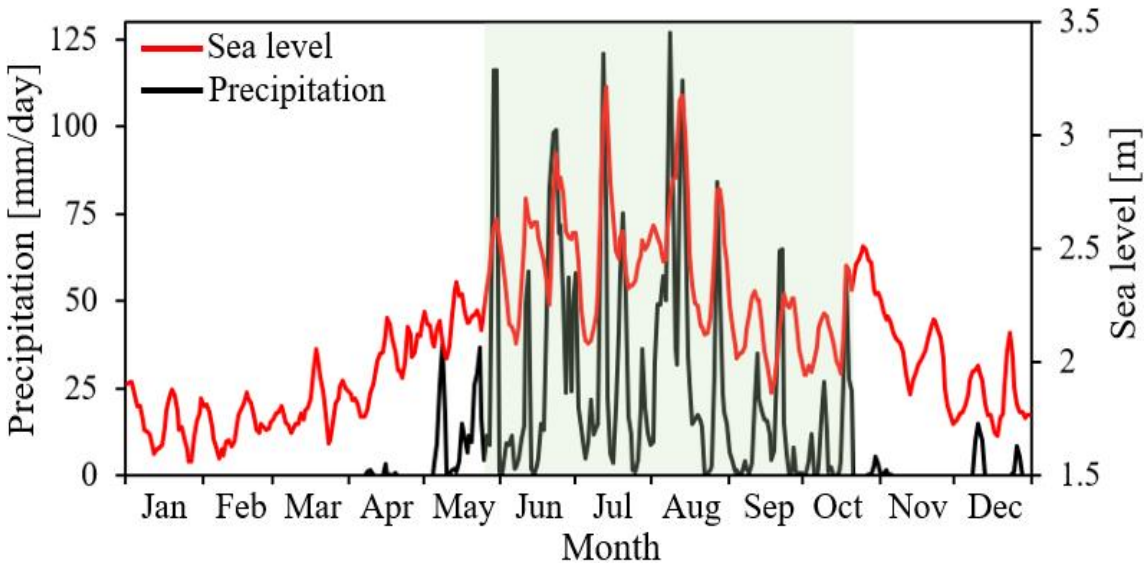

Figure 1.5 The time series of daily observed sea level (red) at Cox's Bazar station and daily area averaged precipitation (black) near Cox's Bazar area (22°–22.5°N and 92°–92.5°E) in 1999. The shaded period represents the period for monsoon season (late May to early October).

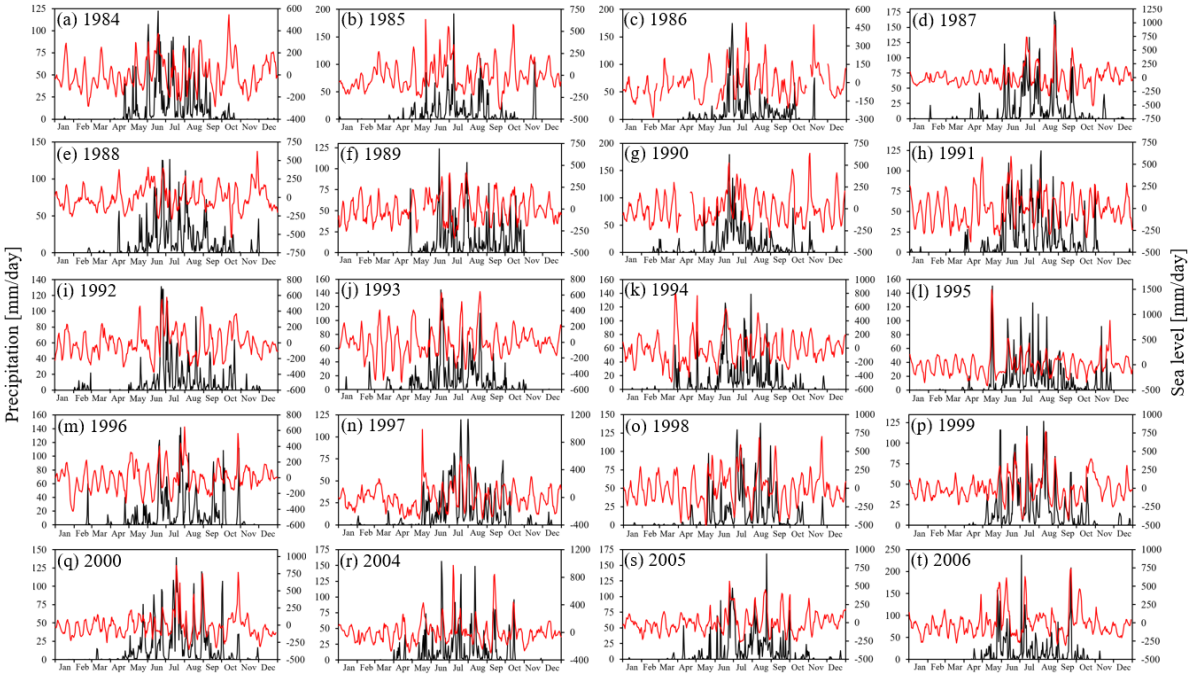

Figure 1.6 The time series of daily observed sea level (red) at Cox's Bazar station and daily area averaged precipitation (black) near Cox's Bazar area (22°–22.5°N and 92°–92.5°E) during 1984–2006. The figure for 1999 (p) is identical to Figure 1.5 and the years of 2001–2003 were excluded due to data unavailability.

1.5. The objective of the study

The coastal area of Bangladesh is highly vulnerable to ESL hazards and in the context of changing climate, the vulnerability of the coast is increasing severely. The variability of ESL is a short-term phenomenon, which is influenced by the ocean and atmospheric disturbances. To address the long-term variability of sea level, the role of different ocean and atmospheric factors along the coast of Bangladesh was studied intensively (Singh et al., 2001; Vialard et al., 2009; Iskandar and McPhaden, 2011; Lee, 2013; Tazkia et al., 2016). It is expected that the high precipitated-water discharge from upstream may enhance the ESL along the coast of Bangladesh. The earlier studies mentioned the effect of river discharge, different ocean and atmospheric factors to the intraseasonal and interannual sea level variations over BoB (Vialard et al., 2009; Cheng et al., 2013; Antony et al., 2016; Ghosh et al., 2018; Dandapat et al., 2020). However, the influence of precipitation on ESLs at daily time scale along the coast of Bangladesh remains unknown. Therefore, the main objective of this study is to investigate the effect of precipitation on ESLs at a daily time scale. The ESL was determined using a threshold value, and the daily variation of SL within ESL event was studied for seven days period. The

effect of precipitation on the variability of ESL will be also examined for all daily samples derived from seven days in prior to the ESLs.

The investigation of precipitation effect on ESL events at daily time scale represents the novelty of this study. It is hypothesized that the effect of precipitation has a significant influence on the variability of ESL along the coast of Bangladesh. The expected outcomes will contribute to improve the forecast of ESL events and to reduce the hazards along the vulnerable coastal regions. The predictions of ESL will be helpful for coastal beneficiaries and policy makers for planned coastal management as well as to ensure the sustainability of the vulnerable coast.

Chapter 2: Data and methodology

2.1. Selection of the study sites for ESL analysis

The variability of ESL was investigated at three selected study sites along the coast of Bangladesh and their names are Cox's Bazar, Charchanga, and Khepupara. These sites are located in different geographical settings (Fig. 2.1). The elevation of Cox's Bazar, Charchanga, and Khepupara area is 4.5 m, 4.0 m, and 3.5 m above MSL, respectively (CCC, 2016). Based on the tide gauge record during 1977–1998, it was mentioned that the increasing coastal water level at Cox's Bazar, Charchanga, and Khepupara is 7.8 mm/yr, 6.0 mm/yr, and 4.0 mm/yr, respectively (Mondal, 2001; Sarwar, 2013; Antony et al., 2016). Cox's Bazar is located in the eastern coastal area (21.45°N and 91.95°E) and characterized by a hilly landscape. The location of Cox's Bazar makes it more vulnerable to cyclones and surge-induced coastal floods (Unnikrishnan et al., 2011; Dastagir, 2015). Cox's Bazar is popular for tourism, having the world's largest sea beach (Brammer, 2014). Charchanga is located in the lower estuary of the GBM river system (22.22°N and 91.06°E) and famous for river port and fishing. Khepupara is located in the low-lying deltaic plain of the western coast (21.85°N and 90.08°E) and has potential for agriculture. The selection of three study sites from three different topographic areas will be useful to investigate the spatial variations of ESL along the coast of Bangladesh.

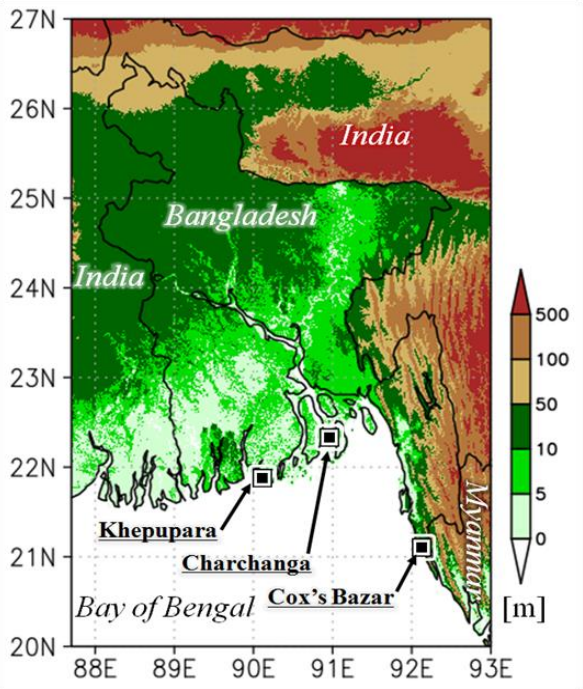

Figure 2.1 Selected study sites along the coast of Bangladesh.

2.2. Data and variables

The studied periods are 1983–2006 for Cox's Bazar, 1980–2000 for Charchanga, and 1987–2000 for Khepupara. The difference in study period is due to the availability of the in-situ sea level data. The daily station-observed sea level data, provided by the University of Hawaii Sea Level Center (UHSLC, Caldwell et al., 2015) were used. The satellite-observed daily gridded (0.25° × 0.25°) anomalous sea level product of the Copernicus Climate Change Service (C3S) was adopted to investigate the spatial pattern of coastal sea levels during 1993–2006 (Taburet et al., 2019). Daily precipitation data were obtained from APHRODITE-V1003R1 (Yatagai et al., 2012), which covers land area at a spatial resolution of 0.25° × 0.25°. The daily sea level pressure (SLP) and wind data were obtained from the Japanese 55-year Reanalysis (JRA55, Kobayashi et al., 2015), whose horizontal grid size is 1.25° × 1.25°. Daily discharge data of the Bangladesh Water Development Board (BWDB, 2005) for Bahadurabad point of the Brahmaputra River and for Hardinge Bridge point of the Ganges River were used for the period of 1990–2000. The Indian Meteorological Department (IMD, 2008) best-track data was used to identify the location of cyclone over the targeted BoB area during ESLs for the period of 1993–2006.

The Oceanic Niño Index (ONI) and the Dipole Mode Index (DMI) obtained from the National Weather Service and Physical Sciences Laboratory of NOAA, respectively were used to explore the role of large-scale atmosphere-ocean coupled modes. The ONI was determined from the three-month running mean of ERSST.v5 (Huang et al., 2017) SST anomalies over Niño 3.4 region (5°S–5°N and 120°W–170°W). The DMI is the difference in anomalous SST between the western (10°S–10°N and 50°E–70°E) and southeastern (10°S–0°N and 90°E–110°E) equatorial Indian Ocean (Rayner et al., 2003). Here, the anomaly means the deviation of daily SST from a three-month running mean of daily SST. Aside from these two modes, local SST in the BoB was also analyzed to investigate the relationship between the local SST and interannual variation of high sea level and precipitation in the studied region. For local SST in the BoB, the Optimum Interpolation Sea Surface Temperature (OISST, Reynolds et al., 2007) data from NOAA was used. The monthly mean SST anomaly was adopted to represent the warm and cold BoB (17°N–23°N and 83°W–95°W) SST, which was determined from daily climatology during 1983–2006.

For the statistical analysis, four explanatory variables of precipitation, SLP, zonal wind (U), and meridional wind (V) were used and their influences on ESL variations were evaluated.

2.3. Methods

2.3.1. Determination of sea level anomaly (SLA)

The sea level near the Bangladesh coast exhibits prominent seasonal variation (Cheng et al., 2013) corresponding to the monsoon (Khandaker, 1997; Anoop et al., 2015) and regular tidal cycles (Tazkia et al., 2016). The sea level anomaly (hereafter referred to as SLA) was used to remove the seasonal component of the sea level variation. An example of the seasonal variation of the daily sea level at Cox's Bazar station for a one-year period of 1998 is shown in Figure 2.2. The figure shows a seasonal variation in sea level corresponding to pre-monsoon, monsoon, and post-monsoon seasons. The variation in equatorial wind-driven waves (Han, 2005; Vialard et al., 2009), changes in SST by atmospheric factors (Han, 2005), variation in tides with lunar phases (Tazkia et al., 2016), and storm-driven oceanic surges (Iskandar et al., 2011) are the important factors for seasonal variation of sea level along the coast. To remove the seasonality in observed sea level, daily sea level anomalies relative to the 91 days running mean were used. The removal of the seasonal effects of atmospheric and oceanic forcings from regular sea levels will be necessary to investigate the role of other factors (e.g., precipitation) to the variation of anomalous sea level. To calculate the anomaly, 91 days (seasonal) running mean time series was constructed from the daily observed sea level data. The seasonal running mean with 91 days was determined for each 91-sea level event from the beginning of the study period. Then, the anomaly was calculated from the differences between the daily sea levels and its 91 days (seasonal) running mean (Equation 1).

$$SL' = SL_{obs} - \overline{SL_{obs}} \qquad (1)$$

where, SL´ represents SLA, SL_{obs} for daily observation of sea level, and $\overline{SL_{obs}}$ for 91 days running mean of the observation data. An example of the calculation process of the SLA at Cox's Bazar station for the one-year period of 1998 is shown in Figure 2.3. It is noted that there is a regular tidal cycle in SLA data. As the daily variation of ESL generally arises with regular tides (Mondal, 2001; Cheng et al., 2013; Sarwar, 2013; Tazkia et al., 2016), the effects of tide were not removed from observed sea level.

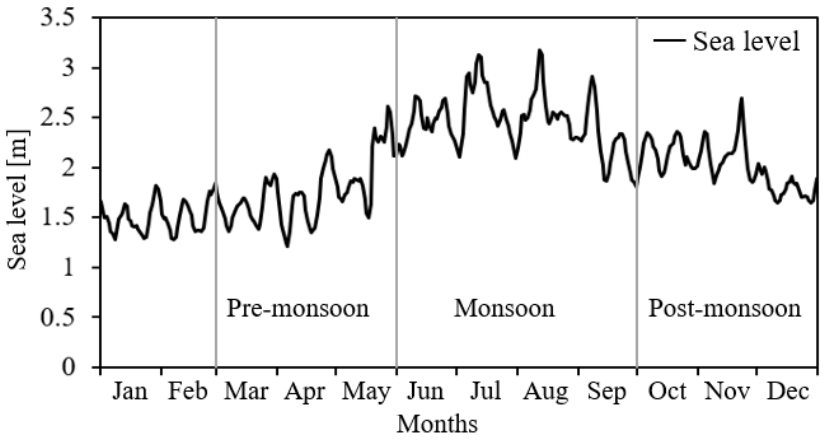

Figure 2.2 Time series for the seasonal variation of sea levels in 1998 at Cox's Bazar Station. The sea level is varied by the seasonal effects of the pre-monsoon (March–May), monsoon (June–September) and post-monsoon (October–December).

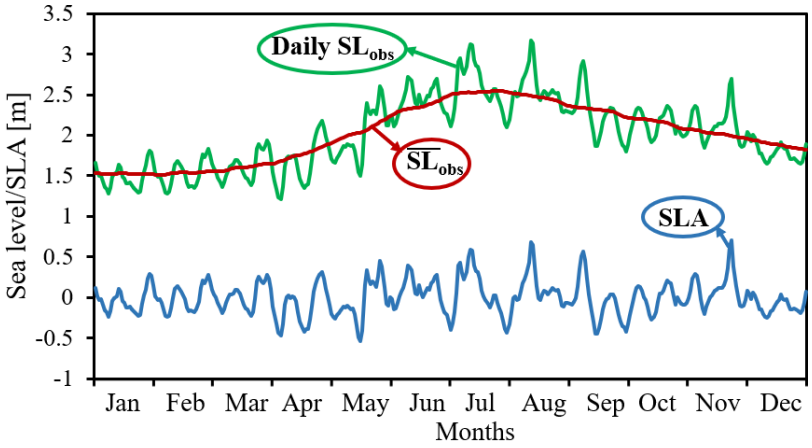

Figure 2.3 Process for the estimation of SLA. Sea level in 1998 at Cox's Bazar. The green line represents the daily sea level. Red line represents its 91-day running mean and the blue line represents SLA.

2.3.2. Identification of the ESL events

As the ESL is the key term of this study, the steps for identification of the ESL events will be explained in this section. The ESL events were determined by applying the threshold value of the 99th percentiles in the daily SLA time series, following the method of previous studies (Woodworth and Blackman, 2004; Kirezci et al., 2020). The 99th percentile high SLA values were 0.562 m, 0.486 m, and 0.427 m (indicated by red lines in Fig. 2.4). The determined values were used as a threshold for identification of ESL events, and the number of identified ESL events were 69, 62, and 37, respectively, for Cox's Bazar, Charchanga, and Khepupara station. However, it was found that there is consecutiveness in those identified ESL events.

Therefore, to select the independent ESL events, a peak over threshold (POT) approach was adopted for the identification of the events (Ward et al., 2018; Kirezci et al., 2020). The peaks over the threshold were identified, and then, the consecutive days before and after the peak sea level was excluded to select an independent ESL event. Applying the POT approach, the number of selected independent ESL events were 35, 30, and 18, respectively, for Cox's Bazar, Charchanga, and Khepupara station. It was confirmed that most of the selected ESL events occurred during summer monsoon, and their number are 28, 27, and, 15 for Cox's Bazar, Charchanga, and Khepupara, respectively. The number of ESL events are many during June–July for Cox's Bazar, August–September for Charchanga, and October–November for Khepupara.

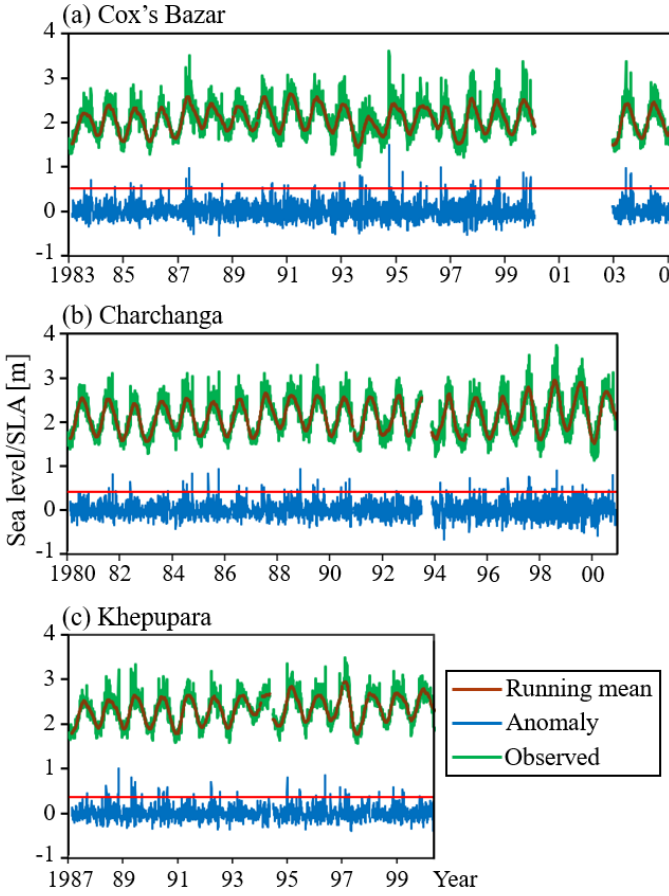

Figure 2.4 (a) Time series of daily sea levels at Cox's Bazar during 1983–2006. The green line represents the observed daily sea level. The dark orange line shows the 91-day running mean and the blue line shows SLA. The discontinuity in the time series denotes the missing data. (b) Same as (a) but for Charchanga during 1980–2000. (c) Same as (a) but for Khepupara during 1987–2000. The red lines in a, b, and c represent the 99th percentile values used for the selection of ESL events, which were 0.562 m, 0.486 m, and 0.427 m for Cox's Bazar (a), Charchanga (b), and Khepupara (c), respectively.

2.3.3. Estimation of sea level using multivariate linear regression (MLR) analysis

In Section 2.3.1, it was mentioned that the observed sea level is influenced by the effects of different meteorological variables. It is important to investigate the contribution of the meteorological variables to the variability of sea levels. Therefore, the estimated sea level was calculated here using the contribution of the four explanatory variables of precipitation, SLP, zonal and meridional wind. The SLP and wind are selected as dominant factors for the sea level change as discussed earlier (Singh et al., 2001; Suresh et al., 2013; Iskandar and McPhaden, 2011; Anoop et al., 2015; Tazkia et al., 2016). However, the present research is a pioneer study to investigate the influence of precipitation on ESL variability combined with other variables. A multivariate linear regression (MLR) analysis was used to investigate the effect of precipitation on the daily variability of sea level during the selected ESL events. The MLR has been widely used to discuss the mechanisms of sea level variations at various timescales (Hünicke and Zorita, 2006; Zhang and Church, 2012; Karabil et al., 2017). Using MLR statistics, the targeted variable (observed daily SLA) could be described by the linear combination of the explanatory variables. Previous studies analyzed the linear relationship between sea level and explanatory variables of SLP, precipitation, air temperature, winds, and climate variability indices (Mehra et al., 2010; Zhang and Church, 2012; Karabil et al., 2017; Kumar et al., 2018). This study adopted two approaches of MLR for estimation of ESL for the selected events. The MLR model was created for each ESL event and for all events at each station to study how contributions of the meteorological factors depend on the events and stations. The MLR approach for each event is referred to as "MLR for each event" and for all events at each station is referred to as "MLR for all events. The MLR equations were adopted using four explanatory variables. The details of these two approaches are discussed below.

a. *MLR for each event*

The first method described here is MLR created for each event and for each station. The results are presented in Chapter 3. The prediction equation for the observed SLA is described as

$$SL'(t) = a_1 \times SLP(t) + b_1 \times U(t) + c_1 \times V(t) + d_1 \times Pre(t) + e_1 \quad (2)$$

Herein, t represents the duration of the event, which ranged from −6 to 0, corresponding to six days before the targeted ESL ($t = -6$) to the day of the ESL event ($t = 0$). SL´ represents the predicted SLA. Pre represents the accumulated precipitation over the preceding five days for each t. The explanatory variables were standardized and the MLR analysis was performed for

each ESL event. The regression coefficients are represented as a_1, b_1, c_1, and d_1, while e_1 represents the intercept value. The coefficients were determined for each site and for each selected event.

To elucidate the impact of precipitation on the SLA, the MLR without precipitation was also created, which is described as

$$SL'(t) = a_2 \times SLP(t) + b_2 \times U(t) + c_2 \times V(t) + e_2 \quad (3)$$

Where a_2, b_2, and c_2, are regression coefficients and e_2 represents the intercept value. The obtained coefficients are presented and discussed in section 5.2. The predicted sea level anomalies obtained from MLR Equations (2) and (3) were evaluated using the same seven-day time series of the observed daily SLA as reference data. The goodness of fit of each prediction was evaluated by the coefficient of determination (R^2). Since the degree of freedom for predictand (i.e., seven days) is closer to the number of explanatory variables (three or four), that will lead to very high R^2. Under this condition, the evaluation of precipitation effect using the comparison of R^2 for MLRs in equation 2 and 3 may be distorted by the difference in the number of explanatory variables rather than the physical impact of the precipitation term. To avoid such an effect, this study used *adjusted* R^2. The *adjusted* R^2 values were expected to be different between two predictions and an *adjusted* R^2 close to one denotes that the MLR is very skillful. If the prediction using Equation (2) outperforms the prediction using Equation (3), it means that adding precipitation data could improve the prediction of SLA during the ESL event. Here, the MLR performance was evaluated in terms of *adjusted* R^2 to argue the biasedness of the MLR output related to the effect of adding variables (Draper and Smith, 1998). The *adjusted* R^2 was calculated by

$$Adjusted\ R^2 = 1 - (1 - R^2)\frac{n - 1}{n - p - 1}$$

Herein, p is the number of explanatory variables and n is the sample size. It was assumed $p = 4$ (i.e., SLP, zonal and meridional winds, and precipitation) for the prediction of sea level with precipitation, whereas $p = 3$ was assumed for the prediction without precipitation. The sample size was set as $n = 7$, considering the seven-day variations of meteorological variables (Section 2.3.3.1).

In this study, the difference in *adjusted* R^2 between the two predictions was regarded as the significance of the effect of precipitation. If *adjusted* R^2 for the prediction with precipitation

(i.e., Equation (2); hereafter referred to as WP) is greater than that without precipitation (i.e., Equation (3); hereafter referred to as WOP), it means that the precipitation is crucial for the targeted extreme event. Thus, a larger difference in *adjusted* R^2 between predictions WP and WOP denotes a stronger influence of precipitation on sea level variations. The *adjusted* R^2 value was evaluated for all selected events to determine the spatial and temporal characteristics of the effect of precipitation on the predictions of ESL. One may anticipate that the contribution of precipitation to the prediction of ESL might be influenced by the multicollinearity of the variables. To argue this point, a correlation analysis was performed among the variables for each ESL event of the three study stations (Section 2.3.3.4).

b. *MLR for all events*

In the previous MLR method (i.e., MLR for each event), the MLR was created for each event. That method falls short because the number of explanatory variables is too close to the degree of freedom of the predictand. To overcome this deficit, the MLR here was created using all ESL events at each station. In other words, "MLR for each event" introduced above used only seven samples as input for three (or four) explanatory variables. The sample size was obviously too small, and this will lead to too high predictability. Therefore, it is needed to discuss carefully the impact of adding precipitation effect by adjusted R^2. The adopted MLR was performed using all daily samples derived from seven days in prior to the ESLs. Therefore, the sample size is 7 × event number for each station. The explanatory variables are identical with those addressed in "MLR for each event" (Equation 2), but the number of samples is increased. The details of the adopted MLR equations and results are presented in Chapter 4.

2.3.3.1. Period of ESL events

In this study, the ESL as a dependent variable and its controlling factors were studied for a seven-day period. The data period for seven days (including the day of ESL and six days before the ESL day) was determined by considering the fact that the duration of the ESL events are generally around seven days (Fig. 2.5). Figure 2.5 displays the time series of observed SLA averaged for all selected ESL events at three study stations. For all three of the stations, the mean SLA is highest on the day of the extreme (t = 0), with a gradual increase from the prior days. During extremes, the evolution of SLA with a gradual increase from prior days to the day of extreme may represent the period ($t = -6$ to 0) of an ESL event for seven days. Although the period for the decline of ESL from its peak to the normal sea level was not considered here, it is known to be influenced by the coastal waves (Han and Webster, 2002; Suresh et al., 2013).

The seven days period of ESL coincides with the high tidal phase of a fifteen-day tide cycle, which possibly influence the evolution of the ESL events. However, during the selected ESL events the coastal water level was generally higher than the regular tidal height. In addition, it was observed that many ESL events occurred during the low tidal phase. These facts denote that there is strong influence of the atmospheric forcing on ESL. It was mentioned that the ESL is enhanced during cyclones and surges (Zhang and Church, 2012; Lee, 2013). Therefore, the determination of the ESL period for seven days also reflects the life span of storm-induced surges and cyclones (Unnikrishnan et al., 2011; Zhang and Church, 2012). Considering the period of ESL, the daily SLP and wind data for seven days in prior to the ESL day were used.

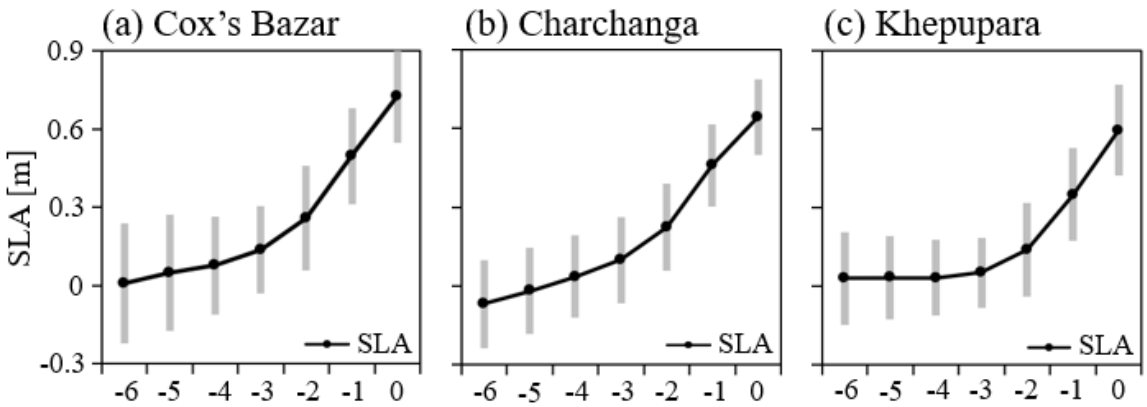

Figure 2.5 The average time series (line) of SLA for all ESL events at Cox's Bazar (a), Charchanga (b) and Khepupara (c). The error bars represent the standard deviation of the cases. The x-axes represent the day corresponding to the six days before ($t = -6$) to the ESL day ($t = 0$).

2.3.3.2. Area setting for the explanatory variables

As addressed in Section 1.2, Bangladesh is located in downstream of the GMB river basin and it receives almost a hundred percent of the precipitated-water discharge from the upstream of the basin. Therefore, it is necessary to delineate the proper basin area for accurate estimation of the precipitation amount that causes discharge for the selected stations of Charchanga and Khepupara (Fig. 2.1). At the determination of this area, a pre-analysis was conducted, aiming to identify the source area from where the precipitated-water could influence the coastal water levels. It was found that the available daily discharge at the downstream area is highly correlated with the daily precipitation over the upper GBM basin area for the period of 1990–2000 (Fig. 2.6). The discharge station is located near the upper basin area and it is assumed that the discharge at this station is influenced by the daily precipitation from the upper

basin. Therefore, the daily precipitation was used instead of accumulated precipitation. The daily discharge at Bahadurabad point shows high correlation with the daily precipitation of the upper basin of the Brahmaputra River (Fig. 2.6a). In comparison with the Brahmaputra river, the daily discharge of the Ganges River at Hardinge Bridge point shows relatively low correlation with the daily precipitation of its upper basin area (Fig. 2.6b). This might reflect the effects of humans' control of the Ganges River water in the upper river basin (Adel, 2002; Rahman and Rahaman, 2018; Hassan, 2019), which results in a low correlation between the precipitation in upstream and discharge at the downstream. The basin area that causes discharge to the downstream through GBM river system is not properly represented by the correlation between precipitation and discharge. The insignificant correlation was noticed for almost all over the basin area. The low correlation between precipitation and discharge may be influenced by the days without precipitation during the study period. The correlation between SLA and precipitation over the targeted area for some ESL days which occurred in the post-monsoon season also represents the insignificant or negative correlation at Charchanga and Khepupara stations (Fig. 2.12b,c). It is assumed that the discharge in the downstream through GBM river is mainly influenced by the precipitated-water from the eastern Himalaya and Meghalaya area rather than the precipitation from the western Himalaya and Ganges area over India. Therefore, the eastern Himalaya and Meghalaya area with adjacent lower catchment of the GBM river over Bangladesh, indicated by light pink in Figure 2.7, was adopted as the area for areal precipitation.

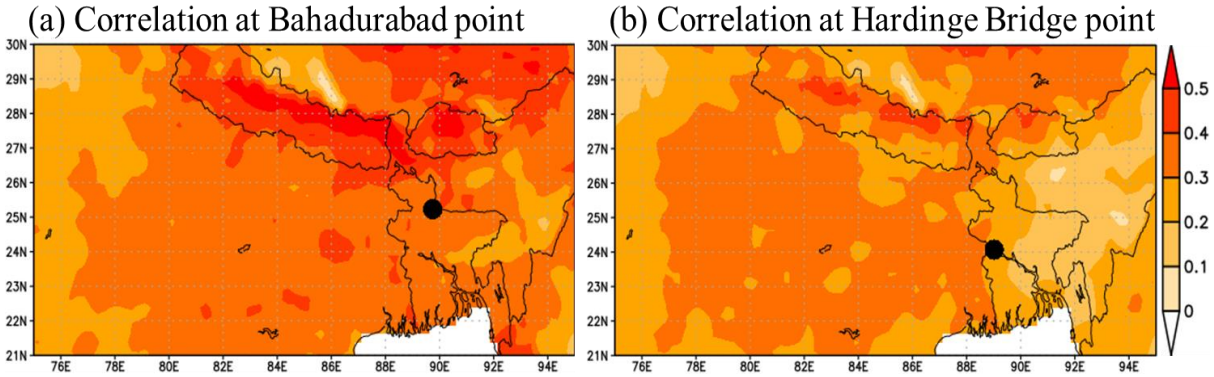

Figure 2.6 Correlation between the daily precipitation and discharge for the Brahmaputra River at Bahadurabad point (a) and for the Ganges River at Hardinge Bridge point (b).

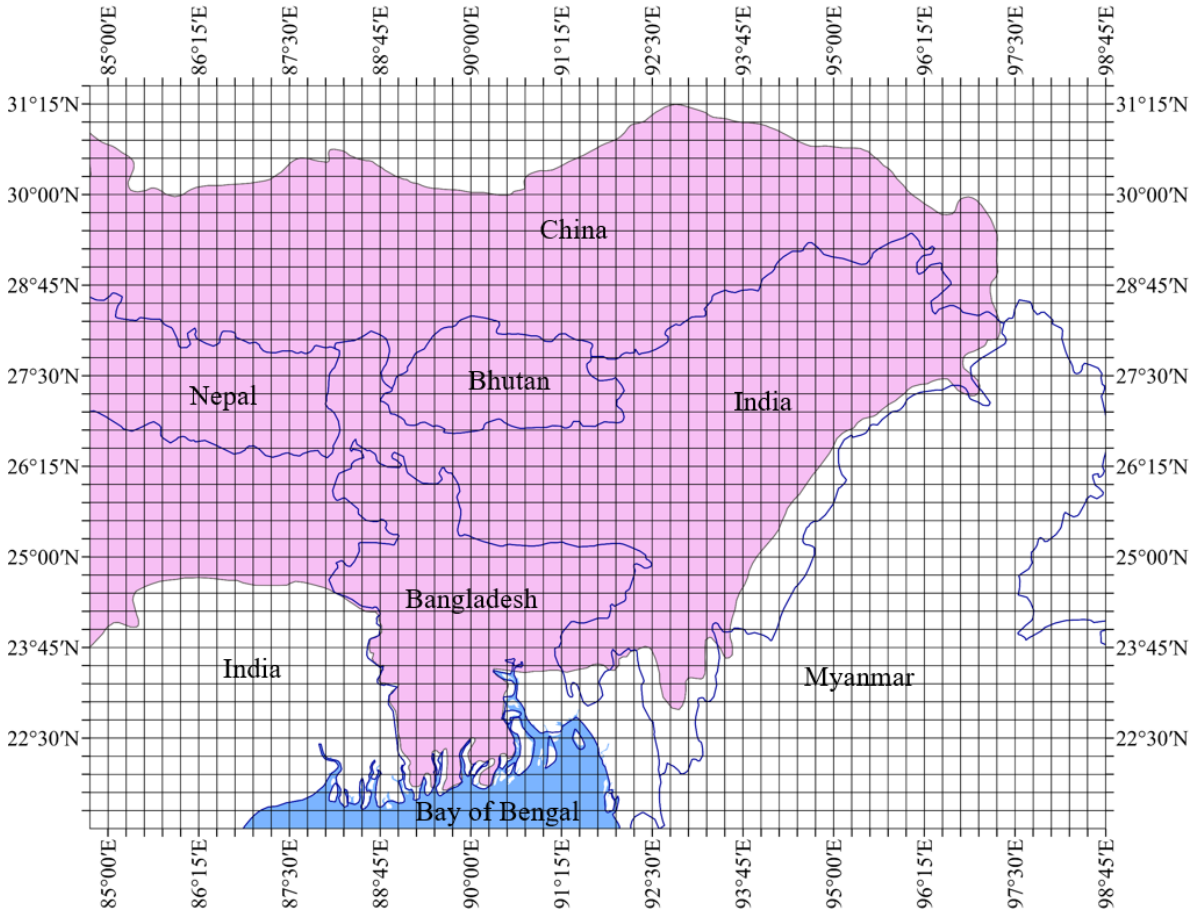

Figure 2.7 Selected area for precipitation over GBM basin. The shaded area (light pink) represents the grids, whose precipitation was used for estimation of sea level at Charchanga and Khepupara.

The Cox's Bazar station in the eastern coast is a hydrologic catchment area of the Sangu, Matamuhuri, and Karnafuli River systems. This basin area is relatively small and explicitly isolated by the Arakan Mountain range (Xie et al., 2006; Adnan et al., 2019). Following the topographic boundary of this catchment, a proper basin area was identified for Cox's Bazar station (Fig. 2.8), that is also consistent with earlier studies (Smith et al., 2001; Xie et al., 2006; Adnan et al., 2019).

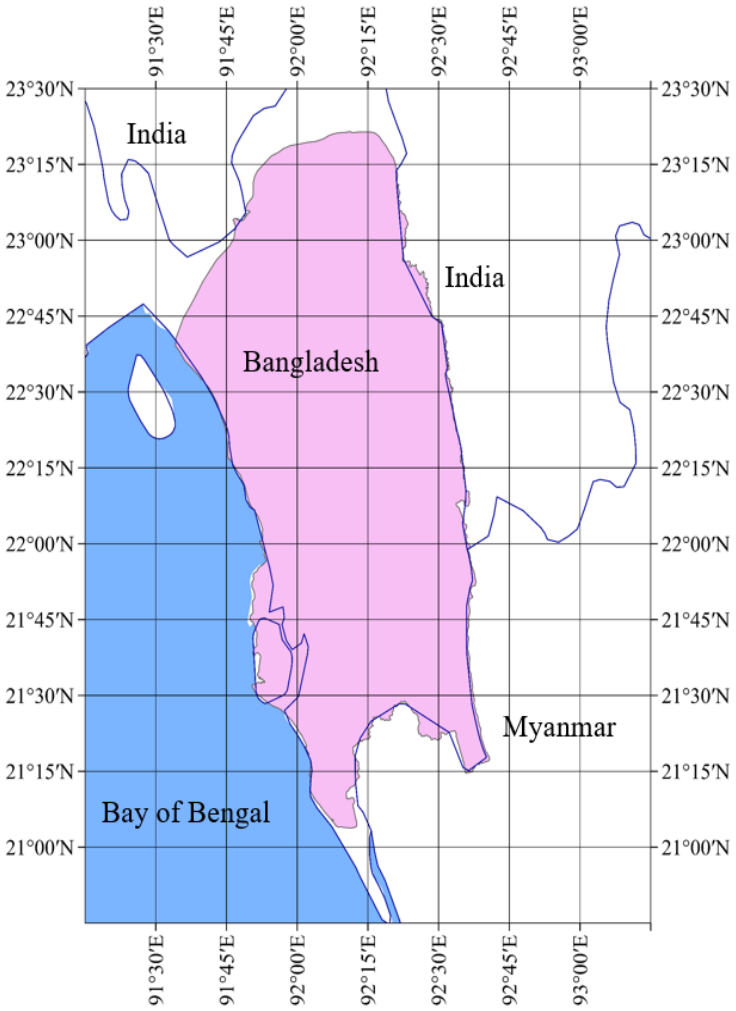

Figure 2.8 Selected basin area (light pink) for estimation of precipitation at Cox's Bazar station.

For SLP and winds, the daily area-averaged values over the northern BoB area (16°–22° N and 85°–95° E) were commonly used for all three sites. The BoB area was considered because the high intensity of cyclone-generated winds and surges over this area enhances the ESL along the coast (Unnikrishnan et al., 2011; Iskandar and McPhaden, 2011; Lee, 2013). In this study, the oceanic precipitation over BoB was not considered in the MLR. This is because the precipitation over the large area of sea surface rapidly merges with the sea water and its direct contribution to sea level change is negligible (Perigaud and McCreary, 2003; Prakash et al., 2012). On the other hand, the effect of terrestrial precipitation is expected to have influence on ESL because the river water enters the shallow coastal sea as plumes and these plumes of freshwater floats over the salty sea water. The rotation of the Earth pushes the flow of water plumes up against the shoreline and raises the sea level along the coast (Piecuch et al., 2018).

2.3.3.3. Duration of accumulated precipitation

For precipitation, the accumulation of preceding five days was used to account for the delayed effect of precipitated-water runoff from the upstream to downstream. To investigate the effect of different lengths of accumulated precipitation on ESL, a correlation analysis between the SLA and different lengths of accumulation was performed for two different basin areas of Cox's Bazar and Charchanga (Fig. 2.9). As the basin area for Charchanga and Khepupara are same, the correlation analysis was not performed for Khepupara. The correlation analysis was conducted for seven-day period of each ESL event and the accumulated precipitation for three, five, and seven days was considered. The result shows similar significant correlations ($r > 0.67$ or $r < -0.67$) between the different lengths of accumulated precipitation and SLA for more than half of the selected ESL events at two stations. The variations in correlation among the different lengths of accumulation are similar for both stations. Hence, the accumulation over five days was arbitrarily adopted to account the effect of precipitation.

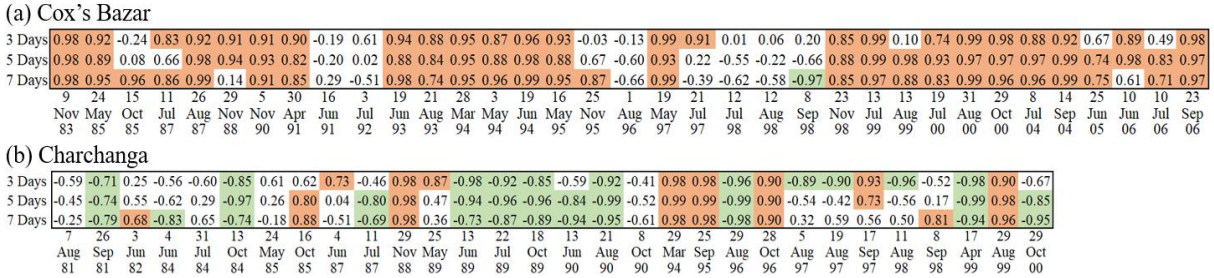

Figure 2.9 Correlation between the seven-day time series of SLA and accumulated precipitation for each selected ESL event at Cox's Bazar (a) and Charchanga (b) station. The analysis was conducted for different lengths of precipitation accumulation (3, 5, and 7 days). The statistically significant positive (negative) correlations were highlighted with orange (green) color shading.

In addition, to evaluate the delay in precipitated-water to reach at river mouth, a pre-analysis using MLRs for WP (Equation 2) and WOP (Equation 3) was conducted for three different accumulation periods of precipitation over three, five, and seven days at Charchanga station (Fig. 2.10). The Charchanga station was selected considering the expected delay in precipitated-water runoff from the large upper basin area. The result shows that the predicted ESLs for three, five, and seven days setting of accumulated precipitation were similar. This is because the precipitation time series are similar regardless of the accumulation period (Fig. 2.11). The previous study mentioned that the river discharge in the downstream area increases

with one to ten days delay after the precipitation peak over middle Himalaya and Meghalaya hilly areas (Webster et al., 2010). In this study, the lower Himalaya and Meghalaya hilly areas were selected as basin area where approximately five days delay is expected (Webster et al., 2010). Considering these results this study subjectively determined the period of precipitation accumulation as five days. The validity of this assumption needs to be investigated in future using reliable river discharge data.

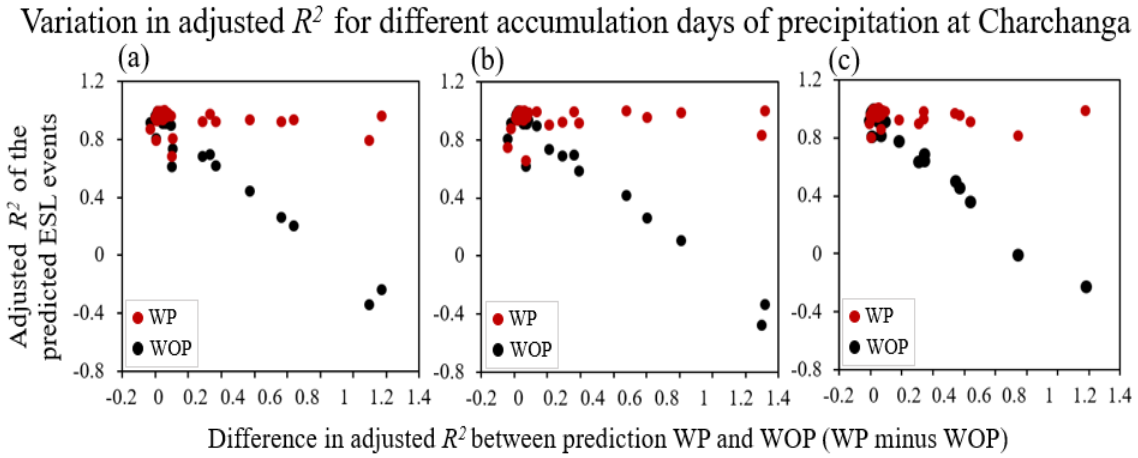

Figure 2.10 The relationship between the *adjusted* R^2 values of sea level predictions at Charchanga based on MLR for WP and WOP using different accumulation days for precipitation. In (a), 3 days accumulated precipitation was used. (b) and (c) same as (a) but for 5 days and 7 days, respectively. Each dot corresponds to an ESL event. Red and black dots represent *adjusted* R^2 for predictions WP and WOP, respectively. The y-axis represents the *adjusted* R^2 for predictions WP. The x-axis represents the differences in *adjusted* R^2 between WP and WOP predictions.

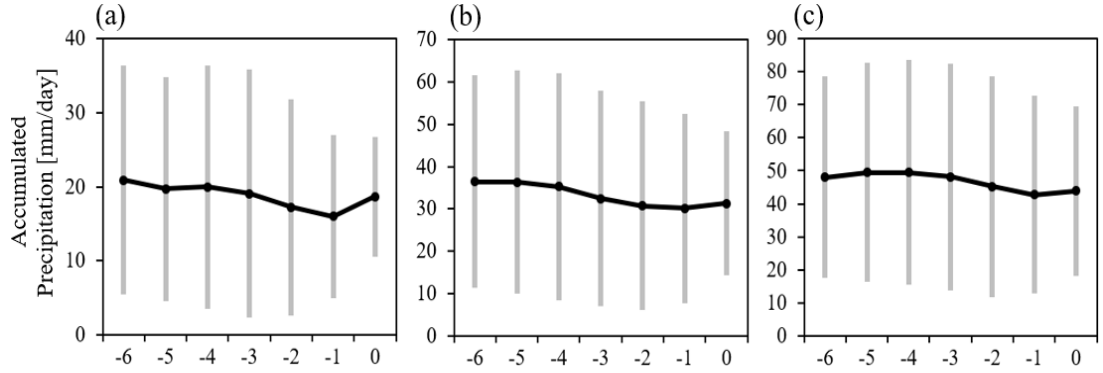

Figure 2.11 (a) Average time series of the 3 days accumulated precipitation for the selected ESL events at Charchanga. (b) and (c) same as (a) but for 5 days and 7 days accumulated precipitation, respectively. The error bars represent the standard deviation of the cases. The x-axes represent the day corresponding to the six days before ($t = -6$) to the ESL day ($t = 0$).

2.3.3.4. Independency among the explanatory variables

The prediction of a dependent variable in MLR is influenced by the interdependency of the explanatory variables (Hünicke and Zorita, 2006; Zhang and Church, 2012; Karabil et al., 2017). It is anticipated that the predictability of ESL using MLR predictions is influenced by the multicollinearity of the variables. To argue this point, the independency of the explanatory variables was investigated using a correlation analysis among the variables for each ESL event of the three study stations of Cox's Bazar, Charchanga, and Khepupara (Fig. 2.12). It shows high correlation among the explanatory variables for many events at all three stations. To evaluate the significance of the obtained correlation coefficients a significance test was performed at 90% confidence level (Table 2.1). The result shows the nonsignificant correlation among the explanatory variables (i.e., Pre, SLP, U, and V) for many events at three stations. For example, at Cox's Bazar out of 35 ESL events there are 24, 23, 22, 29, 27, and 20 events which show nonsignificant correlation for Pre-SLP, Pre-U, Pre-V, SLP-U, SLP-V, and U-V, respectively (Table 2.1). The nonsignificant correlation represents that the explanatory variables are independent and they are useful in MLR analysis. On the other hand, some of the explanatory variables (i.e., Pre, SLP, and V) shows significant correlation with SLA, that denote their high effect on the sea level variations for three stations (upper part of Fig. 2.12). For SLP, many events show significant negative correlation with SLA. Some events, however, show non-significant correlation. The significant correlation between SLA and SLP implies the strong effect of atmospheric load on the sea level variations.

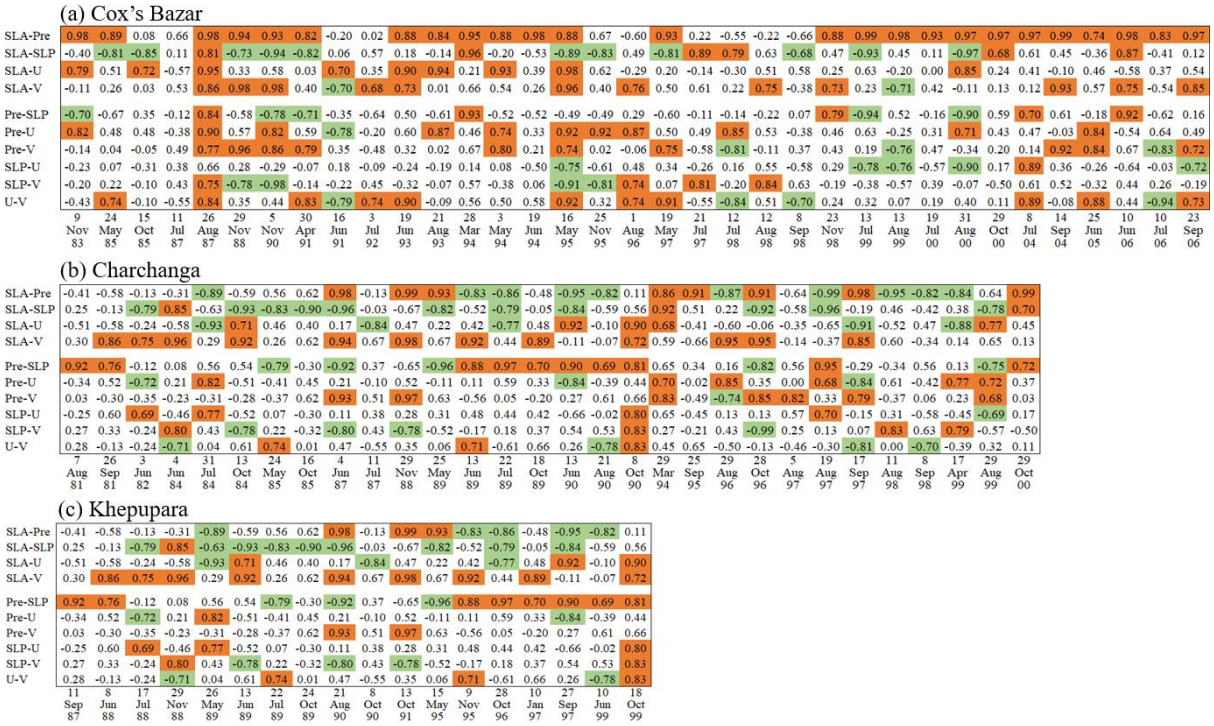

Figure 2.12 Correlation coefficients among the explanatory variables for the selected ESL events at three study stations of Cox's Bazar (a), Charchanga (b), and Khepupara (c). The statistically significant positive (negative) correlations were highlighted with orange (green) color shading.

Table 2.1 Number of ESL events for significant (S) and non-significant (NS) correlation at 90% confidence level among the explanatory variables. The analysis was performed for each ESL event for three study stations of Cox's Bazar, Charchanga, and Khepupara.

Station	SLA-Pre		SLA-SLP		SLA-U		SLA-V		Pre-SLP		Pre-U		Pre-V		SLP-U		SLP-V		U-V	
	S	NS	S	NS	S	NS	S	NS	S	NS	S	NS	S	NS	S	NS	S	NS	S	NS
Cox's Bazar	25	10	17	18	9	26	15	20	11	24	12	23	13	22	6	29	8	27	15	20
Charchanga	18	12	14	16	10	20	14	16	15	15	9	21	8	22	5	25	8	22	7	23
Khepupara	8	10	10	8	6	12	9	9	11	7	3	15	2	16	3	15	5	13	5	13

Chapter 3: Influence of the meteorological variables to the predictions of ESLs

3.1. Introduction

The contribution of the different meteorological factors to the variability of sea level was addressed in Section 1.3 (Chapter 1). The reviewed earlier study mainly focuses the contribution of a specific factor for sea level change in different coastal regions of the world as well as for the coast of Bangladesh (Singh et al., 2001; Svensson and Jones, 2002; Moron and Ullmann, 2005; Unnikrishnan et al., 2011; Lee, 2013; Anoop et al., 2015; Tazkia, et al., 2016; Kuang et al., 2017). The ESL change along the coast is influenced by the combined influences of the different meteorological factors (IPCC, 2013). Details on the combined influences were discussed in Section 1.3. Consideration of the combined influences of different meteorological factors for the predictability of ESL will be useful to understand the contribution of a specific factor. Here, the predictability of sea level was estimated considering the contribution of four explanatory variables. The study was mainly conducted based on statistical analysis using MLR for each event. The spatiotemporal variations of the sea level and explanatory variables were evaluated to understand their evolution pattern during the extremes. As discussed in Section 2.3.3a (Chapter 2), two different settings of MLR (Equation 2 and Equation 3) were adopted for each event to evaluate the contribution of precipitation effect in comparison with other factors. The contribution of the precipitation for each ESL event is presented in this Chapter.

It is well known that the intensity of precipitation in this area varies with pre-monsoon, monsoon, and post-monsoon seasons (Vialard et al., 2009; Turner and Annamalai, 2012; Suresh et al., 2013). The monsoon is the peak season for high precipitation over this area (Singh, 2001; Ahasan et al., 2010). The occurrence of severe cyclones and associated surges are also frequent during monsoon over this region (Unnikrishnan et al., 2011; Lee, 2013). It was mentioned that the high precipitated-water runoff and storm-induced strong winds and surges during monsoon accelerate the sea level along the coast of Bangladesh (Ali, 1999; Cheng et al., 2013; Caesar et al., 2015). Therefore, this study investigates the seasonal variations of the impact of precipitation on the variability of ESL along the coast.

The objective of this chapter is to evaluate the spatiotemporal variations of the meteorological variables during ESL events and to investigate the contribution of precipitation to the predictability of ESL. It is also aimed to investigate the seasonal variations of the impact of precipitation on the variability of ESLs. The rest of the sections of this Chapter are outlined

as follows. Section 3.2 explains the analytical procedures. Section 3.3 shows the results for contribution of the meteorological variables to the predictions of ESL. Section 3.4 discusses the outcomes and summary.

3.2. Analytical procedures: MLR for each ESL event

In section 2.3.3.4, the independency of the explanatory variables in MLR analysis was investigated using a correlation analysis among the variables for each ESL event at three stations. The significance of the correlation coefficients was tested at 90% confidence level. In this Chapter, the effect of precipitation on ESL was investigated using the MLR for each event with seven-day period. Here, a composite analysis was performed for spatiotemporal variations of sea level and forcing parameters for all ESL events. The time series of SLA and meteorological variables were averaged for all selected ESL events at three stations. Similarly, a composite spatial distribution of the meteorological variables has been presented for ESL events at Cox's Bazar, Charchanga, and Khepupara. The composite analysis was performed for the ESL events which occurred after the year 1992, considering the availability of the daily gridded sea level anomaly data from 1993. Details of the datasets for each variable were the same as those presented in Chapter 2, except the gridded sea level anomaly data for composite analysis over BoB. Here, the used daily gridded sea level anomaly data represents the deviation of the daily sea level from 20-year mean and is different from the one mentioned for station data in Chapter 2. Here, the influence of precipitation on the predictability of ESL was evaluated by the difference in *adjusted* R^2 between the outcomes of MLR Equation 2 and Equation 3, as addressed in Chapter 2.

The seasonal variation of the impact of precipitation was investigated considering the relationship between the SLA and *adjusted* R^2 difference between two predictions of with precipitation (Equation 2) and without precipitation (Equation 3). Here, the effect of precipitation on ESL change was evaluated on a monthly basis for selected ESL events at each of the study stations. To confirm the effect of precipitation on the monthly variability of ESL events, a comparative analysis was performed between the frequency of ESL events at each month and the mean precipitation of that month at Cox's Bazar station.

3.3. Results

3.3.1. Spatiotemporal variations of sea level and meteorological variables

A composite analysis for all ESL events was performed to understand the spatiotemporal variations of sea level and forcing parameters. Figure 3.1 displays the time series of SLA and meteorological variables, averaged for all selected ESL events. For all three of the stations, the mean SLA is highest on the day of the extreme (t = 0), with a gradual increase from the prior days (Fig. 3.1a-c). The precipitation at Cox's Bazar shows a similar evolution with SLA, in which the amount of precipitation increases gradually towards the day of ESL (Fig. 3.1d). In comparison with Cox's Bazar, the amount of precipitation for Charchanga (Fig. 3.1e) and Khepupara (Fig. 3.1f) are very less and their evolutions are almost stable during extremes. The time series of SLP at all three stations shows a gradual decline from the prior days to the day of the extreme (Fig. 3.1g-i), suggesting that a low-pressure system is approaching the targeted area. The SLP decrease is relatively steady at Khepupara (Fig. 3.1i). The southerly wind velocities at the three stations increased and reached the maximum on the day of ESL (Fig. 3.1j-l). In Charchanga and Khepupara, the southerly wind was intensified from t = −2, denoting a strong effect of a wind-induced surge for these locations. The westerly wind increased during the ESL events at Cox's Bazar, while the zonal wind speed is near zero at Charchanga and an easterly wind is dominated at Khepupara (Fig. 3.1m-o).

Similarly, a composite spatial distribution of the meteorological variables has been presented for ESL events at three study stations of Cox's Bazar, Charchanga, and Khepupara. For each station, the composite analysis was performed for those ESL events, which occurred after the year 1992, because the daily gridded sea level anomaly data is available from the year 1993. Figure 3.2 demonstrates that at Cox's Bazar the sea level anomaly along the coast is high throughout the targeted seven-day duration and increased until the day of ESL, which is consistent with the time evolution in the station data (Fig. 3.1a). In comparison with Cox's Bazar the magnitude of the high sea level anomaly is comparatively low throughout the targeted seven-day duration for Charchanga (Fig. 3.3a-g) and Khepupara (Fig. 3.4a-g), which is consistent with the time evolution in the station data for Charchanga (Fig. 3.1b) and Khepupara (Fig. 3.1c). For Cox's Bazar (Fig. 3.2), the accumulated precipitation over the coastal area remained high from t = −6 through to t = 0, presumably reflecting the strong enhancement of orographic rain along the Arakan Mountains (Xie et al., 2006). The rainfall began to increase from t = −1 and reached a maximum on the ESL day near Cox's Bazar area (Fig. 3.2a-g). The

high orographic rain appeared to be intensified in accordance with strong southerly-southwesterly winds toward the coast, which are part of synoptic-scale flow surrounding the low-pressure center, located over western India (Fig. 3.2g).

For Cox's Bazar the composite analysis suggests that high precipitation concentrated on the narrow hilly slope increased sea level anomaly along the coast, together with the effects of low SLP and associated strong surface winds (Fig. 3.2). The steeper slope in this hilly area enhances the surface runoff to the downstream coast. The short distance between the downstream coast and upstream hilly area reduces the delay in precipitated water runoff. In the eastern hilly area approximately 78% of the area is covered by the fine textured clay loam soils (Zzaman et al., 2021). Hence, infiltration and percolation rates are low, which support the faster surface runoff to the downstream. Since this area is occupied with many hilly rivers and their tributaries, the drainage density (i.e., the total length of streams per unit area) is high. The high drainage density denotes that the precipitated-water is well drained and the discharge is enhanced in the downstream. Furthermore, the upper basin area is not under human economic activities (e.g., agriculture, infrastructures). This encourages the direct runoff of the huge precipitated-water toward the downstream Cox's Bazar area (Adnan et al., 2019; Zzaman et al., 2021). These geomorphological settings and low anthropogenic controls suggest the strong influence of upstream precipitation to ESL at Cox's Bazar area.

In comparison with Cox's Bazar, the gradual increase in precipitation from prior days to the day of ESL is comparatively less for Charchanga (Fig. 3.3a-g) and Kehpupara (Fig. 3.4a-g), which is highly consistent with the temporal evolution during seven days for Charchanga (Fig. 3.1e) and Khepupara (Fig. 3.1f). However, there is presence of strong low pressure and associated high winds with a gradual increase from prior days to the day of extreme for Charchanga (Fig. 3.3a-g) and Khepupara (Fig. 3.4a-g). The intensity of strong low pressure and winds are high in the day of extreme for Charchanga (Fig. 3.3g) and Khepupara (Fig. 3.4g). During the extreme events, the high sea level along the coast of Charchanga and Khepupara may be influenced by the effect of strong low pressure and high winds. The earlier studies also mentioned that the storm-induced surges, associated with low pressure and high winds, accelerate the sea level rise along the coast of Bangladesh (Unnikrishnan et al., 2011; Iskandar and McPhaden, 2011; Lee, 2013). The result denotes that, likewise the discussed effect of high precipitation, the strong low pressure induced surges and high winds are also the important factors for ESL variability along the coast of Bangladesh.

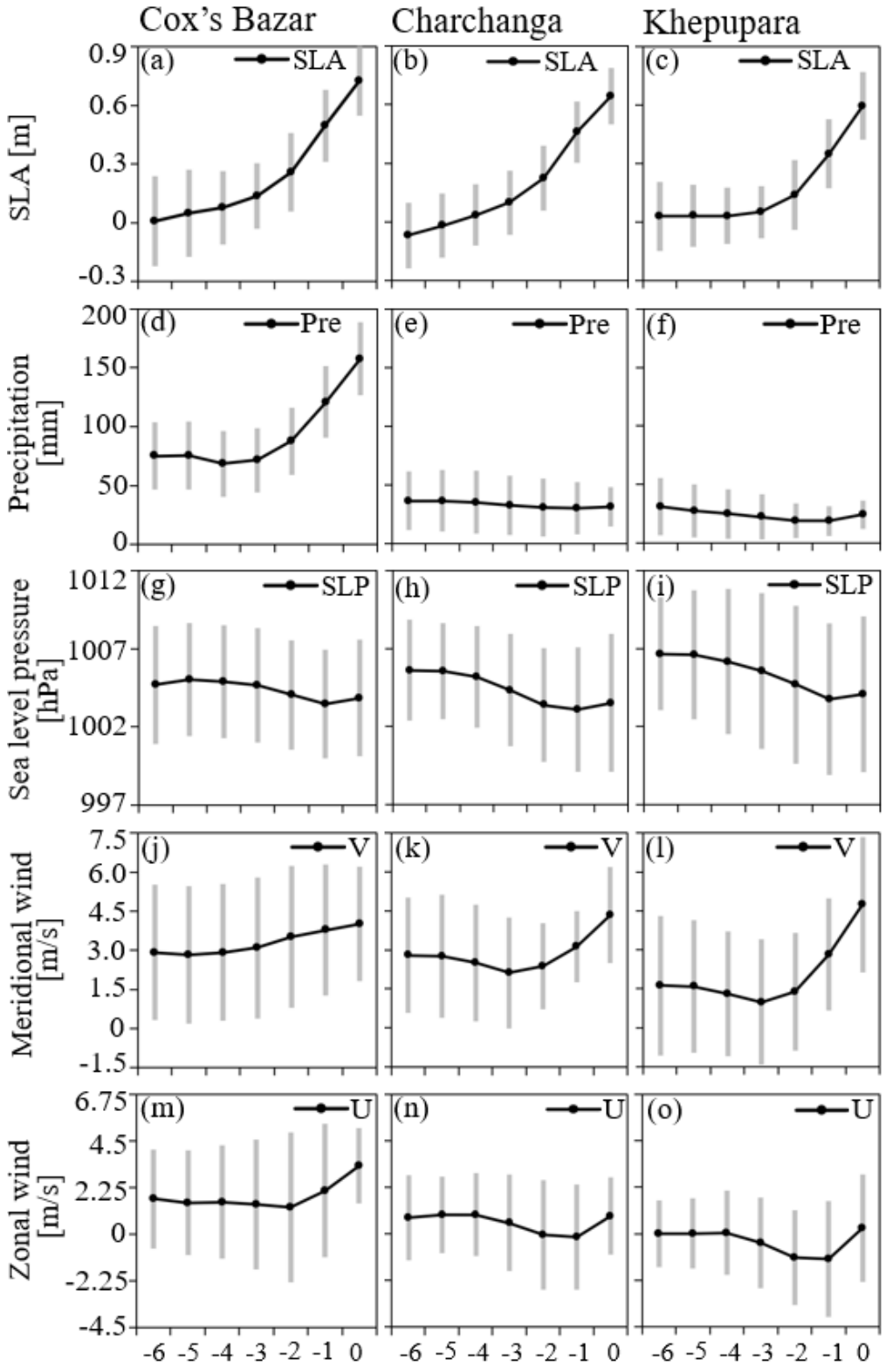

Figure 3.1 The average time series (line) of SLA, Pre, SLP, U, and V for all ESL events at Cox's Bazar (a, d, g, j, and m), Charchanga (b, e, h, k, and n) and Khepupara (c, f, i, l, and o). The error bars represent the standard deviation of the cases. The x-axes represent the day corresponding to the six days before ($t = -6$) to the ESL day ($t = 0$).

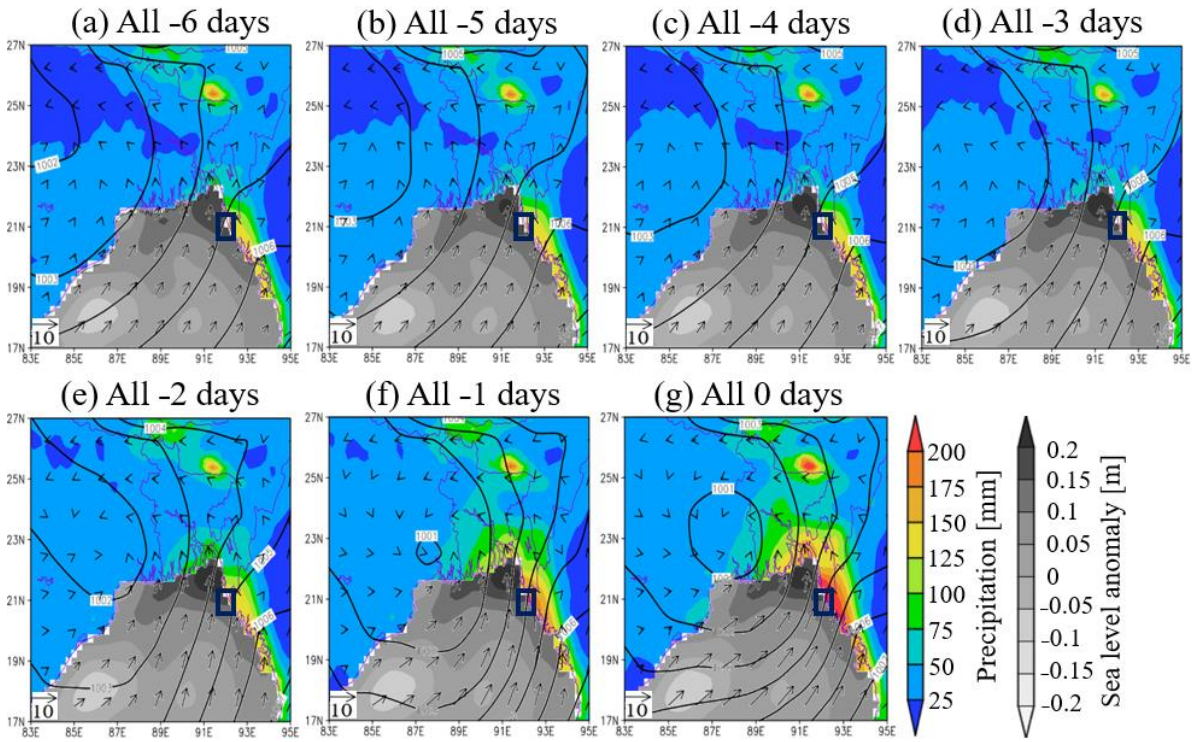

Figure 3.2 Composite map of the variables for each prior day (a-f) and the day of extreme (g) for all ESL events at Cox's Bazar during 1993–2006. Here, the analysis was performed for the ESL events during 1993–2006, considering the availability of gridded sea level anomaly data from 1993. The gray shading over the ocean represents sea level anomaly (m) and the color shading over the land represents accumulated precipitation during the five preceding days (mm). The contour and vector are for SLP (hPa) and surface wind (m/s), respectively. The rectangles denote the location of the Cox's Bazar station. It is noted that the sea level anomaly drawn here is defined as the deviation of sea level from its 20-year (1993–2012) climatological mean (Taburet et al., 2019).

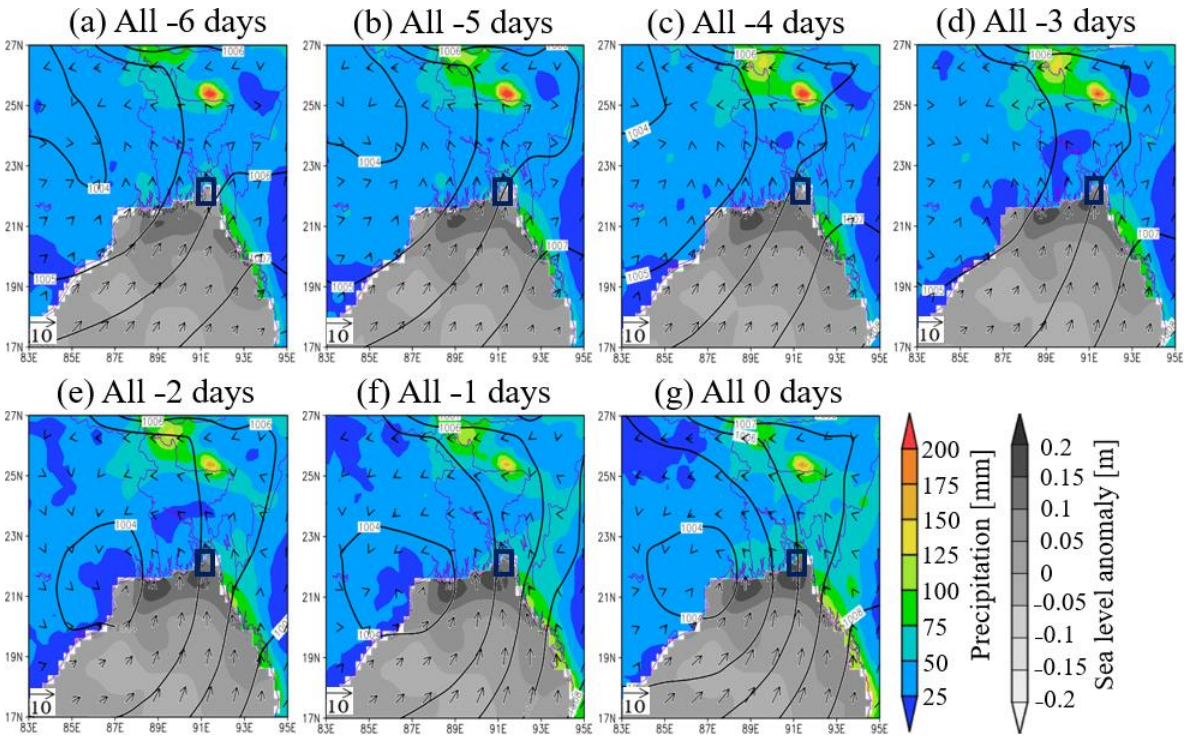

Figure 3.3 Composite map of the variables for each prior day (a-f) and the day of extreme (g) for all ESL events at Charchanga during 1993–2000. Here, the analysis was performed for the ESL events during 1993–2000, considering the availability of gridded sea level anomaly data from 1993. The gray shading over the ocean represents sea level anomaly (m) and the color shading over the land represents accumulated precipitation during the five preceding days (mm). The contour and vector are for SLP (hPa) and surface wind (m/s), respectively. The rectangles denote the location of the Charchanga station. It is noted that the sea level anomaly drawn here is defined as the deviation of sea level from its 20-year (1993–2012) climatological mean (Taburet et al., 2019).

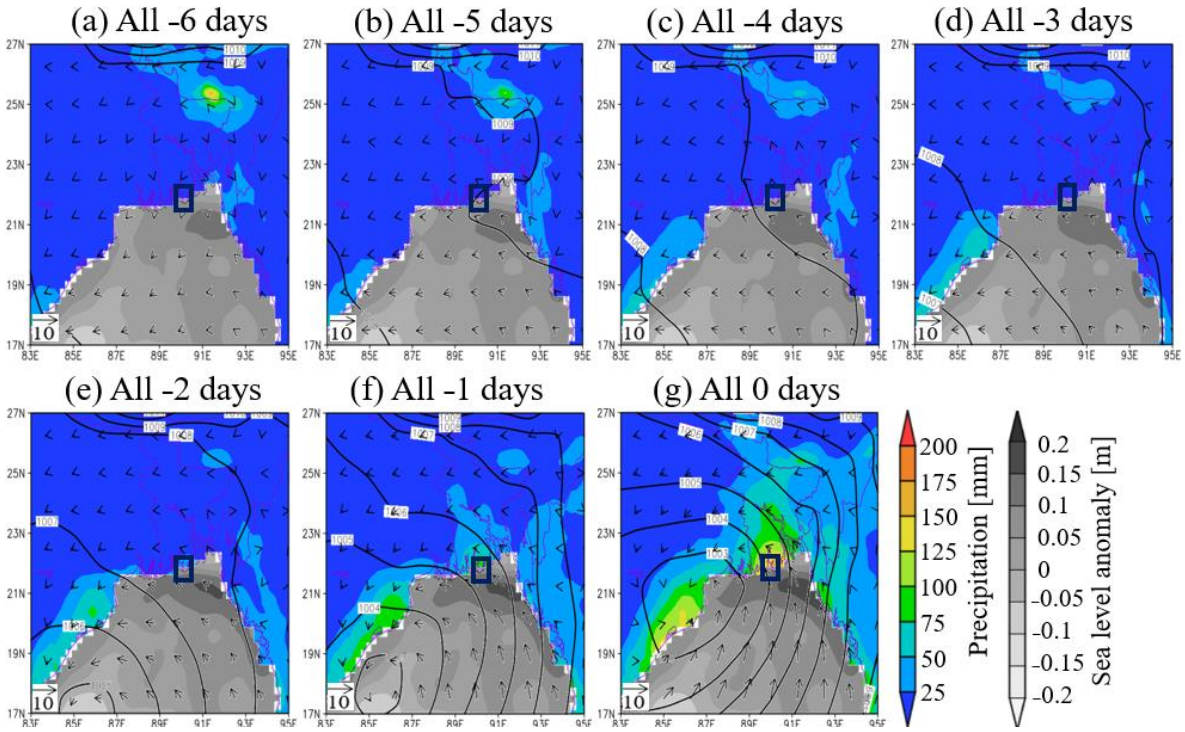

Figure 3.4 Composite map of the variables for each prior day (a-f) and the day of extreme (g) for all ESL events at Khepupara during 1993–2000. Here, the analysis was performed for the ESL events during 1993–2000, considering the availability of gridded sea level anomaly data from 1993. The gray shading over the ocean represents sea level anomaly (m) and the color shading over the land represents accumulated precipitation during the five preceding days (mm). The contour and vector are for SLP (hPa) and surface wind (m/s), respectively. The rectangles denote the location of the Khepupara station. It is noted that the sea level anomaly drawn here is defined as the deviation of sea level from its 20-year (1993–2012) climatological mean (Taburet et al., 2019).

3.3.2. Contribution of precipitation to the predictions of ESL

In this section, the influence of precipitation on SLA was evaluated using MLR statistics. Figure 3.5 compares the variations of predicted and observed sea levels for a typical event at each station. Here, only successful cases are presented, in which the sea level prediction is nicely improved by adding the precipitation effect. The remaining cases will be also studied in this Section. At Cox's Bazar, the observed daily sea level on 19 July 2000 is well captured by the prediction with precipitation (i.e., Equation (2)), which achieved *adjusted* R^2 = 0.994 (Fig. 3.5a) and the root mean squared error (*rmse*) is 0.01. This result suggests that the evolution of ESL is mainly controlled by meteorological factors. However, when the effect of precipitation is excluded, the *adjusted* R^2 decreased to −0.591 (Fig. 3.5a) and the *rmse*

became 0.22. At Charchanga on 25 September 1995, the prediction with precipitation is more skillful (*adjusted* R^2 = 0.954, *rmse* = 0.03) than the prediction without precipitation (*adjusted* R^2 = 0.258, *rmse* = 0.18) (Fig. 3.5b). At Khepupara on 13 October 1991, the prediction with precipitation also performed better, although the differences in *adjusted* R^2 between the prediction with (*adjusted* R^2 = 0.999, *rmse* = 0.01) and without precipitation (*adjusted* R^2 = 0.941, *rmse* = 0.03) are small (Fig. 3.5c) compared with those of Cox's Bazar and Charchnaga stations. The difference in *adjusted* R^2 between the two predictions implies that the impact of precipitation on ESL differed for each station.

Figure 3.6 examines the *adjusted* R^2 of the SLA predictions for all ESL events. The higher *adjusted* R^2 is commonly seen for the prediction with precipitation. This is a common character for the *rmse* (Table 3.1). The distribution of *rmse* values for the predictions with precipitation shifted lower in comparison to that for the prediction without precipitation; the lower shift of the mean *rmse* value is statistically significant ($p < 0.05$ for the three stations). These results show the importance of precipitation variability in predicting sea level variation along the coast of Bangladesh. The improvement in *adjusted* R^2 for WP predictions is greater at Cox's Bazar than at Charchanga and Khepupara. Figure 3.6 shows that the increase of *adjusted* R^2 is large for the event whose *adjusted* R^2 value is low for the prediction WOP. For such cases, the daily variation of sea level is likely to be influenced by the precipitation that accompanies river discharge and therefore, the consideration of the precipitation effect would improve the predictability of ESL. Studies have shown that the high river discharge modulates the long-term sea level variability along the coast of Bangladesh (Singh, 2001, 2002a; Caesar et al., 2015; Dandapat et al., 2020).

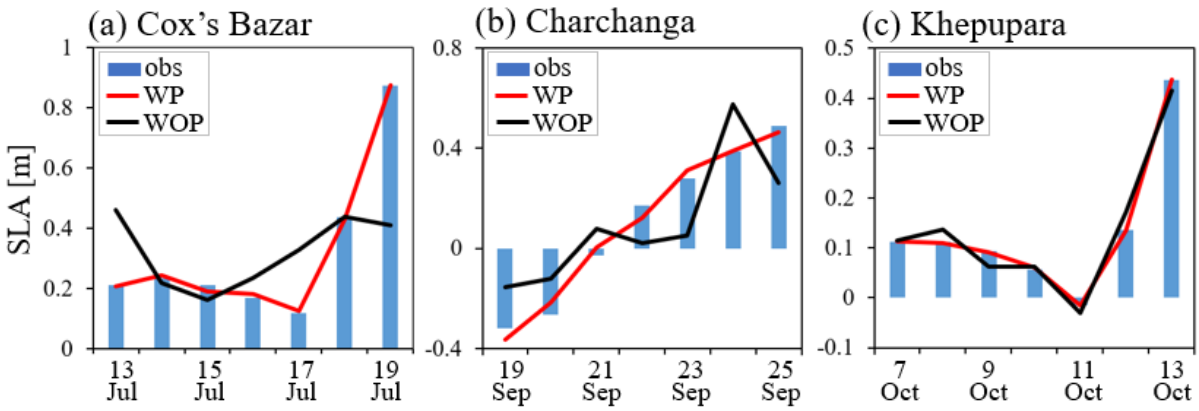

Figure 3.5 (a) The observed SLA (bar) and predicted SLAs for prediction with precipitation (WP, red line) and without precipitation (WOP, black line) at Cox's Bazar for the case of ESL on 19 July 2000. (b) and (c) same as (a) but for Charchanga on 25 September 1995 and Khepupara on 13 October 1991, respectively. The MLR equations are

$$SL' = 0.06 \times SLP - 0.04 \times U - 0.05 \times V + 0.23 \times Pre + 0.32 \quad \text{(WP, Cox's Bazar)}$$

$$SL' = -0.06 \times SLP - 0.06 \times U + 0.14 \times V + 0.20 \quad \text{(WOP, Cox's Bazar)}$$

$$SL' = 0.01 \times SLP - 0.14 \times U + 0.03 \times V + 0.29 \times Pre + 0.10 \quad \text{(WP, Charchanga)}$$

$$SL' = 0.15 \times SLP + 0.09 \times U - 0.23 \times V + 0.10 \quad \text{(WOP, Charchanga)}$$

$$SL' = -0.11 \times SLP + 0.05 \times U + 0.08 \times V + 0.04 \times Pre + 0.13 \quad \text{(WP, Khepupara)}$$

$$SL' = -0.17 \times SLP + 0.13 \times U + 0.08 \times V + 0.13 \quad \text{(WOP, Khepupara)}$$

Table 3.1 The evaluation of the root mean square error (*rmse*) for WP and WOP predictions.

	Cox's Bazar (No. of cases)		Charchanga (No. of cases)		Khepupara (No. of cases)	
	WP	**WOP**	**WP**	**WOP**	**WP**	**WOP**
rmse < 0.01	2	0	3	0	1	0
0.01 ≤ rmse < 0.03	11	1	15	3	4	4
0.03 ≤ rmse < 0.06	14	8	10	11	12	10
0.06 ≤ rmse < 0.09	5	9	1	8	1	3
0.09 ≤ rmse	3	17	1	8	0	1
Total	35	35	30	30	18	18

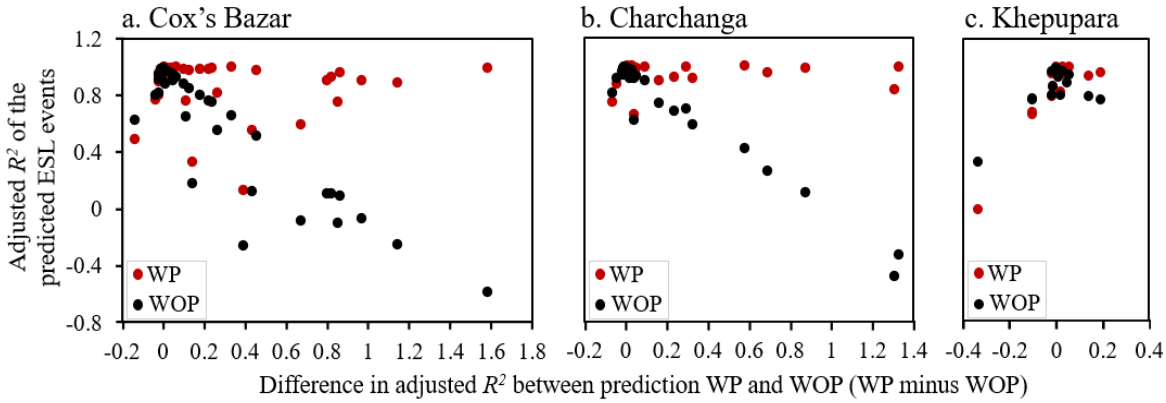

Figure 3.6 The relationship between the *adjusted* R^2 values of sea level predictions based on MLR for WP and WOP at (a) Cox's Bazar, (b) Charchanga, and (c) Khepupara. Each dot corresponds to an ESL event. Red and black dots represent *adjusted* R^2 for predictions WP and WOP, respectively. The y-axis represents the *adjusted* R^2 for predictions WP. The x-axis represents the differences in *adjusted* R^2 between WP and WOP predictions.

3.3.3. Seasonal variations of the impact of precipitation

The seasonal variations of precipitation effect to ESL events are presented in Figure 3.7. Here, the effect of precipitation was measured from the *adjusted* R^2 difference of the two predictions and then its relationship with SLA was evaluated. In Cox's Bazar, ESL events with a high influence of precipitation tended to occur in June and July (Fig. 3.7a), which may correspond to the peak precipitation season of the summer monsoon. Interestingly, the highest SLAs are observed in May (Fig. 3.7a) and the difference in *adjusted* R^2 for these events are generally small. It was confirmed that these events mostly occurred in early May in 1995 and 1997 and there were tropical cyclones or tropical depressions over the study area (Ali, 1999; Wahiduzzaman, 2021). Hence, it is very likely that these ESL events are strongly influenced by SLP and winds, rather than the precipitation effect. For such cases, since *adjusted* R^2 is originally very high, predictions WP and WOP do not differ largely. In June and July, the effect of precipitation at Cox's Bazar is thought to be enhanced because the precipitation amount is high in these months. In Charchanga, the ESL events with a large *adjusted* R^2 difference occurred during the post-monsoon period from August through to September (Fig. 3.7b). The frequency of heavy precipitation events remained high in these months, leading to the possibility of a large contribution of precipitation. At Khepupara, the differences in *adjusted* R^2 are found during October and November, corresponding to the post-monsoon season, although the magnitude of the *adjusted* R^2 difference is smaller than other stations (Fig. 3.7c).

The impact of precipitation on the skill of MLR predictions varied among stations and seasons. It has been suggested that the impact is high in Cox's Bazar and Charchanga for July and September–October, respectively. These months agree well with the month of highest precipitation for the study area, as mentioned in previous studies (Shahid, 2011; Ahasan et al., 2010; Mohsenipour et al., 2020).

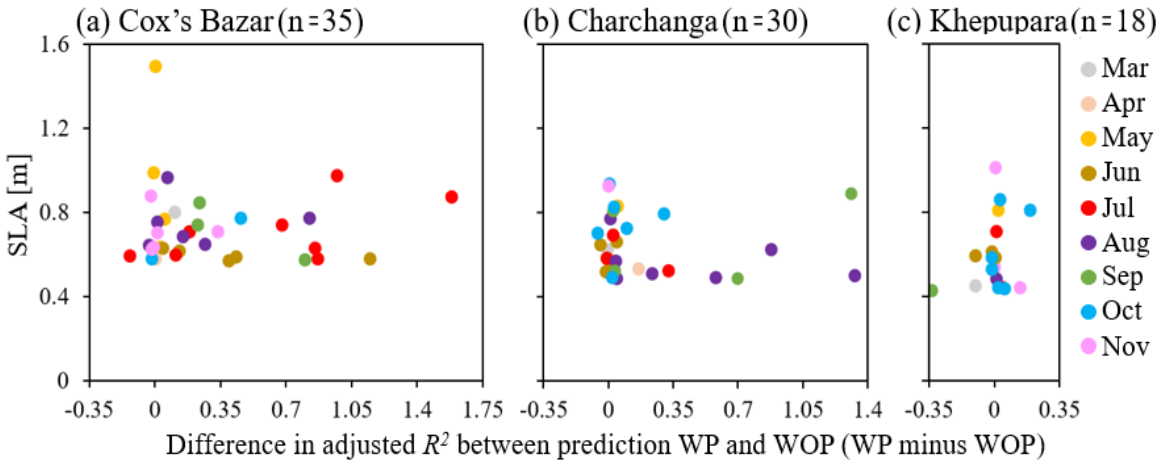

Figure 3.7 Monthly variations in *adjusted* R^2 difference between predictions WP and WOP at (a) Cox's Bazar, (b) Charchanga, and (c) Khepupara. Dots represent ESL events and the colors indicate the months when they occurred.

In Cox's Bazar, the ESL events with a high influence of precipitation tended to occur during the peak precipitation of the summer monsoon. Figure 3.8b confirmed that the occurrence of ESL events with a high influence of precipitation is corresponding to the peak precipitation of June and July during monsoon. It is also confirmed the amount of precipitation in June and July is high at Cox's Bazar (Fig. 3.8b). Figure 3.8b represents the high seasonal variability of monthly precipitation in Bangladesh, associated with the summer monsoon, which typically ranges from June through to September. According to the submonthly-scale, intraseasonal variability is dominant in this region (Fujinami et al., 2017), there is a prominent increase of heavy precipitation events (>50 mm/day) from pre-monsoon (May) to post-monsoon (October) seasons. The frequency of ESL events shows a similar seasonal variation with the heavy precipitation event, indicating that ESL events are triggered by high precipitation events (Fig. 3.8a). Figure 3.8a,b also confirmed that the simultaneous increases of ESL events and heavy precipitation in 1999, as shown in Figure 1.3 (Chapter 1), are common characters for many years. Figure 3.8a shows five ESL events in November, which denotes there are different processes in comparison to those occur during peak monsoon season. Among the five ESL events, the ESL on 29 November 1988 and 25 November 1995 are influenced by

the effect of tropical cyclone rather than the precipitation. The presence of tropical depression and associated small precipitation might influence the ESL on 9 November 1983 and 23 November 1998. The small precipitation over a small area along the eastern coast was observed during the ESL event on 9 November 1990. These are the possible cause of the November ESLs.

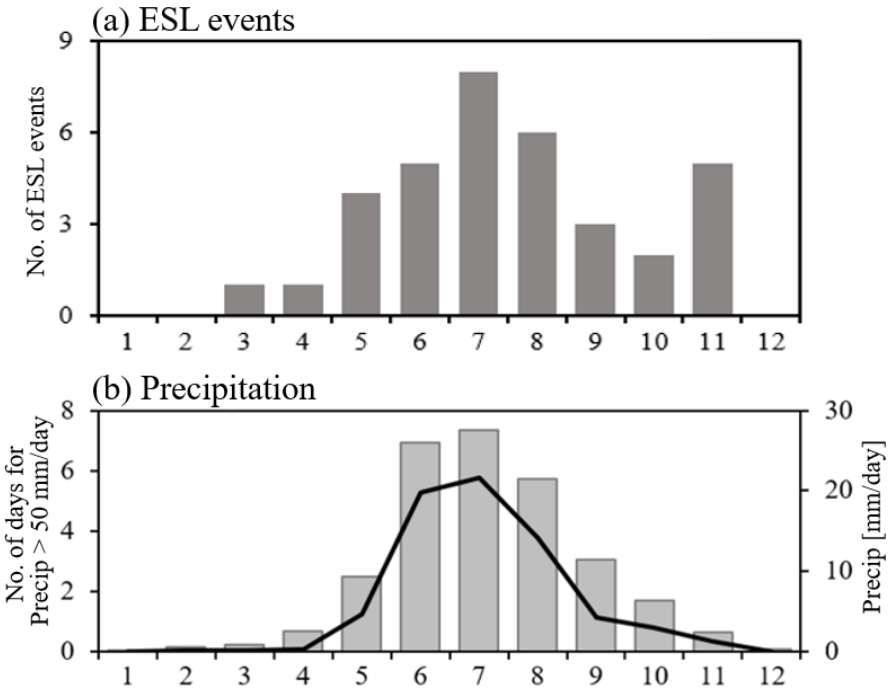

Figure 3.8 (a) Monthly variation of ESL events at Cox's Bazar averaged during 1983–2006. Note that years of 2001–2003 were excluded due to data unavailability. (b) Monthly variations of mean precipitation (mm/day; bar) during 1983–2006 averaged near Cox's Bazar area (20.60°–22.00° N and 91.90°–92.75° E) and the number of days exceeding 50 mm/day of area-mean precipitation (line).

3.4. Discussion and summary

In section 3.3.2, it was confirmed that the predictability of ESL is highly influenced by the effect of precipitation. The MLR performs well for predictions of ESL with the effect of precipitation than that without precipitation, which denotes high contribution of precipitation for predictions of ESL. To understand the causality of precipitation to enhance ESL, the MLR with precipitation term (Equation 2) was decomposed into two parts, one for the term of precipitation (Equation 4) and another for the term of other effects (Equation 5).

$$SL'_{Pre\text{-}term}(t) = d_1 \times \mathrm{Pre}(t) \quad (4)$$

$$SL'_{Other\ terms}(t) = a_1 \times \mathrm{SLP}(t) + b_1 \times \mathrm{U}(t) + c_1 \times \mathrm{V}(t) + e_1 \quad (5)$$

Figure 3.9 shows the decomposition of predicted SLA with WP setting at Cox's Bazar. The predicted SLA without the term of precipitation shows large uncertainty although it shows a weak increase toward the ESL day (Fig. 3.9b). This means SLA variations driven by meteorological elements (air pressure and wind) are strongly case-dependent. The precipitation term also shows large uncertainty among cases but shows a steady increase (Fig. 3.9a). The negative SLAs in Figure 3.9a during the first half of the episode is because of the use of normalized precipitation. The result shows that during extreme events the SLA explained by the precipitation term is smaller than that of other terms. From prior four day ($t = -4$) to the day of extreme ($t = 0$), however, the SLA explained by the precipitation term shows high increase from -0.08 m to 0.32 m (about 0.40 m). In contrast, for this period there is a weak increase from 0.22 m to 0.38 m (about 0.16 m) in SLA explained by the other terms. This analysis suggested that the large increase in SLA toward the ESL day is mainly governed by the contribution of precipitation rather than other effects.

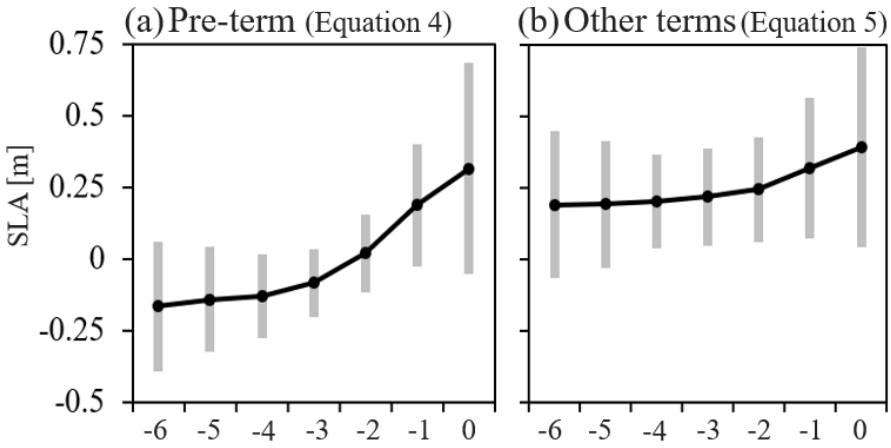

Figure 3.9 (a) and (b) represent the average time series of the decomposed SLA variations due to Pre-term (Equation 4) and other terms (Equation 5), respectively at Cox's Bazar. The error bars represent the standard deviation of the cases. The x-axes represent the day corresponding to the six days before ($t = -6$) to the ESL day ($t = 0$).

The results indicate that the precipitation has significant contribution to ESL. It denotes the importance for consideration of high precipitation over Bangladesh area to predict the ESL change along its coast. Likewise, the revealed importance of high precipitation, the composite analysis in Section 3.3.1 confirmed that the low-pressure generated strong winds and surges influence the sea level during extreme SL events. The influence of cyclones and associated winds to the sea level change during extremes was evaluated along the coast of Bangladesh. A composite analysis was performed for cyclone-induced ESL days to understand the effect of cyclones and associated winds to the sea level change. Figure 3.10 shows the composite of

cyclone-induced ESL days at the three study sites during 1993–2006. Here, the cyclone-induced ESL days means the ESL days when the tropical cyclone was observed in the targeted area (17°–27°N and 83°–95°E) based on the IMD best track data (IMD, 2008). It is revealed that during the cyclone-induced ESL days, there are high sea levels along the coast of the three stations, which denotes the strong effect of low SLP and high winds toward the coast (Fig. 3.10). The composite analysis shows that during extremes the center of the cyclones are generally located over land and western coast of the BoB, which may reflect their active influence on the variability of ESL along the coast. The effect of cyclones to accelerate the sea level during some ESL events (i.e., ESL events in May) is also evident in this region (Fig. 3.7a). The role of cyclone-induced surges and winds to enhance the sea level rise along the coast of Bangladesh was mentioned in earlier studies (Unnikrishnan et al., 2011; Iskandar and McPhaden, 2011; Lee, 2013). Therefore, the consideration of the cyclone effect is important for studying the ESL variability along the coast.

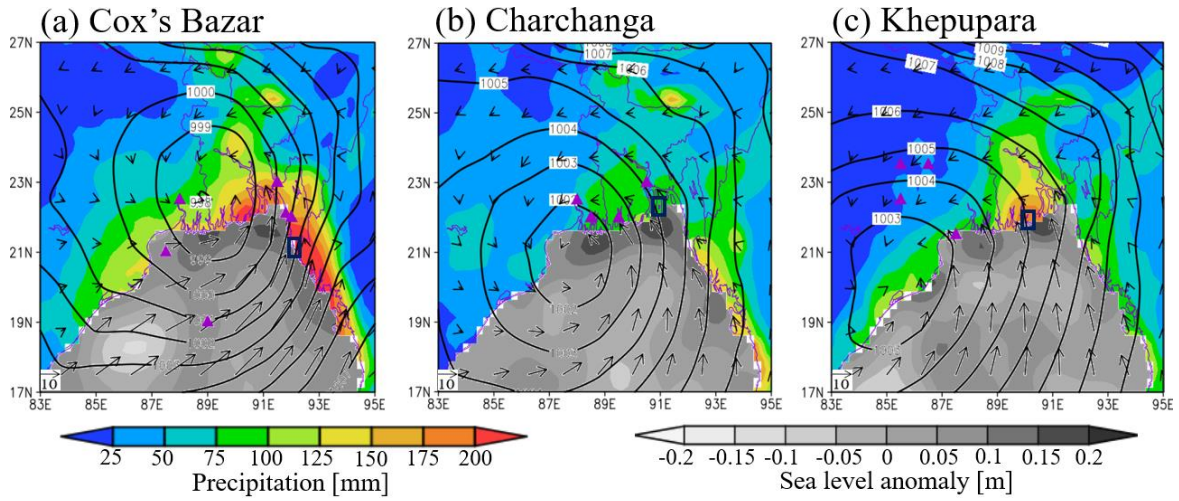

Figure 3.10 (a) Composite map of the variables for six cyclone-induced ESL days at Cox's Bazar during 1993–2006. Here, the analysis was performed for the period 1993–2006, considering the availability of gridded sea level anomaly data from 1993. The gray shading over the ocean represents sea level anomaly (m) and the color shading over the land represents accumulated precipitation during the five preceding days (mm). The contour and vector are for SLP (hPa) and surface wind (m/s), respectively. The purple triangle indicates the location of cyclone on each ESL day. (b) and (c) same as (a) but for five and four cyclone-induced ESL days during 1993–2000 for Charchanga and Khepupara, respectively. At Charchanga, it is noted that the two different cyclones during two different days are occurred over same location. The sea level anomaly drawn here is defined as the deviation of sea level from its 20-year (1993–2012) climatological mean (Taburet et al., 2019).

In this study, it is revealed that the ESL variability along the coast of Bangladesh is influenced by the seasonality of precipitation. The previous studies mentioned that the seasonal variation of precipitation in this area was modulated by the high precipitation during the monsoon season (Shahid, 2010; Ahasan et al., 2010; Turner and Annamalai, 2012; Cheng et al., 2013; Ahmed et al., 2017; Mohsenipour et al., 2020). The high precipitation during the monsoon season may reflect the revealed effect of high monsoonal precipitation on the variability of ESL over this region. The effect of high monsoonal precipitation and associated runoff on the coastal sea level change was mentioned in some earlier researches, but there have lack of focus on precipitation effect to the variability of ESL at daily time scale along the coast of Bangladesh (Singh, 2001; Mondal, 2001; Dewan, 2003; Sarwar, 2013; Antony et al., 2016). In this regard, it is expected that this is a pioneer study to investigate the influence of precipitation on ESL change along the coast of Bangladesh.

The composite map of the sea level anomaly and meteorological variables for three stations shows the distribution of high sea level anomaly near the eastern and central coastal area (Fig. 3.2-3.4). The spatial extent of this high sea level anomaly is approximately 100–200 kilometer from the coastline. The presence of high sea level anomaly over this small area adjacent with coastline might reflect the effect of terrestrial precipitated-water discharge over there. The heavy precipitation and its high effect on ESL were found at Cox's Bazar along the eastern coastal area. The risen sea level along the eastern coast possibly influences the distribution of sea level anomaly in the central and western coast in the following days due to the propagation of coastal Kelvin wave in the funnel shape northern BoB (Han and Webster, 2002; Suresh et al., 2013). Previous study suggested that the equatorial Kelvin wave over Indian Ocean tends to propagate to the east and after arriving at Malay Archipelago it turns into coastal Kelvin wave and propagate to the north along the eastern coast of the BoB (Webster et al., 1999; Han and Webster, 2002). The northward propagation of this coastal Kelvin wave might force the high sea level near Cox's Bazar, and it can further propagate toward the central and western coast. Therefore, the coastal Kelvin wave is one of the important forcings which possibly influence the spatial variability of coastal high sea levels along the coast of Bangladesh.

However, some shortcomings are also addressed on the performances of MLR for predictions of ESL. It is recognized that, in a few cases, the *adjusted* R^2 of the MLR is not high, even with the consideration of precipitation (Fig. 3.5). For such cases, nonlinear effects may play an important role and the adopted MLR do not work as expected. The result represents

that likewise the high predictability of ESL considering with precipitation, some events show high predictability for without precipitation. The high predictability of ESL in MLR without precipitation indicates the high contribution of SLP and meridional wind (V) to sea level. Therefore, it is revealed that the variations in the predictability of ESL for two different MLRs are mainly influenced by the variations in the contribution of the explanatory variables. In addition, this study assesses the causal effect of precipitation on the predictability of ESL by means of statistical analysis. However, the adoption of a physical model is desirable to understand the causality of precipitation to increase ESL.

Nevertheless, the novel outcomes of this study will be to meet up the study gap on the effects of high precipitation on the ESL variability along the vulnerable coast of Bangladesh. It is revealed that the high precipitation over this region has a large contribution to the ESL. Therefore, it is expected that the consideration of the effect of precipitation will help to improve the forecast of ESL events. This study has importance to represent the effect of precipitation on ESL variations and to reduce the vulnerabilities of ESL-induced hazards along the coast of Bangladesh.

Chapter 4: Performance of the MLR for predictions of ESL

4.1. Introduction

In Chapter 3, it was confirmed that the MLR for each event using seven-day period performs well for predictions of ESL. It was revealed that the performance of MLR for predictions of ESL considering with precipitation (Equation 2) outperformed predictions without precipitation (Equation 3). In MLR for each event three (or four) explanatory variables were used as input to explain seven-day evolution of sea level. Since the MLR is sensitive to the sample size (Hünicke and Zorita, 2006; Zhang and Church, 2012; Karabil et al., 2017), the sample size might be too small. This small sample size in comparison to the number of explanatory variables will lead to too high predictability. Therefore, to avoid such a deficit in the MLR for each event, the sample size was increased here. The MLR adopted here uses daily samples of all ESL events including seven days before each ESL day. This MLR is referred to as MLR for all events. The sample size is 7 × event number for each station. The explanatory variables are identical with those addressed in MLR for each event (Equation 2), but the number of samples is increased. Here, the effect of precipitation on ESL will be investigated using a large sample size.

In Chapter 3, the MLR for each event confirmed that the variability in the predictions of ESL are influenced by the variation of precipitation effect among the stations. In a similar manner, here the contribution of precipitation will be investigated to understand the variations in predicted sea level among the stations using MLR for all events.

The objective of this chapter is to investigate the effect of precipitation on the predictability of ESLs using MLR for all events at three study stations. It is also aimed to investigate the contribution of precipitation to the variations of ESLs among the stations. The rest of the sections of this Chapter are outlined as follows. Section 4.2 explains the analytical procedures. Section 4.3 shows the results of the MLR predictions for all ESL events. Section 4.4 discusses the outcomes and summary.

4.2. Analytical procedures: MLR for all events

In Chapter 3, the MLR was performed for seven-day period of each ESL event. Here, MLR was created using all ESL events. The daily samples of seven days in prior to all ESL events for each station were used at once. The MLR equation for each station is presented as

$$SL'_{Cox's\ Bazar}(t) = a_3 \times SLP(t) + b_3 \times U(t) + c_3 \times V(t) + d_3 \times Pre(t) + e_3 \quad (6)$$

$$SL'_{Charchanga}(t) = a_4 \times SLP(t) + b_4 \times U(t) + c_4 \times V(t) + d_4 \times Pre(t) + e_4 \quad (7)$$

$$SL'_{Khepupara}(t) = a_5 \times SLP(t) + b_5 \times U(t) + c_5 \times V(t) + d_5 \times Pre(t) + e_5 \quad (8)$$

Herein, SL′ represents the predicted SLA at each station and t represents the number of samples. At Cox's Bazar (Equation 6), the sample size (t) is 245 days, which was derived from 7 days in prior to 35 ESLs events (35 × 7 = 245). Similarly, for Charchanga (Equation 7) and Khepupara (Equation 8) the sample size (t) is 210 days (30 × 7) and 126 days (18 × 7), respectively. The coefficients were determined for all sample sizes at each station. The derived coefficients are presented in Table 4.1.

Table 4.1 Coefficients of the explanatory variables of Pre, SLP, U, and V obtained from the MLR for Cox's Bazar (Equation 6), Charchanga (Equation 7), and Khepupara (Equation 8).

Stations	Coefficients for explanatory variables			
	Pre	SLP	U	V
Cox's Bazar	0.187	−0.002	0.019	0.079
Charchanga	−0.016	−0.091	−0.004	0.148
Khepupara	0.045	−0.076	−0.016	0.141

To examine the causality of precipitation to enhance ESL, the MLR (Equation 6, 7, and 8) was decomposed into two parts. One is for the precipitation term and the another for other terms. These two terms were compared to understand their contribution for predictions of sea level during extremes.

For Cox's Bazar:

$$SL'_{Cox's\ Bazar\ (Pre\text{-}term)}(t) = d_3 \times Pre(t) \quad (9)$$

$$SL'_{Cox's\ Bazar\ (Other\ terms)}(t) = a_3 \times SLP(t) + b_3 \times U(t) + c_3 \times V(t) + e_3 \quad (10)$$

For Charchanga:

$$SL'_{Charchanga\ (Pre\text{-}term)}(t) = d_4 \times Pre(t) \quad (11)$$

$$SL'_{Charchanga\ (Other\ terms)}(t) = a_4 \times SLP(t) + b_4 \times U(t) + c_4 \times V(t) + e_4 \quad (12)$$

For Khepupara:

$$SL'_{Khepupara\ (Pre\text{-}term)}(t) = d_5 \times Pre(t) \quad (13)$$

$$SL'_{Khepupara\ (Other\ terms)}(t) = a_5 \times SLP(t) + b_5 \times U(t) + c_5 \times V(t) + e_5 \quad (14)$$

4.3. Results

4.3.1. Performance of MLR for all events

Here, the result for predictions of ESL using MLR for all events at Cox's Bazar (Equation 6), Charchanga (Equation 7), and Khepupara (Equation 8) is presented. To represent the predictability of ESL, the time series of the predicted sea level was compared with the observed sea level. Figure 4.1 displays the average time series of the observed and predicted SLA at three study stations. For all three stations, similar to the observed SLA, the predicted mean SLA is highest on the day of the extreme (t = 0), with a gradual increase from the prior days. The predicted SLA on the day of the extreme shows large uncertainty, which represents the high variations in predicted ESLs among the events. In the day of extreme, the observed SLA is 0.72 m, 0.64 m, and 0.59 m and the predicted SLA is 0.53 m, 0.37 m, and 0.43 m, respectively, for Cox's Bazar (Fig. 4.1a,b), Charchanga (Fig. 4.1c,d), and Khepupara (Fig. 4.1e,f). The result shows that in comparison with Charchanga (Fig. 4.1c,d), and Khepupara (Fig. 4.1e,f) the observed sea level is well predicted in the day of extreme at Cox's Bazar (Fig. 4.1a,b). Using MLR for all events, the predicted variability in ESL among stations are consistent with those using MLR for each event presented in Chapter 3. To examine the main driver to the variability among stations, the contribution of precipitation and other explanatory variables in the MLR for all events were investigated in the following section.

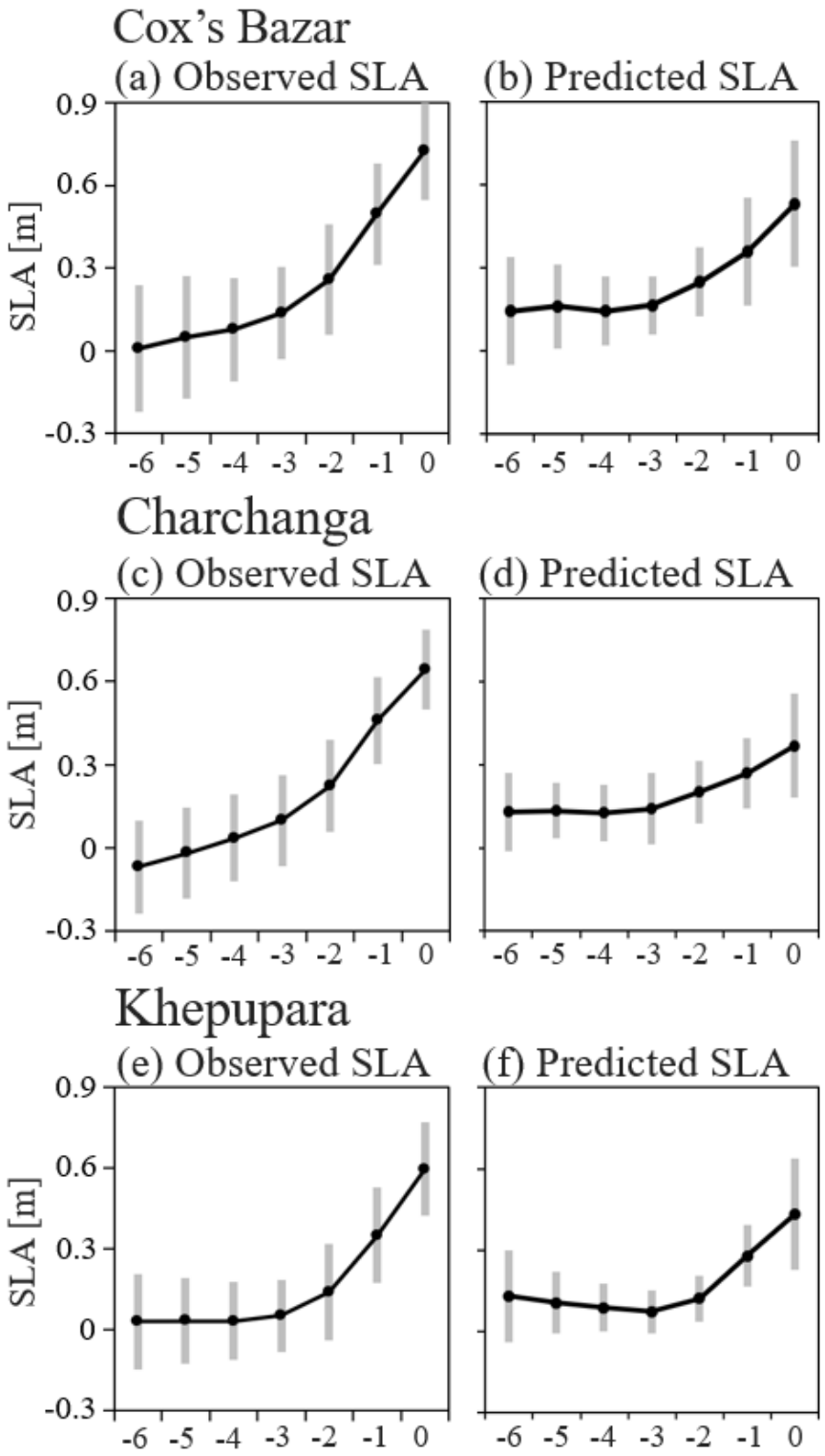

Figure 4.1 (a) and (b) represent average time series of the observed and predicted SLA, respectively at Cox's Bazar. (c), (d) and (e), (f) same as (a), (b) but for Charchanga and Khepupara, respectively. The error bars represent the standard deviation of the cases. The x-axes represent the day corresponding to the six days before ($t = -6$) to the ESL day ($t = 0$).

4.3.2. Variations in the contribution of precipitation among the stations

In Section 4.3.1, it was confirmed that the predictability of ESL considering precipitation is high at Cox's Bazar than Charchanga and Khepupara. It is hypothesized that the variabilities in ESL predictions among the stations may be influenced by the variations in the contribution of precipitation. Therefore, to investigate the contribution of precipitation to the variabilities in ESLs, the MLR for all events was decomposed into two parts, one for the precipitation term and another for the other terms. The contribution of the precipitation term was determined using Equation 9, 11, and 13 for Cox's Bazar, Charchanga, and Khepupara, respectively. Similarly, Equation 10, 12, and 14 were used to determine the contribution of other terms for Cox's Bazar, Charchanga, and Khepupara, respectively. Figure 4.2 shows the decomposition of the predicted SLA for precipitation term and other terms at three stations. For Cox's Bazar, the SLA explained by the precipitation term (Fig. 4.2a) is smaller than that of other terms (Fig. 4.2b). However, the other terms show almost stable evolution from prior days towards the day of extreme ($t = 0$). In contrast, the contribution of precipitation term shows gradual increase especially from prior three day ($t = -3$) toward the day of extreme ($t = 0$), although it shows large uncertainty among the events (Fig. 4.2a). For this period, there is high increase in SLA from –0.07 m to 0.23 m (about 0.30 m) explained by the precipitation term. In contrast, there is a very weak increase in SLA from 0.24 m to 0.29 m (about 0.05 m) explained by the other terms, which denotes that the high increase in SLA toward the ESL day is mainly governed by the precipitation term. In comparison with Cox's Bazar, the contribution of precipitation term is very small than the contribution of other terms for Charchanga (Fig. 4.2c) and Khepupara (Fig. 4.2e). The SLA explained by other terms shows a steady increase from prior three day ($t = -3$) toward the ESL day with large uncertainty among the events for Charchanga (Fig. 4.2d) and Khepupara (Fig. 4.2f). It indicates that the high increase in sea level toward the ESL day is mainly driven by the contribution of the other terms rather than the precipitation term for Charchanga and Khepupara. The high contribution of precipitation at Cox's Bazar is influenced by the high coefficient value of precipitation (coeff. = 0.187), and the low coefficient values of precipitation for Charchanga (coeff. = −0.016) and Khepupara (coeff. = 0.045) reflect the small effect of precipitation for these two stations (Table 4.1).

To discuss the relationship between precipitation and sea level, their time series were compared in Figure 4.3. Figure 4.3a shows that at Cox's Bazar the amount of precipitation is high during the ESL events, which denotes the evidence of high precipitation effect for ESL variability at Cox's Bazar. On the other hand, for Charchanga (Fig. 4.3b) and Khepupara (Fig.

4.3c) the amount of precipitation is very small during the ESL events. The small amount of precipitation at Charchanga and Khepupara may be due to the use of precipitation averaged over a large basin, which may reduce the amount when dry area is included. Figure 4.3 indicates that the variations in predictability of ESLs among the stations are highly influenced by the variations in precipitation. For Cox's Bazar, it shows high precipitation during ESL. In comparison with Cox's Bazar, the amount of precipitation is very small in Charchanga and Khepupara. The small precipitation at Charchanga and Khepupara may be the reason for relatively high contribution of other factors (i.e., SLP and winds) for the predictions of ESL.

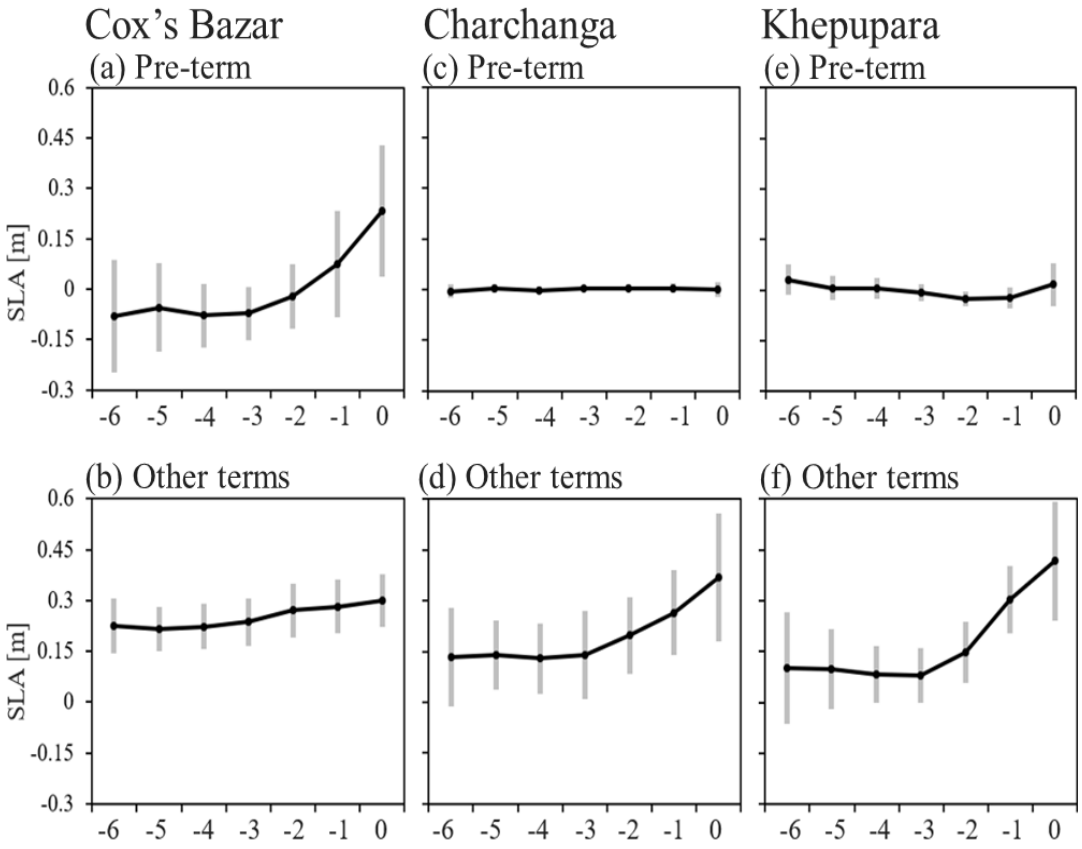

Figure 4.2 (a) and (b) represent the average time series of the decomposed SLA for Pre-term and other terms, respectively at Cox's Bazar. (c), (d) and (e), (f) same as (a), (b) but for Charchanga and Khepupara, respectively. The error bars represent the standard deviation of the cases. The x-axes represent the day corresponding to the six days before ($t = -6$) to the ESL day ($t = 0$).

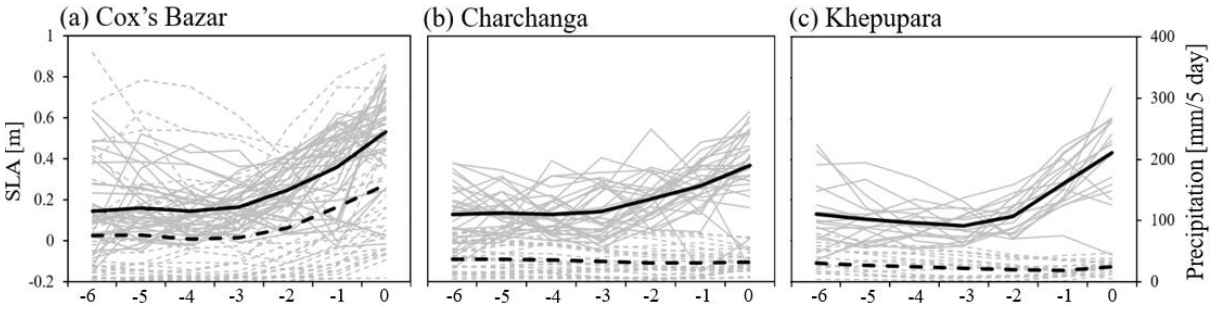

Figure 4.3 (a) Time series of five-day accumulated precipitation (thin dash lines) and estimated SLA (thin solid lines) during each ESL event at Cox's Bazar. The thick lines represent their averages. The x-axis represents the day corresponding to the six days before ($t = -6$) to the ESL day ($t = 0$). The left axis is for SLA and the right axis is for precipitation. (b) and (c) same as (a) but for Charchanga and Khepupara station, respectively.

4.4. Discussion and summary

In the results section, it was revealed that the ESL is well predicted using MLR for all events. The variations in the contribution of precipitation influence the predictions of ESL among the stations. Considering precipitation term the predicted high SLA at Cox's Bazar in comparison to Charchanga and Khepupara reflects the high precipitation over Cox's Bazar area (Fig. 4.2). Here, a composite analysis of the meteorological variables was performed to represent their spatial variations in the day of ESL. Figure 4.4 shows the composite map of the variables for all days of extreme ($t = 0$) of the selected ESL events at three stations. It denotes that during extreme days the precipitation remains high over Cox's Bazar which may contribute to the high sea level along the coastal ocean (Fig. 4.4a). For Charchanga (Fig. 4.4b) and Khepupara (Fig. 4.4c), the intensity of precipitation seems less, which results in the relatively low sea level along the coast of Charchanga and Khepupara. Figure 4.4 shows that for Cox's Bazar, the high precipitation and low-pressure induced strong wind enhance the sea level. However, for Charchanga and Khepupara low-pressure associated storms and winds play an important role for high sea level rather than precipitation. At Cox's Bazar, precipitation along the coast remains high during ESL event (Fig. 4.4), which is consistent with the temporal evolution shown in Figure 4.3. For Charchanga and Khepupara, the small precipitation in Figure 4.4 is also consistent with their temporal evolutions in Figure 4.3.

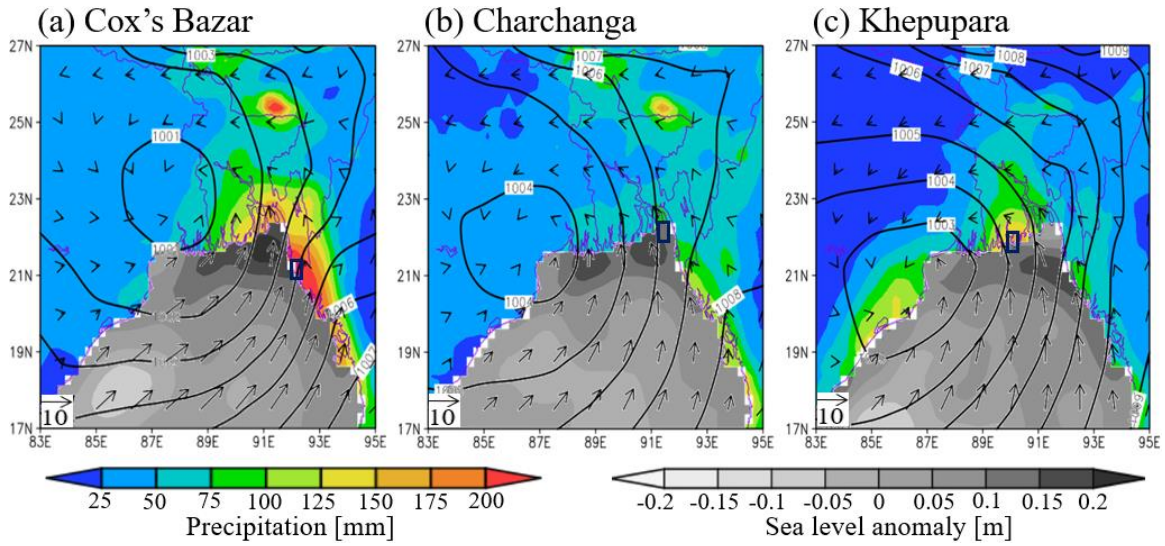

Figure 4.4 (a) Composite map of the variables for all day of extreme (t = 0) of the selected ESL events at Cox's Bazar. Here, the analysis was performed for 25 days of ESL for the period of 1993–2006. Only the ESL events after 1992 were used because of the availability of gridded sea level anomaly data from 1993. The gray shading over the ocean represents sea level anomaly (m) and the color shading over the land represents accumulated precipitation during the five preceding days (mm). The contour and vector are for SLP (hPa) and surface wind (m/s), respectively. The rectangles denote the location of the Cox's Bazar station. (b) same as (a) but for Charchanga station and the analysis was performed for 12 days during extremes for the period of 1993–2000. (c) same as (a) and (b) but for Khepupara station and the analysis was performed for 7 days during extremes for the period of 1993–2000. It is noted that the sea level anomaly drawn here is defined as the deviation of sea level from its 20-year (1993–2012) climatological mean (Taburet et al., 2019).

The main objective of this study is to investigate the effect of precipitation on ESL events. The effect was evaluated using the MLR for each event (Equation 2). In section 3.3.2, it was confirmed that the observed ESL is well predicted by the MLR with consideration of precipitation effect. However, the MLR created for each event may be sensitive to the sample size (Hünicke and Zorita, 2006; Zhang and Church, 2012; Karabil et al., 2017). Therefore, in Chapter 3 the MLR built using all ESL events (Equation 6, 7, and 8) was evaluated. The sample size is increased to be in total 245, 210, and 126 for Cox's Bazar (Equation 6), Charchanga (Equation 7), and Khepupara (Equation 8), respectively. The MLR for all events performed well for the predictions of sea level. Figure 4.5 shows the average time series of SLA from two MLRs at Cox's Bazar. The predicted SLA using MLR for each event shows a gradual increase toward the day of extreme (Fig. 4.5a). The predictions of SLA using MLR for all events also

shows monotonic increase toward the day of ESL (Fig. 4.5b). For both MLRs, the gradual increase in SLA towards the day of ESL is mainly attributable to the contribution of precipitation at Cox's Bazar (Fig. 3.9a, 4.2a).

To evaluate the consistency of two MLR predictions, the coefficients in the two MLRs were compared. At Cox's Bazar, there are positive coefficients of precipitation for 28 ESL events out of total 35 events (Fig. 4.6a). For Charchanga, 18 ESL events out of total 30 shows negative coefficients and the remaining 12 ESL events shows positive coefficients (Fig. 4.6e). At Khepupara, 11 ESL events out of total 18 shows positive coefficients for precipitation (Fig. 4.6i), although the values of the coefficients are small. In comparison with Charchanga and Khepupara, the positive coefficient values of precipitation are found for many events at Cox's Bazar. This result implies the fact that precipitation is more influential for ESL at Cox's Bazar. At three stations, many events shows negative coefficients for SLP (Fig. 4.5b,f,j), negative and small coefficients for U (Fig. 4.6c,j,k), and also relatively small coefficients for V (Fig. 4.6d,h,l). The strong negative coefficients of SLP for many events at Charchanga rather than other stations highly influence the predictions of ESL. The coefficients of the explanatory variables in MLR for all events are presented in Table 4.1 (Section 4.2). The result shows that likewise the MLR for each event, the coefficient of precipitation in MLR for all events is positive at Cox's Bazar (coeff. = 0.187), and it is higher than that in Charchanga (coeff. = −0.016) and Khepupara (coeff. = 0.045) (Table 4.1). Table 4.1 also shows that the coefficients for other variables (i.e., SLP, U, and V) are small and negative at three stations, which is consistent with the MLR for each event (Fig. 4.6). The negative coefficients for other explanatory variables (i.e., SLP) also denotes their high influence on ESL, especially for Charchanga and Khepupara (Table 4.1). At Cox's Bazar, for both MLR predictions (Fig. 4.5), the increasing SLA toward the day of extreme are mainly attributable to the precipitation term in MLR for each event (Fig. 3.9a) and MLR for all events (Fig. 4.2a). The consistency between two different MLRs is owing to the similarities of the coefficients, which denotes that the positive effect of terrestrial precipitation to enhance sea level is robust at Cox's Bazar.

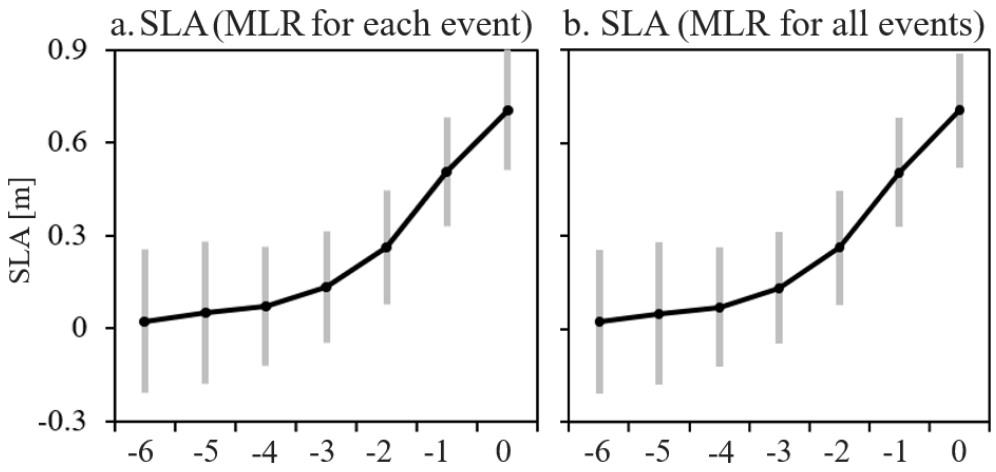

Figure 4.5 (a) Average time series of the predicted SLA at Cox's Bazar using MLR for each event. (b) same as (a) but for the MLR for all events. The error bars represent the standard deviation of the cases. The x-axes represent the day corresponding to the six days before (t = −6) to the ESL day (t = 0).

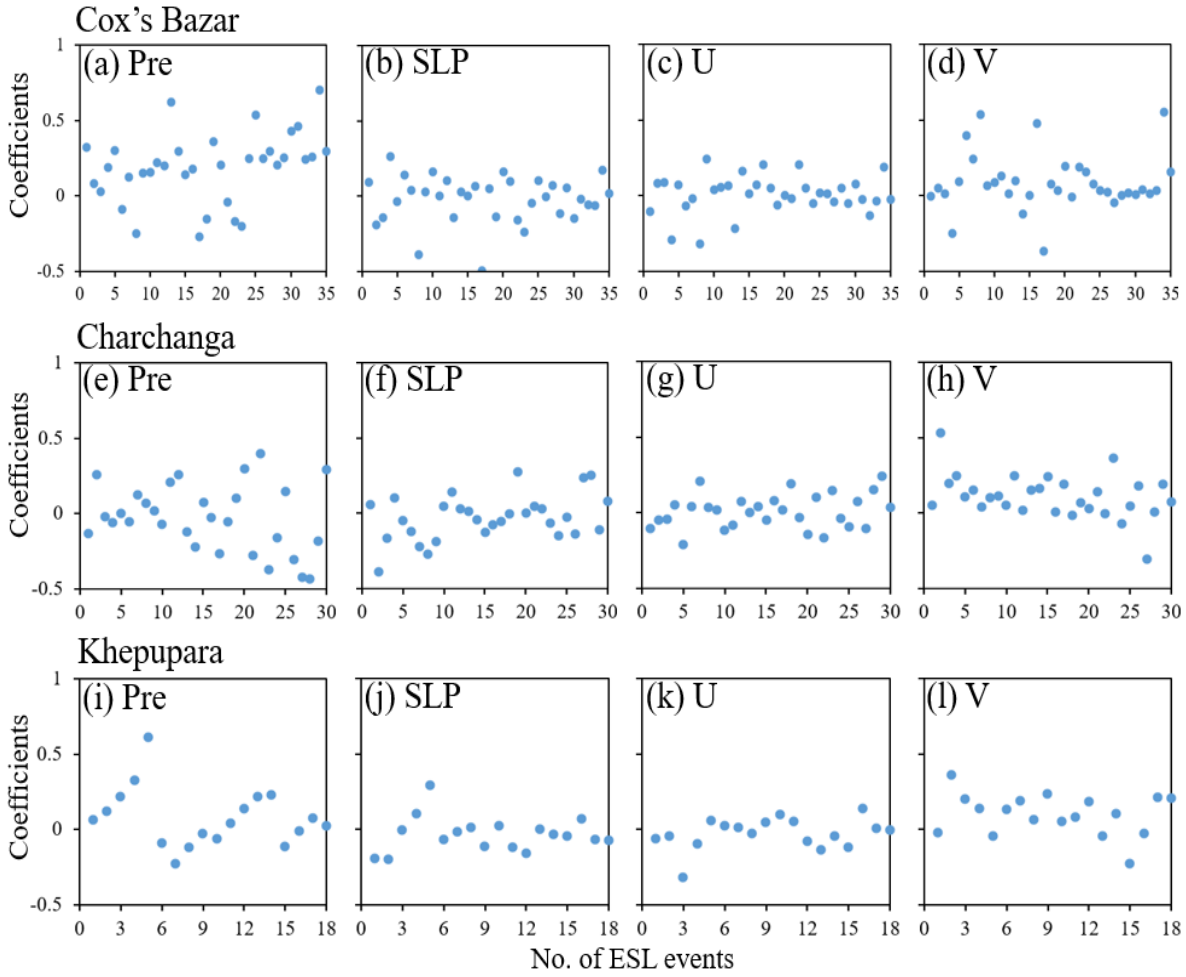

Figure 4.6 Scatter plots of the coefficients obtained from the MLR for each event (Equation 2). (a), (b), (c), and (d) represent the coefficients of Pre, SLP, U, and V, respectively, for 35 ESL events at Cox's Bazar. (e), (f), (g), and (h) are the same but for 30 ESL events at Charchanga. Similarly, (i), (j), (k), and (l) represents the same but for 18 ESL events at Khepupara.

Likewise the MLR for each event in Chapter 3, the ESL is nicely predicted by the MLR for all events at three stations. In comparison to Charchanga and Khepupara, the predicted high SLA considering precipitation term at Cox's Bazar is presumably due to the high precipitation. At Cox's Bazar the consistency in predictions of ESL using two different MLR is governed by the dominant effect of precipitation which were revealed by both MLRs. In contrast, for Charchanga and Khepupara it is influenced by the effect of SLP and winds. Both MLR approaches commonly capture this feature.

Chapter 5: General discussion

5.1. Influence of remote and local SST

It is known that the monsoonal precipitation has interannual variation in relation to the large-scale ocean and atmosphere dynamics (Salahuddin et al., 2006; Fan et al., 2016; Ahmed et al., 2017). The El Niño–Southern Oscillation (ENSO) and Indian Ocean Dipole (IOD) are the dominant climate modes that modulate the interannual variability of precipitation in this region (Singh et al., 2001; Salahuddin et al., 2006; Ahmed et al., 2017; Wahiduzzaman, 2021). In Chapter 3, it was addressed that the precipitation contributes to the ESL along the coast of Bangladesh. Considering the importance of precipitation for ESL, the spatial distributions of terrestrial precipitation were investigated with respect to the remote effect of ENSO, IOD, and local SST conditions. Here, it is hypothesized that the variations in precipitation related to the ENSO and IOD index, and local SST effect may influence the ESL variability over this region. Therefore, the interannual variations of the ESL modulated by the influence of ENSO, IOD, and BoB SST were investigated in this section.

The frequency of ESL events during the positive and negative phases of ENSO, IOD, and local BoB SST was investigated for Cox's Bazar station. The ESL events were targeted to investigate how they are associated with the effect of large-scale ocean conditions. The spatial distributions of terrestrial precipitation and its significance were investigated for the remote effect of ENSO, IOD, and local SST conditions. Details of the used datasets for each parameter were same as those mentioned in Chapter 2.

In Section 3.3.3, it was confirmed that the predictability of ESL varies with the seasonal march of monsoonal precipitation. The earlier studies mentioned that the monsoonal precipitation have interannual variation in relation to the large-scale ocean and atmosphere dynamics (Salahuddin et al., 2006; Fan et al., 2016; Ahmed et al., 2017). Therefore, considering the effect of the large-scale ocean and atmosphere forcings on monsoonal precipitation, the influence of ENSO, IOD, and local SSTs (BoB SST) on precipitation and ESL events was investigated for Cox's Bazar station. Figure 5.1 depicts the interannual time series of ENSO, IOD, BoB SST, and the daily SLA at Cox's Bazar during 1983–2006. The positive and negative phases for each ocean index were determined based on the threshold values, and then the analysis was conducted to characterize ESL and precipitation in each phase. One standard deviation of their monthly interval data (see Section 2.2) was used to determine the threshold

value. For ENSO, ONI index above +0.8K and below –0.8K are defined as positive phase and negative phase, respectively (Fig. 5.1a). For IOD, DMI index above +0.4K and below –0.4K are defined as positive phase and negative phase, respectively (Fig. 5.1b). These threshold values are similar to the threshold values adopted by the Bureau of Meteorology, Australia (BOM, 2022). For BoB SST, the area-averaged SST above +0.2K and below –0.2K are defined as warm and cold phase, respectively (Fig. 5.1c). Among the total of 35 ESL events at Cox's Bazar, those occurred during positive and negative phases of ENSO, IOD, and BoB SST are very small (Table 5.1). For ENSO, the number of days for positive, negative, and normal phases are 1339, 1220, and 5028, respectively, and among them the number of ESL events are 3, 8, and 24, respectively. For IOD, the number of days for positive, negative, and normal phases are 671, 817, and 6099, respectively and among them the number of ESL events are 4, 3, and 28, respectively. Similarly, for BoB SST, the number of days are 1489, 1609, and 4489, respectively and among them the number of ESL events are 7, 6, and 22, respectively. The small number of ESL events during negative and positive phases likely reflects their shorter duration than normal phase, rather than the less likelihood of ESL at these phases. These results denote that the effect of ENSO, IOD, and BoB SST on ESL is not strong.

However, it is expected that the SST serves as an indirect forcing agent for ESL through enhancing the high precipitation when SST is high (Salahuddin et al., 2006; Roxy et al., 2013: Rahman et al., 2013). Therefore, it was aimed to investigate the effect of SST on precipitation around Bangladesh area. Considering the importance of precipitation for ESL, spatial distributions of terrestrial precipitation were investigated for positive and negative years of ENSO, IOD, and local SST. The positive year means the year in which more than six months belong to the positive phase, and vice versa for the negative phase. The analysis presented here used annual total precipitation, not monsoon precipitation. It was confirmed that the main claim remain unchanged if monsoon precipitation is analyzed. This is because of the large fraction of monsoon precipitation to annual precipitation. A year list of the status for ENSO, IOD, and BoB SST during 1983–2006 is given in Table 5.2. The result shows that the difference in precipitation between the positive and negative years of ENSO (Fig. 5.2a-c) and IOD (Fig. 5.2d-f) over the Bangladesh area is not significant, suggesting that the effect of remote SST is not a dominant factor altering the terrestrial precipitation variability over Bangladesh in terms of the annual timescale. For the positive IOD year, positive precipitation anomaly is found only in the narrow area near Cox's Bazar (Fig. 5.2d-f). Such a weak response of precipitation to remote SST has been noted by previous studies (Ahasan et al., 2010; Rahman et al., 2013;

Ahmed et al., 2017). Figure 5.2g-i shows that the Bangladesh area receives more precipitation during positive BoB SST years than negative years and their difference is significant. It is hypothesized that this is the reason for more ESL events during the warm SST years (n = 7) than the negative years (n = 6) (Table 5.1). However, their difference is small. The effect of BoB SST to enhance precipitation (Roxy et al., 2013) and the role of precipitation-induced high discharge to sea level change along the coast were reported in previous studies (Dandapat et al., 2020). The BoB SST-enhanced precipitation and associated discharge may have contributed to the variation in sea level along the coast of Bangladesh.

The result in this section shows the number of ESL events are small during the positive and negative phases of ENSO, IOD, and BoB SST. Therefore, the remote effect of ENSO and IOD on the local sea level variations at Cox's Bazar is uncertain. It is revealed that the precipitation over the Bangladesh area is insensitive to the ENSO and IOD which denotes their weak effect on local precipitation variability in this area as reported previously (Rahman et al., 2013; Ahmed et al., 2017). The precipitation over northern Bangladesh tended to be high in the year of high SST over the BoB, which may have contributed to the variation in sea level.

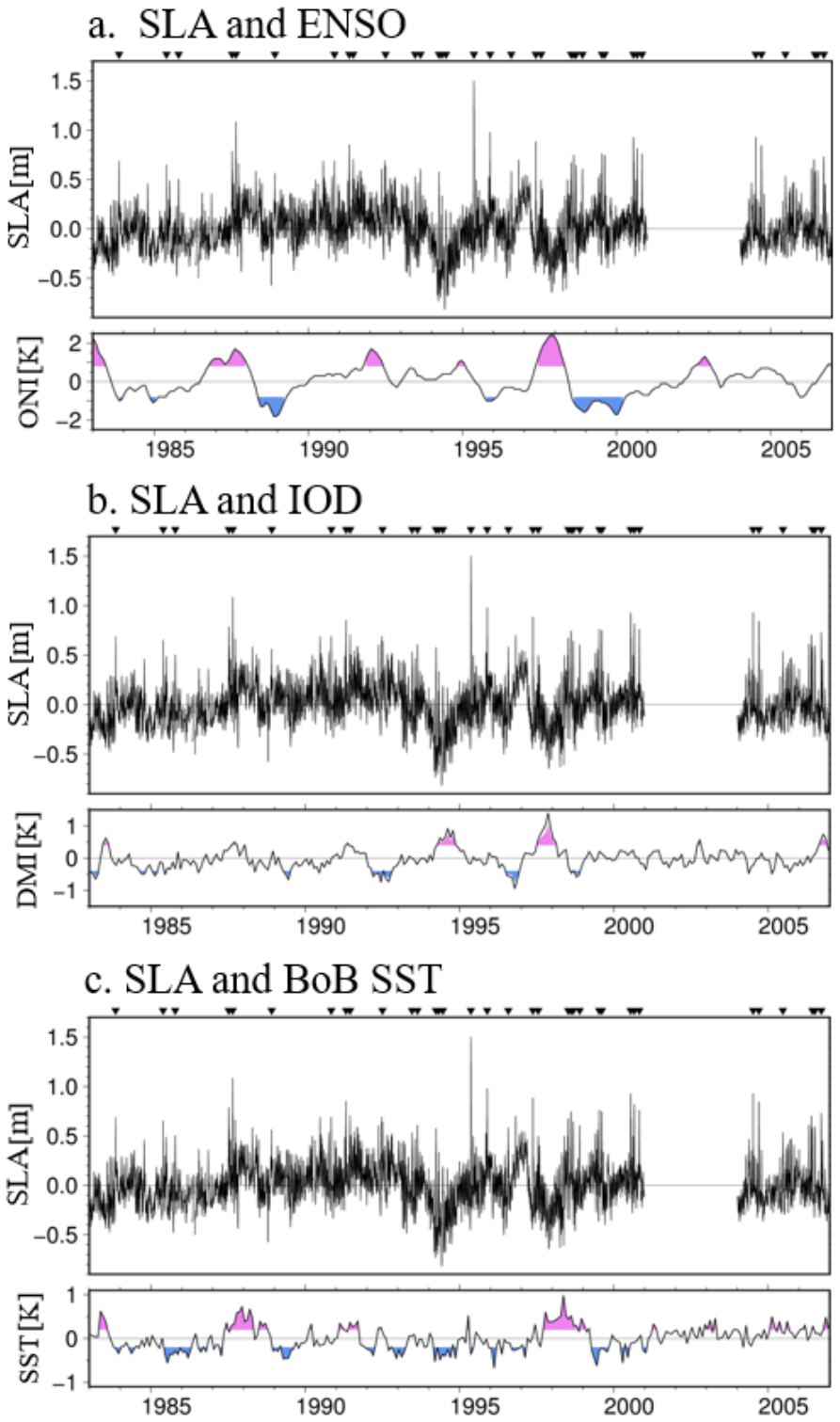

Figure 5.1 (a) Time series of (upper) daily SLA at Cox's Bazar and (lower) ENSO index during 1983–2006. The station SLA data are missing during 2001–2003. Shading in ENSO index indicates the period above (purple) and below (blue) threshold values. The triangle plotted on the top denotes the day of the ESL event. (b) and (c) Same as (a) but for IOD index and monthly mean SST anomaly over the BoB (5°–23° N and 80°–99° E), respectively.

Table 5.1 Number of SLA days and ESL events during different phases of ENSO, IOD, and BoB SST anomaly over the BoB (5°–23°N and 80°–99°E).

	Indices	No. of SLA days	No. of ESL events
ENSO	Positive (ONI > 0.8K)	1339	3
	Negative (ONI < -0.8K)	1220	8
	Normal (-0.8K < ONI < 0.8K)	5028	24
IOD	Positive (DMI > 0.4K)	671	4
	Negative (DMI < -0.4K)	817	3
	Normal (-0.4K < DMI < 0.4K)	6099	28
BoB SST	Warm (SST > 0.2K)	1489	7
	Cold (SST < -0.2K)	1609	6
	Normal (-0.2K < SST < 0.2K)	4489	22

Table 5.2 List of positive and negative years for ENSO, IOD, and BoB SST.

ENSO	Positive years :1987, 1991, 1992, 1997, 2002
	Negative years :1985, 1988, 1989, 1999, 2000
IOD	Positive years :1987, 1991, 1994, 1997, 2006
	Negative years :1984, 1985, 1989, 1992, 1996
BoB SST	Positive years :1987, 1988, 1991, 1998, 2003, 2005, 2006
	Negative years :1984, 1985, 1986, 1989, 1992, 1993, 1994, 1996, 1999

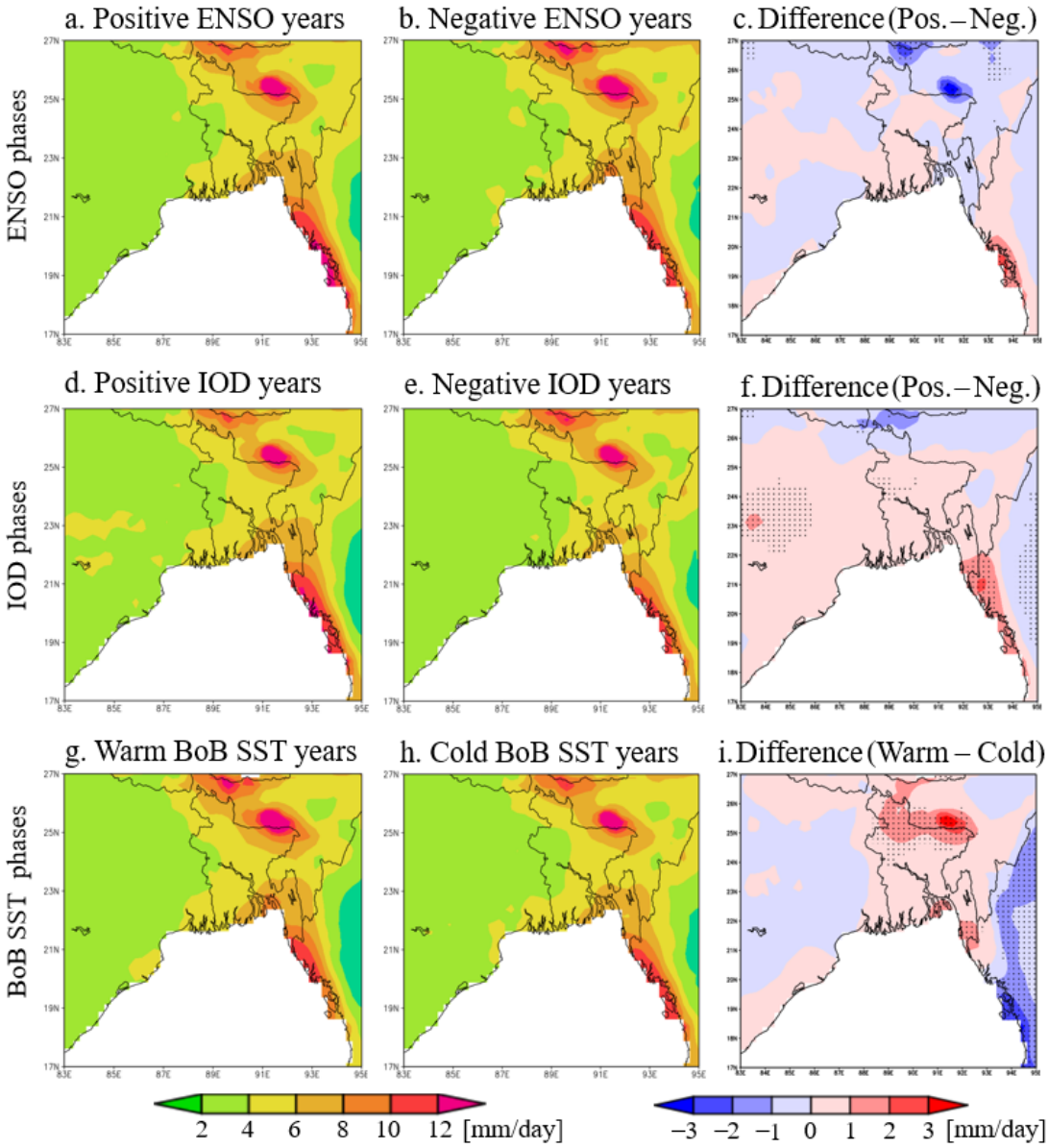

Figure 5.2 Average precipitation (mm/day) during (a) positive and (b) negative ENSO years. (c) Difference in precipitation between positive and negative ENSO year. (d) and (e) same as (a) and (b) but for positive IOD and negative IOD years and (f) their difference. Similarly, (g) and (h) for warm and cold BoB SST years and (i) their difference. The dots in (c), (f), and (i) represent the difference is statistically significant at 95% confidence level.

5.2. Contribution to coastal management

This study found that the ESL along the eastern coast of Bangladesh is mainly influenced by the effect of terrestrial precipitation. In contrast, for many events the ESL along the central and western coast are highly influenced by the strong low pressure and associated winds rather than precipitation. In Bangladesh the prediction of ESL has not been developed

yet and the role of site-dependent key meteorological factor for ESL is still out of consideration by the coastal managers. At present, the daily observed water level at available gauge stations is used for monitoring the sea level change (BWDB, 2020). The task of the coastal managers is to monitor the daily sea level. Their ongoing activities are also to investigate the forcing factors (e.g., precipitation) for ESL and to develop prediction models for ESL. However, the effect of precipitation is not accounted yet. The finding of this study suggests that the coastal managers should monitor the high precipitation and incorporate its effect to ESL warning at Cox's Bazar area. The available observation of daily precipitation conducted by the Meteorological Department of Bangladesh (BMD, 2020) will be effective for the monitoring of precipitation. In contrast, for Charchanga and Khepupara the coastal managers should incorporate the effect of strong low-pressure and winds for prediction of ESL, which has been suggested by previous studies (Dube et al., 2009; Mehra et al., 2010; Lee, 2013; Dastagir, 2015). It is hoped that the formulation of ESL prediction considering the effect of a site-dependent key factor and the development of early warning system will help coastal peoples to reduce the losses in lives and properties. The people should be aware of the key factors and follow the predictions which will be essential to take proper measures against ESL hazards. The construction of coastal embankment is considered as an important measure to prevent the inundation of extreme water into the low-lying coast and to control the flood risk (Adel, 2002; Rahman and Rahaman, 2018; Hassan, 2019). The design and construction of disaster resilient houses, rescue center, public institutions, and effective communication system are necessary to reduce the vulnerability of the people (Ali, 1999; Dewan, 2003; Karim and Mimura, 2008). The development of proper drainage system will reduce the water logging problem and help to minimize the flood risk (Mirza, 2003; Brammer, 2014; Dastagir, 2015). The public awareness on the causes of ESL hazards and follow the aforementioned measures are essential for sustainable coastal management.

Bangladesh is located in the highest precipitation-prone area of the world. The novel finding of this study highlights the influence of precipitation on ESL combined with other meteorological variables in this area. The consideration of upper basin precipitation will improve the prediction of ESL for Cox's Bazar area, which will be effective to reduce the impact of ESL hazards. This study mentioned that the high precipitation over hilly areas plays a key role for ESL along the eastern coast of Bangladesh. The geomorphological settings of this hilly area may favor the high precipitated-water runoff, which enhance the sea level to be extreme along the eastern coast. Such role of precipitation is expected to be present in different global coasts that have similar geographical settings. In contrast, the upper GBM basin receives

high precipitation, but its effect in the central and western downstream is relatively small. The variation in precipitation over large upper basin and effect of human activities on discharge may lead to small amount of precipitated-water in the downstream. In addition, the small effect of precipitation for ESL is possibly influenced by the low pressure and winds rather than precipitation. It indicates that the effect of precipitation is not crucial for ESL in river basins where the discharge in the downstream is affected by the anthropogenic controls and other meteorological forcings are stronger (e.g., low pressure, winds) than precipitation.

In this study the area averaged precipitation over the selected basin is used to investigate the effect of precipitation on ESL using statistical analysis. It suggests that the accurate estimation of precipitated-water discharge in the downstream is important to investigate the effect of upper basin precipitation on ESL. For this densely populated area, the runoff of the precipitated-water from upper basin is influenced by the human activities before it reaches the downstream (Adel, 2002; Rahman and Rahaman, 2018; Hassan, 2019). Therefore, it is necessary to account the withdrawal of river water in the upper basin. Considering the withdrawal of upstream water, precipitation-runoff models will be useful for the estimation of net precipitated-water discharge in the downstream (Zarriello and Ries, 2000; Degefu et al., 2019). For example, the VIC-WUR (Variable Infiltration Capacity, developed by the Wageningen University and Research) hydrological model accounts the water withdrawal by human activities (Droppers et al., 2020). The use of surface and groundwater for various human activities (e.g., irrigation, industrial, domestic, and livestock) and dam operation were considered. The developed datasets on sectoral water demands were used for simulation of water withdrawal using VIC-WUR model. It is expected that the adoption of such hydrological models will be effective to estimate the net precipitated-water discharge, leading to more reliable prediction of coastal sea level change. The source area for precipitated-water discharge over GBM river basin extends over many countries. The precipitated-water discharge in the downstream is influenced by the water resource management in the upstream regions which might relate to the policy of multi-countries. The data on water withdrawal in each country is needed for the accurate estimation of net-precipitated water discharge in the downstream. Therefore, an international cooperation among countries will be essential for the improved prediction of coastal ESL.

At present, the coastal hazards (e.g., flood, inundation, and erosion) are frequent and intense due to the changing climate forcings (Turner and Annamalai, 2012; Wahl et al., 2017; Kirezci, et al., 2020). In the context of climate change, the ESL-induced hazards are a

great concern to the sustainability of the coastal communities (Antony et al., 2016; Wahl et al., 2017). The climate change induced heavy precipitation, strong cyclones, and high winds enhance the occurrence of ESL events along the coasts (Dube et al., 2009; Piecuch et al., 2018; Singh et al., 2021). The intensity of heavy precipitation, strong winds, and severe cyclone events are projected to increase in future due to anthropogenic greenhouse gas emissions (Singh et al., 2000, Mirza, 2003; Mehra et al., 2010; Lee, 2013). The extremeness in precipitation is projected to increase by the late 21st century, which might raise flood risk in low-lying global deltas (Karim and Mimura, 2008; IPCC, 2013). The change in oceanic and atmospheric forcings will intensify the cyclones and associated cyclonic circulation over the coastal regions (Dube et al., 2009; Mehra et al., 2010; Lee, 2013). Under the projected warming in the 21st century, the frequency of intense cyclones is projected to increase substantially and the precipitation near the cyclone center becomes more extreme during landfall over the South Asia region (IPCC, 2013). Thus, the role of terrestrial precipitation to ESL in the studied area remains high in future. Further understanding on the process of terrestrial hydrological cycle including human activities will help reduce the vulnerability of the coastal community and ensure coastal sustainability.

Chapter 6: Conclusion

The main objective of this study is to investigate the effect of precipitation on the variability of ESL at daily time scale along the coast of Bangladesh. The study was conducted at three different coastal stations of Cox's Bazar, Charchanga, and Khepupara. The effect of precipitation on ESL was investigated mainly using MLR statistics. The explanatory variables of precipitation, SLP, zonal, and meridional winds were incorporated for predictions of SLA during the ESL events. The 99th percentiles values of daily SLA were used as threshold for the identification of ESL events. Then, after removing overlapped ESL events in total 35, 30, and 18 independent ESL events were selected for Cox's Bazar, Charchanga, and Khepupara, respectively. For precipitation, two different settings of the domain were used: one is for Cox's Bazar and another for Charchanga and Khepupara. For Cox's Bazar the hydrologic catchment area of the Sangu, Matamuhuri, and Karnafuli River system was used, which is isolated by the Arakan Mountain range. The GBM river basin area was used for Charchanga and Khepupara. The basin average precipitation over five days accumulation was used to account the delay effect in precipitation runoff. For SLP and winds, the daily area-averaged data over the BoB area was used considering the storm-induced surges and strong winds towards the coast. Two MLRs, one for with precipitation (WP) and another for without precipitation (WOP) were developed for each event and for each station to investigate the effect of precipitation. To confirm the independency of the explanatory variables, a correlation analysis among the explanatory variables was performed. It was confirmed that the explanatory variables contribute independently to SLA. The contribution of precipitation was evaluated from the differences of WP and WOP settings of the MLR for each event with seven-day period. It was revealed that the estimation of ESLs considering precipitation effects outperformed the estimation of ESLs without precipitation. The lower root mean squared error values were found for many cases for prediction of sea level with precipitation than without precipitation, which means the better prediction of SLA if precipitation data is incorporated. To understand the causal effect of the precipitation the MLR equation was decomposed into two parts, one is the term for precipitation effect and another to represent the effects of other terms (i.e., winds and sea level pressure). It was confirmed that the gradual increase in SLA towards the day of extreme is mainly governed by the contribution of precipitation term than the contribution of other atmospheric forcings for Cox's Bazar. In contrast, the influence of precipitation on ESL is relatively small for Charchanga and Khepupara. The larger influence of precipitation at Cox's Bazar reflects the high precipitation over this hilly area. The results demonstrated that

the effect of precipitation on ESL is robust and the effect of precipitation on the variability of ESL has spatial variation, with strong effects in the central and eastern parts of the coast. It was also noticed that the variability in ESLs among the stations are influenced by the variations in spatiotemporal evolutions of the explanatory variables during extremes. For Cox's Bazar, the sea level in the day of extreme is highly influenced by the intense precipitation and strong low-pressure induced winds towards the coast. In the day of extreme, the sea level for Charchanga and Khepupara are influenced by the low-pressure associated surges and winds rather than precipitation.

The influences of precipitation on the local variability of ESL events were investigated based on the seasonal effects of the precipitation. It was found that the ESLs are influenced by the seasonality of precipitation. The peak precipitation of the monsoon season has high influence on the variability of ESL. It was revealed that the ESLs at Cox's Bazar are influenced by the high precipitation of monsoon during June and July. For Charchanga, the influence of precipitation is prominent during the post-monsoon period (August to September). At Khepupara, the effect of high precipitation was found during October and November. For Cox's Bazar station, the high frequency of ESLs during monsoon is influenced by the prominent increase of heavy precipitation events. There are variations in the predictability of ESL among the stations, and the high predictability in ESL at Cox's Bazar reflects the high precipitation over this area in comparison with Charchanga and Khepupara. Therefore, it was confirmed that the precipitation plays an important role for ESL variability along the coast of Bangladesh.

Likewise the MLR for each event, another MLR was developed by using all ESL events. The MLR for all events was performed at each station using all daily samples derived from seven days in prior to the ESLs. For Cox's Bazar in total 245 samples were used, accounting the 35 ESL events and the 7 days for each ESL event. In the similar manner, in total 210 samples (30 × 7) and 126 samples (18 × 7) were used for Charchanga and Khepupara, respectively. The MLR for all events well predicted the daily sea level during ESL events. The predictions of ESL is high at Cox's Bazar than Charchanga and Khepupara, which is consistent with the MLR for each event. It is confirmed that the precipitation is a dominant factor for variations in the predictions of ESL among the stations. In addition, the coefficients of the two different MLR denotes that the predictions of ESL are highly influenced by the high coefficient values of precipitation than the other variables. For both the MLR predictions, the high coefficient values of precipitation at Cox's Bazar reflect the high effect of precipitation there

than Charchanga and Khepupara. The consistency in the two different settings of MLR prediction denotes the insensitivity of MLR for the sample size.

This study investigated the likelihood of ESL events during the positive and negative phases of ENSO, IOD, and BoB SST. It was revealed that the number of ESL events are very small during the positive and negative phases of ENSO, IOD, and BoB SST, which denotes that the effect of positive and negative phases of ENSO, IOD, and BoB SST on ESL is not strong. There is no significant precipitation difference over Bangladesh area corresponding to the remote SST effect induced by ENSO and IOD. The upper Bangladesh area receives high precipitation during the warm phase of BoB SST than the cold phase, and the warm BoB SST-induced high precipitation may have contributed to the variation in sea level.

The study will be considered as one of the pioneer studies for consideration of the effect of abundant precipitation in this area to predict the ESL. In the IPCC's report, it was mentioned that the precipitation as a part of the hydrological cycle modulates the regional and local sea level (IPCC, 2019). Therefore, it is hoped that the findings of this study will highlight the importance of precipitation to improve the forecast of ESL events and disaster prevention.

This study revealed the high effect of precipitation on ESL for Cox's Bazar area along the eastern coast. The hilly geomorphological characteristics accelerates abundant precipitated-water discharge in the downstream, which enhance the sea level to be extreme along the eastern coast. It is expected that such role of precipitated-water discharge will influence the ESL in different global coasts that have similar geographical settings. In contrast, the ESL for Charchanga and Khepupara area are influenced by the SLP and winds rather than precipitation. The understanding on the effect of site-dependent key meteorological factor for ESL will help the coastal managers to monitor crucial factor at each location, and the consideration of their effect will improve the prediction of ESL. The improved prediction will be effective for the preparation of the action plan for better coastal management. Furthermore, the prediction of ESL will help the coastal managers and stakeholders in the coastal communities to consider proper measures against ESL hazards. The construction of embankment, well drainage, disaster resilient buildings, and public awareness on extremeness of sea level will be effective to reduce the risk of ESL hazards. Considering the application of this study, the forecast datasets of daily sea level, precipitation, SLP, and winds are publicly available via internet. Hence, it is expected that the coefficients of the explanatory variables determined in MLR analysis for all ESL events will be useful for the prediction of sea level during extreme event. This study suggests that the

accurate estimation of precipitated-water discharge in the downstream using hydrological models will help to get more reliable prediction of ESL.

In the context of changing climate, the intensity of extreme precipitation, strong cyclones, and high winds are projected to increase in future due to anthropogenic greenhouse gas emission. Under changing climate forcings, the ESLs will be more intense in future and the increasing intensity of ESL-induced hazard will enhance the vulnerability of the coastal communities to adapt with disaster risk. The prediction of ESL has importance to prevent the associated disaster risk, which leads to reduce the vulnerability of the coastal communities and ensure the coastal sustainability.

References:

Adel, M. M., 2002. Man-made climatic changes in the Ganges basin. *International Journal of Climatology*, 22, 993–1016. https://doi.org/10.1002/joc.732

Adnan, M. S. G., Dewan, A., Zannat, K. E., 2019. The use of watershed geomorphic data in flash flood susceptibility zoning: a case study of the Karnaphuli and Sangu river basins of Bangladesh. *Natural Hazards*, 99, 425–448. https://doi.org/10.1007/s11069-019-03749-3

Ali, A., 1999. Climate Change Impacts and Adaptation Assessment in Bangladesh. *Climate Research*, 12, 109–116. https://doi.org/10.3354/CR012109

Ahasan, M. N., Chowdhary, M. A. M., Quadir, D. A., 2010. Variability and Trends of Summer Monsoon Rainfall over Bangladesh. *Journal of Hydrology and Meteorology*, 1–17. https://doi.org/10.3126/jhm.v7i1.5612

Ahmed, M. K., Alam, M. S., Yousuf, A. H. M., Islam, M. M., 2017. A long-term trend in precipitation of different spatial regions of Bangladesh and its teleconnections with El Niño/Southern Oscillation and Indian Ocean Dipole. *Theoretical and Applied Climatology*, 473–486. https://doi.org/10.1007/s00704-016-1765-2

Anoop, T. R., Kumar, S. V., Shanas, P. R., Johnson, G., 2015. Surface wave climatology and its variability in the North Indian Ocean based on ERA-interim reanalysis. *Journal of Atmospheric and Oceanic Technology*, 32, 1372–1385. https://doi.org/10.1175/JTECH-D-14-00212.1

Antony, C., Unnikrishnan, A. S., Woodworth, P. L., 2016. Evolution of extreme high waters along the east coast of India and at the head of the Bay of Bengal. *Global and Planetary Change*, 140, 59–67. https://doi.org/10.1016/j.gloplacha.2016.03.008

BMD, 2020. Climate and Weather Data: Observation of daily precipitation over Bangladesh. *Bangladesh Meteorological Department,* Agargaon, Dhaka-1207, Bangladesh.

BOM, 2022. About ENSO and IOD indices. *Bureau of Meteorology, Melbourne, Commonwealth of Australia*. http://www.bom.gov.au/climate/enso/indices/about.shtml

Brammer, H., 2014. Bangladesh's dynamic coastal regions and sea-level rise. *Climate Risk Management*, 1, 51–62. https://doi.org/10.1016/j.crm.2013.10.001

BWDB, 2005. Daily discharge data for the Ganges River at Hardinge Bridge and Brahmaputra River at Bahadurabad. *Bangladesh Water Development Board*, Dhaka-1215, Bangladesh.

BWDB, 2020. Flood forecast and warning center, Bangladesh. *Bangladesh Water Development Board*, Dhaka-1215, Bangladesh.

Caesar, J., Janes, T., Lindsay, A., Bhaskaran, B., 2015. Temperature and precipitation projections over Bangladesh and the upstream Ganges, Brahmaputra and Meghna systems. *Environmental Science: Processes and Impacts*, 17, 1047–1056. https://doi.org/10.1039/C4EM00650J

Caldwell, P. C., Merrifield, M. A., Thompson, P. R., 2015. Sea level measured by tide gauges from global oceans-the Joint Archive for Sea Level holdings (NCEI Accession 0019568), Version 5.5, *NOAA, National Centers for Environmental Information, Dataset*. https://doi.org/10.7289/V5V40S7W

CCC, 2016. Assessment of Sea Level Rise on Bangladesh Coast through Trend Analysis, *Climate Change Cell (CCC)*, Department of Environment, Ministry of Environment and Forests, Bangladesh.

Cheng, X., Xie, S. P., McCreary, J. P., Qi, Y., Du, Y., 2013. Intraseasonal variability of sea surface height in the Bay of Bengal. *Journal of Geophysical Research: Oceans*, 118, 816–830. https://doi.org/10.1002/jgrc.20075

Dandapat, S., Gnanaseelan, C., Parekh, A., 2020. Impact of excess and deficit river runoff on Bay of Bengal upper ocean characteristics using an ocean general circulation model. *Deep Sea Research Part II: Topical Studies in Oceanography*, 172, 104714. https://doi.org/10.1016/j.dsr2.2019.104714

Dastagir, M. R., 2015. Modeling recent climate change induced extreme events in Bangladesh: A review. *Weather and Climate Extremes*, 7, 49–60. https://doi.org/10.1016/j.wace.2014.10.003

Degefu, D. M., Liao, Z., He, W., Yuan, L., An, M., Zhang, Z., Xia, W., 2019. The Impact of Upstream Sub-basins' Water Use on Middle Stream and Downstream Sub-basins' Water Security at Country-Basin Unit Spatial Scale and Monthly Temporal Resolution. *International Journal of Environmental Research and Public Health*, 16, 450. https://doi.org/10.3390/ijerph16030450

Dewan, A. M., Nishigaki, M., Komatsu, M., 2003. Floods in Bangladesh: A comparative hydrological investigation on two catastrophic events. *Journal of the Faculty of Environmental Science and Technology*, 8, 53–62. http://ousar.lib.okayama-u.ac.jp/files/public/1/11503/20160527190938720714/008_053_062.pdf

Draper, N. R., Smith, H., 1998. Applied regression analysis (Third Edition). *John Wiley and Sons, Inc*. https://doi.org/10.1002/9781118625590

Droppers, B., Franssen, W. H. P., van Vliet, M. T. H., Nijssen, B., Ludwig, F., 2020. Simulating human impacts on global water resources using VIC-5. *Geoscientific Model Development*,13, 5029–5052. https://doi.org/10.5194/gmd-13-5029-2020

Dube, S. K., Jain, I., Rao, A. D., Murty, T. S., 2009. Storm surge modelling for the Bay of Bengal and Arabian Sea. *Natural Hazards*, 51, 3–27. https://doi.org/10.1007/s11069-009-9397-9

Endo, N., Matsumoto, J., Hayashi, T., Terao, T., Murata, F., Kiguchi, M., Yamane, Y., Alam, M. S., 2015. Trends in precipitation characteristics in Bangladesh from 1950 to 2008. *SOLA*, 11, 113–117. https://doi.org/10.2151/sola.2015-027

Fan, F., Mann, M. E., Lee, S., Evans, J. L., 2012. Future changes in the south Asian summer monsoon: an analysis of the CMIP3 multimodel projections. *Journal of Climate*, 25, 3909–3928. https://doi.org/10.1175/JCLI-D-11-00133.1

Fan, L., Shin, S., Liu, Z., Liu, Q., 2016. Sensitivity of Asian Summer Monsoon precipitation to tropical sea surface temperature anomalies. *Climate Dynamics*, 2501–2514. https://doi.org/10.1007/s00382-016-2978-x

Fujinami, H., Sato, T., Kanamori, H., Murata, F., 2017. Contrasting features of monsoon precipitation around the Meghalaya Plateau under westerly and easterly regimes. *Journal of Geophysical Research: Atmosphere*, 9591–9610. https://doi.org/10.1002/2016JD026116

Ghosh, S., Hazra, S., Nandy, S., Mondal, P. P., Watham, T., Kushwaha, S. P. S., 2018. Trends of sea level in the Bay of Bengal using altimetry and other complementary techniques. *Journal of Spatial Science*, 6, 49–62. https://doi.org/10.1080/14498596.2017.1348309

Habib, S. M. A., Sato, T., Hatsuzuka, D., 2019. Decreasing number of propagating mesoscale convective systems in Bangladesh and surrounding area during 1998–2015. *Atmospheric Science Letters*, 20, e879. https://doi.org/10.1002/asl.879

Han, W., Webster, P., 2002. Forcing mechanisms of sea level interannual variability in the Bay of Bengal. *Journal of Physical Oceanography*, 32, 216– 239. https://doi.org/10.1175/1520-0485(2002)032<0216:FMOSLI>2.0.CO;2

Han, W., 2005. Origins and dynamics of the 90-day and 30-60-day variations in the equatorial Indian Ocean. *Journal of Physical Oceanography*, 35, 708–728. https://doi.org/10.1175/JPO2725.1

Hassan, A. B. M. E., 2019. Indian hegemony on water flow of the Ganges: Sustainability challenges in the southwest part of Bangladesh. *Sustainable Futures*, 1, 100002. https://doi.org/10.1016/j.sftr.2019.100002

Hatsuzuka, D., Yasunari, T., Fujinami, H., 2014. Characteristics of low pressure systems associated with intraseasonal oscillation of rainfall over Bangladesh during boreal summer. *Monthly Weather Review*, 4758–4774. https://doi.org/10.1175/MWR-D-13-00307.1

Huang, B., Thorne, P. W., Banzon, V. F., Boyer, T., Chepurin, G., Lawrimore, J. H., Menne, M. J., Smith, T. M., Vose, R. S., Zhang, H., 2017. Extended Reconstructed Sea Surface Temperature, Version 5 (ERSSTv5): Upgrades, Validations, and Intercomparisons. *Journal of Climate*, 8179–8205. https://doi.org/10.1175/JCLI-D-16-0836.1

Hünicke, B., Zorita, E., 2006. Influence of temperature and precipitation on decadal Baltic Sea level variations in the 20th century. *Tellus*, 58, 141–153. https://doi.org/10.1111/j.1600-0870.2006.00157.x

IMD, 2008. Tracks of cyclones and depressions (1891–2007), electronic version 1.0/2008. *Indian Meteorological Department*, New Delhi, India.

IPCC, 2013. Climate Change 2013: *The Physical Science Basis. Contribution of Working Group I to the Fifth Assessment Report of the Intergovernmental Panel on Climate Change*. Stocker, T. F., D. Qin, G.-K. Plattner, M. Tignor, S.K. Allen, J. Boschung, A. Nauels, Y. Xia, V. Bex and P.M. Midgley (eds.). Cambridge University Press, Cambridge, United Kingdom and New York, NY, USA: 1535.

IPCC, 2019. IPCC Special Report on the Ocean and Cryosphere in a Changing Climate [H.-O. Pörtner, D.C. Roberts, V. Masson-Delmotte, P. Zhai, M. Tignor, E. Poloczanska, K. Mintenbeck, A. Alegría, M. Nicolai, A. Okem, J. Petzold, B. Rama, N.M. Weyer (eds.)].

Iskandar, I., McPhaden, M. J., 2011. Dynamics of wind-forced intraseasonal zonal current variations in the equatorial Indian Ocean. *Journal of Geophysical Research: Oceans*, 116, C06019. https://doi.org/10.1029/2010JC006864

Islam, M. A., Sato, T., 2021. Influence of terrestrial precipitation on the variability of extreme sea levels along the coast of Bangladesh. *Water*, 13, 2915. https://doi.org/10.3390/w13202915

Karabil, S., Zorita, E., Hünicke, B., 2017. Mechanisms of variability in decadal sea-level trends in the Baltic Sea over the 20th century. *Earth System Dynamics*, 8, 1031–1046. https://doi.org/10.5194/esd-8-1031-2017

Karim. M. F., Mimura, N., 2008. Impacts of climate change and sea-level rise on cyclonic storm surge floods in Bangladesh. *Global Environmental Change*, 18, 490–500. https://doi:10.1016/j.gloenvcha.2008.05.002

Khandker, H., 1997. Mean sea level in Bangladesh. *Marine Geodesy*, 20, 69–76. https://doi.org/10.1080/01490419709388095

Kirezci, E., Young, I. R., Ranasinghe, R., Muis, S., Nicholls, R. J., Lincke, D., Hinkel, J., 2020. Projections of global-scale extreme sea levels and resulting episodic coastal flooding over the 21st Century. *Scientific Reports*, 10, 11629. https://doi.org/10.1038/s41598-020-67736-6

Kobayashi, S., Ota, Y., Harada, Y., Ebita, A., Moriya, M., Onoda, H., Onogi, K., Kamahori, H., Kobayashi, C., Endo, H., Miyaoka, K., Takahashi, K., 2015. The JRA-55 reanalysis: General specifications and basic characteristics. *Journal of the Meteorological Society of Japan*, 93, 5–48. https://doi.org/10.2151/jmsj.2015-001

Kuang, C., Chen, W., Gu, J., Su, T., Song, H., Ma, Y., Dong, Z., 2017. River discharge contribution to sea-level rise in the Yangtze River Estuary, China. *Continental Shelf Research*, 134, 63–75. https://doi.org/10.1016/j.csr.2017.01.004

Kumar, V., Melet, A., Meyssignac, B., Ganachaud, A., Kessler, W. S., Singh, A., Aucan, J., 2018. Reconstruction of Local Sea Levels at South West Pacific Islands-A Multiple Linear Regression Approach (1988–2014). *Journal of Geophysical Research: Oceans*, 123, 1502–1518. https://doi.org/10.1002/2017JC013053

Lee, H. S., 2013. Estimation of Extreme Sea Levels along the Bangladesh Coast Due to Storm Surge and Sea Level Rise Using EEMD and EVA. *Journal of Geophysical Research: Oceans*, 118, 4273–4285. https://doi.org/10.1002/jgrc.20310

Ma, J., Yu, J. Y., 2014. Paradox in South Asian summer monsoon circulation change: Lower tropospheric strengthening and upper tropospheric weakening. *Geophysical Research Letters*, 41. https://doi.org/10.1002/2014GL059891

Mehra, P., Tsimplis, M. N., Prabhudesai, R. G., Joseph, A., Shaw, A. G. P., Somayajulu, Y. K., Cipollini, P., 2010. Sea Level Changes Induced by Local Winds on the West Coast of India. *Ocean Dynamics*, 60, 819–833. https://doi.org/10.1007/s10236-010-0289-z

Mirza, M. M. Q., 2003. Three recent extreme floods in Bangladesh: A hydro-meteorological analysis. *Natural Hazards*, 28, 35–64. https://doi.org/10.1023/A:1021169731325

Mohsenipour, M., Shahid, S., Ziarh, G. F., Yaseen, Z. M., 2020. Changes in Monsoon Rainfall Distribution of Bangladesh Using Quantile Regression Model. *Theoretical and Applied Climatology*, 142, 1329–1342. https://doi.org/10.1007/s00704-020-03387-x

Mondal, A. M., 2001. Sea level rise along the coast of Bangladesh. *Bangladesh Inland Water Transport Authority*, Ministry of Shipping, Dhaka, Bangladesh. www.gloss-sealevel.org/sites/gloss/files/publications/documents/bangladesh_2001.pdf

Moron, V., Ullmann, A., 2005. Relationship between sea-level pressure and sea-level height in the Camargue (French Mediterranean coast). *International Journal of Climatology*, 25, 1531–1540. https://doi.org/10.1002/joc.1200

Nishat, B., Rahman, S. M. M., 2009. Water Resources Modeling of the Ganges-Brahmaputra-Meghna River Basins Using Satellite Remote Sensing Data. *Journal of the American Water Resources Association*, 45, 1313–1327. https://doi.org/10.1111/J.1752-1688.2009.00374.X

Perigaud, C., McCreary Jr., J. P., 2003. Influence of interannual rainfall anomalies on sea level variations in the tropical Indian Ocean. *Journal of Geophysical Research*, 108, 3335. https://doi.org/10.1029/2003JC001857.

Piecuch, C. G., Bittermann, K., Kemp, A. C., Ponte, R. M., Little, C. M., Engelhart, S. E., Lentz, S. J., 2018. River-discharge effects on United States Atlantic and Gulf coast sea-level changes. *Proceedings of the National Academy of Sciences*, 115, 7729–7734. https://doi.org/10.1899/11-177.1

Prakash, S., Mahesh, C., Gairola, R. M., 2012. Sea Level Anomalies in the Tropical Indian Ocean during Two Contrasting Southwest Monsoon Years. *The International Journal of Ocean and Climate Systems*, 127–133. https://doi.org/10.1260/1759-3131.3.2.127

Rahman, M. M., Rafiuddin, M., Alam, M. M., 2013. Teleconnections between Bangladesh Summer Monsoon Rainfall and Sea Surface Temperature in the Indian Ocean. *International Journal of Ocean and Climate Systems*, 231–237. https://doi.org/10.13140/RG.2.1.5186.3446

Rahman, M. M., Rahaman, M. M., 2018. Impacts of Farakka barrage on hydrological flow of Ganges river and environment in Bangladesh. *Sustainable Water Resources Management*, 4, 767–780. https://doi.org/10.1007/s40899-017-0163-y

Rasid, H., Pramanik, M. A. H., 1990. Visual interpretation of satellite imagery for monitoring floods in Bangladesh. *Environmental Management*, 14, 815–821. https://doi.org/10.1007/BF02394176

Rayner, N. A., Parker, D. E., Horton, E. B., Folland, C. K., Alexander, L. V., Rowell, D. P., Kent, E. C., Kaplan, A., 2003. Global analyses of sea surface temperature, sea ice, and night marine air temperature since the late nineteenth century. *Journal of Geophysical Research*, 108, 2156–2202. https://doi.org/10.1029/2002JD002670

Reynolds, R. W., Smith, T. M., Liu, C., Chelton, D. B., Casey, K. S., Schlax, M. G., 2007. Daily high-resolution blended analyses for sea surface temperature. *Journal of Climate*, 5473–5496. https://doi.org/10.1175/2007JCLI1824.1

Roxy, M., Tanimoto, Y., Preethi, B., Terray, P., Krishnan, R., 2013. Intraseasonal SST-precipitation relationship and its spatial variability over the tropical summer monsoon region. *Climate Dynamics*, 45–61. https://doi.org/10.1007/s00382-012-1547-1

Salahuddin, A., Isaac, R. H., Curtis, S., Matsumoto, J., 2006. Teleconnections between the sea surface temperature in the Bay of Bengal and monsoon rainfall in Bangladesh. *Global and Planetary Change*, 188–197. https://doi.org/10.1016/j.gloplacha.2006.06.001

Sarwar, M. G. M., 2013. Sea-level rise along the coast of Bangladesh. In: Shaw R., Mallick F., Islam A. (eds) Disaster risk reduction approaches in Bangladesh. *Disaster Risk Reduction*, 217–231. https://doi.org/10.1007/978-4-431-54252-0_10

Shahid, S., 2009. Spatio-temporal variability of rainfall over Bangladesh during the time period 1969-2003. *Asia-Pacific Journal of Atmospheric Science*, 45, 375–389. https://ssrn.com/abstract=1674429

Shahid, S., 2010. Rainfall variability and the trends of wet and dry periods in Bangladesh. *International Journal of Climatology*, 30, 2299–2313. https://doi.org/10.1002/joc.2053

Shahid, S., 2011. Trends in extreme rainfall events of Bangladesh. *Theoretical and Applied Climatology*, 104, 489–499. https://doi.org/10.1007/s00704-010-0363-y

Singh, O. P., Khan, A. T., Rahman, M., 2000. Changes in the frequency of tropical cyclones over the North Indian Ocean. *Meteorology and Atmospheric Physics*, 11–20. https://doi.org/10.1007/s007030070011

Singh, O. P., 2001. Cause-effect relationships between sea surface temperature, precipitation and sea level along the Bangladesh coast. *Theoretical and Applied Climatology*, 68, 233–243. https://doi.org/10.1007/s007040170048

Singh, O.P., Khan, T. M. A., Murty, T. S., Rahman, M. S., 2001. Sea level changes along Bangladesh coast in relation to the southern oscillation phenomenon. *Marine Geodesy*, 24, 65–72. http://dx.doi.org/10.1080/01490410120192

Singh, O. P., 2002a. Predictability of sea level in the Meghna estuary of Bangladesh. *Global and Planetary Change*, 32, 245–251. https://doi.org/10.1016/S0921-8181(01)00152-7

Singh, O. P., 2002b. Spatial variation of sea level trend along the Bangladesh coast. *Marine Geodesy*, 25, 205–212. https://doi.org/10.1080/01490410290051536

Singh, V. K., Roxy, M. K., Deshpande, M., 2021. Role of warm ocean conditions and the MJO in the genesis and intensification of extremely severe cyclone Fani. *Scientific Reports*, 11, 3607. https://doi.org/10.1038/s41598-021-82680-9

Smith, B. D., Ahmed, B., Ali, M. E., Braulik, G., 2001. Status of the Ganges river dolphin or shushuk Platanista gangetica in Kaptai Lake and the southern rivers of Bangladesh. *Oryx*, 35, 61–72. https://doi.org/10.1046/j.1365-3008.2001.00153.x

Suresh, I., Vialard, J., Lengaigne, M., Han, W., McCreary J., Durand, F., Muraleedharan, P. M., 2013. Origins of wind-driven intraseasonal sea level variations in the North Indian Ocean coastal waveguide. *Geophysical Research Letters*, 40, 5740–5744. https://doi.org/10.1002/2013GL058312

Svensson, C., Jones, D. A., 2002. Dependence between extreme sea surge, river flow and precipitation in eastern Britain. *International Journal of Climatology*, 22, 1149–1168. https://doi.org/10.1002/joc.794

Taburet, G., Sanchez, R. A., Ballarotta, M., Pujol, M. I., Legeais, J. F., Fournier, F., Faugere, Y., Dibarboure, G., 2019. DUACS DT2018: 25 years of reprocessed sea level altimetry products. *Ocean Science*, 15, 1207–1224. https://doi.org/10.5194/os-15-1207-2019

Tazkia, A. R. Krien, Y., Durand, F., Testut, L., Islam, A. K. M. S., Papa, F., Bertin, C., 2016. Seasonal modulation of M2 tide in the Northern Bay of Bengal. *Continental Shelf Research*, 137, 154–162. https://doi.org/10.1016/j.csr.2016.12.008

Turner, A. G., Annamalai, H., 2012. Climate change and the South Asian summer monsoon. *Nature Climate Change*, 2, 587–595. https://doi.org/10.1038/nclimate1495

Unnikrishnan, A. S., Kumar, M. R. R., Sindhu, B., 2011. Tropical cyclones in the Bay of Bengal and extreme sea-level projections along the east coast of India in a future climate scenario. *Current Science*, 101, 327–331. https://www.jstor.org/stable/24078511

Vialard, J., Shenoi, S. S. C., McCreary, J. P., Shankar, D., Durand, F., Fernando, V., Shetye, S. R., 2009. Intraseasonal response of the northern Indian Ocean coastal waveguide to the Madden-Julian Oscillation. *Geophysical Research Letters*, 36, L14606. https://doi.org/10.1029/2009GL038450

Wahiduzzaman, M., 2021. Major Floods and Tropical Cyclones over Bangladesh: Clustering from ENSO Timescales. *Atmosphere*, 12, 692. https://doi.org/10.3390/atmos12060692

Wahl, T., Haigh, I. D., Nicholls, R. J., Arns, A., Dangendorf, S., Hinkel, J., Slangen, A. B. A., 2017. Understanding extreme sea levels for broad-scale coastal impact and adaptation analysis. *Nature Communications*, 8, 16075. https://doi.org/10.1038/ncomms16075

Ward, P. J., Couasnon, A., Eilander, D., Haigh, I. D., Hendry, A., Muis, S., Veldkamp, T. I. E., Winsemius, H. C., Wahl, T., 2018. Dependence between high sea-level and high river discharge increases flood hazard in global deltas and estuaries. *Environmental Research Letters*, 13, 084012. https://doi.org/10.1088/1748-9326/aad400

Webster, P. J., Moore, A. M., Loschnigg, J. P., Leven, R. R., 1999. Coupled ocean–atmosphere dynamics in the Indian Ocean during 1997–98. *Nature*, 401, 356–360. https://doi.org/10.1038/43848

Webster, P. J., Jian, J., Hopson, T. M., Hoyos, C. D., Agudelo, P. A., Chang, H. R., Curry, J. A., Grossman, R. L, Palmer, T. N., Subbiah, A. R., 2010. Extended-range probabilistic forecasts of Ganges and Brahmaputra floods in Bangladesh. *Bulletin of the American Meteorological Society*, 91, 1493–1514. https://doi.org/10.1175/2010BAMS2911.1

Woodworth, P. L., Blackman, D. L., 2004. Evidence for systematic changes in extreme high waters since the mid-1970s. *Journal of Climate*, 1190–97. https://doi.org/10.1175/1520-0442(2004)017<1190:EFSCIE>2.0.CO;2

Wu, S. Y., Yarnal, B., Fisher, A., 2002. Vulnerability of coastal communities to sea-level rise: a case study of Cape May County, New Jersey, USA. *Climate Research*, 22, 255–270. https://doi.org/*10.3354/cr022255*

Xie, S. P., Xu, H., Saji, N. H., Wang, Y., Liu, W. T., 2006. Role of narrow mountains in large-scale organization of Asian monsoon convection. *Journal of Climate,* 3420–3429. https://doi.org/10.1175/JCLI3777.1

Yatagai, A., Kamiguchi, K., Arakawa, O., Hamada, A., Yasutomi, N., Kitoh, A., 2012. APHRODITE: Constructing a long-term daily gridded precipitation dataset for Asia based on a dense network of rain gauges. *Bulletin of the American Meteorological Society*, 93, 1401–1415. https://doi.org/10.1175/BAMS-D-11-00122.1

Zarrielo, P., Ries, K., 2000. A Precipitation-Runoff Model for Analysis of the Effects of Water Withdrawals on Streamflow, Ipswich River Basin, Massachusetts. *USGS Water-Resources Investigations Report 00-4029,* 99.

Zhang, X., Church, J. A., 2012. Sea level trends, interannual and decadal variability in the Pacific Ocean. *Geophysical Research Letters*, 39, L21701. https://doi.org/10.1029/2012GL053240

Zzaman, R. U., Nowreen, S., Billah, M., Islam, A. S., 2021. Flood hazard mapping of Sangu River basin in Bangladesh using multi-criteria analysis of hydro-geomorphological factors. *Journal of Flood Risk Management*, 14:e12715. https://doi.org/10.1111/jfr3.12715

ACKNOWLEDGEMENT

First, I would like to sincerely express my cordial appreciation to Prof. Tomonori Sato who has guided, advised, and motivated me with his valuable time to complete my research. From very beginning of this journey, I have learnt a lot of knowledge from him to conduct and improve my research. I strongly believe that without support of Prof. Tomonori Sato, it was quite difficult to reach the research goal at today. I would like to say my cordial thanks to Prof. Yasuhiro Yamanaka, Prof. Teiji Watanabe, Prof. Tatsufumi Okino, and Prof. Toru Terao for their valuable comments and suggestions to improve my research.

I am grateful to my beloved laboratory members for their time, support, and suggestion for my research. I acknowledge the help of the current and former members of the Regional Climate System Research Group: Prof. Koji Yamazaki, Dr. Tetsu Nakamura, Dr. Daisuke Hatsuzuka, Dr. Enkhbat Erdenebat, Dr. Chinh Ta Huu, Dr. Muhammad Mubashar Ahmad Dogar, Dr. Kenta Tamura, Ms. Keiko Ishizaki, Ms. Keiko Ono, Mr. Shixue Li, Ms. Xiling Zhou, Ms. Yu Gao, Mr. Hiroki Teramura, Mr. Koki Kasai, Mr. Ahsan SM Habib, Ms. Yumi Matsushita, Ms. Yuki Sato, Ms. Nozomi Matsudera, Mr. Hironobu Ochiai, Mr. Yoshihito Higuchi, Mr. Motoharu Sawayanagi, Mr. Kevin Ray E. Lucas, Mr. Deokyoung Han, Mr. Yoshiaki Shirai, Mr. Hiromu Yahata, Mr. Takehiro Morioka, Mr. Kousuke Nagahiro, Mr. Akinobu Ogasawara, Mr. Tatsuro Kotsuji, Ms. Guan Yu Song, and Ms. Ferreira Ramim Bruna. I am also thankful for the co-operation of the members at the Division of Environmental Science Development, Course in Human and Ecological Systems, and Sub-course Seminar for Symbiosis in Nature at the Graduate School of Environmental Science, Hokkaido University. For the grant of my study leave, I would like to thank my Department of Geography and Environment at Shahjalal University of Science and Technology, Bangladesh.

I would like to thank my late parents, my wife, and daughter for their sacrifice and help to overcome the difficulties during my life in Japan.